GENETIC SCREENING OF *NEU/ERBB2*

GENETIC IDENTIFICATION OF NOVEL COMPONENTS OF RECEPTOR TYROSINE KINASE (RTK) DOWN-REGULATION PATHWAYS IN *DROSOPHILA MELANOGASTER.*

By

NOOR HOSSAIN, B.SC. (HONS), M.SC.

A Thesis
Submitted to the School of Graduate Studies
in partial fulfillment of the requirements
for the Degree
Doctor of Philosophy.

McMaster University

DOCTOR OF PHILOSOPHY (2010)
(Biology)

McMaster University
Hamilton, Ontario
Canada.

TITLE: Genetic identification of novel components of receptor tyrosine kinase (RTK) down-regulation pathways in *Drosophila melanogaster*.

AUTHOR: Noor Hossain, M.Sc. (McMaster University)

SUPERVISOR: Professor J. Roger Jacobs.

NUMBER OF PAGES: xii, 224

ABSTRACT:

The type 1 transmembrane receptor tyrosine kinase (RTK), Neu/ErbB2 is a member of the Epidermal Growth Factor Receptor (EGFR) family that functions as a potent mediator of normal cell-growth and development. However, the aberrant expression of RTKs has also been implicated in many human cancers. For example, Neu over-expression has been implicated in human breast and ovarian cancers, and is correlated with poor clinical prognosis. At least one pTyr residue in Neu, Let-23, and PDGFR-β receptor tyrosine kinase is reported to have negative signaling capability. The intrinsic negative signaling behaviour of any of these pTyr residues, such as pTyr at 1028 of Neu (*Neu*^{YA}) has yet to be fully exploited with a view to better understanding of RTK signaling, leading to more precise knowledge in human cancer development and disease treatment.

Here we aimed to determine the role, specificity and the signaling pathway components of rat-*Neu*^{YA} in *Drosophila melanogaster*. Specifically, we asked whether pTyr 1028 of *Neu* could affect signaling from heterologous RTKs. If so, what would be the pathway components? Are they already known or novel? Using a targeted misexpression system, such as the *GAL4*-Upstream Activating Sequence (*GAL4-UAS*) system, we generated graded phenotypes of various *Neu* alleles in adult *Drosophila* eye and wing tissues, suitable for dosage sensitive modifier screening. Taking the advantage of these graded phenotypes, we sought to identify and evaluate the signaling characteristics of Neu/ErbB2. *Neu*^{YA}, in particular, suppressed the rough-eye phenotype of other 'add-back' *Neu* alleles, suggesting an inhibitory role in RTK signaling. The dosage sensitive modifier screen has also shown that the signal attenuating steps, such as receptor-mediated endocytosis, receptor recycling, and lysosomal degradation work in a YA-independent manner. To identify the components of the *Neu*^{YA} signaling pathway in RTK signal attenuation, a genome-wide dominant modifier screen was undertaken to screen over 60,000 F1 progeny either for suppression or enhancement of the rough-eye phenotype of *GMR-Neu*^{YAE} adults. Using deficiency mapping, we isolated and identified that one complementation group of suppressors to be alleles of *lilliputian*. Additionally, we narrowed down several groups of enhancers to certain deficiency regions, uncovering 10-30 genes- previously not known to the receptor tyrosine kinase signaling pathways. Collectively, here we report several novel *Neu*^{YA}-interactors in RTK signal attenuation in *Drosophila*.

ACKNOWLEDGEMENTS:

First of all, I would like to thank my supervisor and mentor Professor Roger Jacobs for his continued support and guidance during this study. I am proud and honoured being able to work with such a supervisor, who never said 'no' to any legitimate academic request. Dr. Jacobs is the best supervisor, anyone can find. I am forever thankful to him for my present growth both in academically and personally. Secondly, I am ever thankful to my co-supervisors, Professor Rama Singh and Dr. Bhagwati Gupta for their enormous help and suggestion during my studies. I am grateful for their tremendous co-operation during my on going job finding as well.

I am grateful to the members of Jacobs lab for their support, friendship and encouragement. I am thankful to Dr. Mihaela Georgescu, Dr. Katie Moyer, Dr. Leena Patel, Enio Polena, Nasrine Yacoub, Jessica and others in Jacobs Lab. I also remember the friendship, help and support from Xiao-Li, Maria, Nadia, Veronica, Jane and others from Dr. Campos lab. I would also like to thank to all of my volunteers from McMaster University and my friends, including Kareem and Ferdous for their invaluable help during the bench work and computer hard-drive mess-up.

Finally, I would like to thank all my family members, including my uncle, Mr. Abdur Rashid; my Father-in-Law, Mr. Zahurul Islam, my mother, and my wife who sacrificed the most during my studies. I am ever grateful to all of my well-wishers and in-laws for their moral and mental support to me over the past few years.

TABLE OF CONTENTS

LIST OF ILLUSTRATIONS, CHARTS, DIAGRAMS

LIST OF ABBREVIATIONS:

A	adenine
APC	Adenomatous Polyposis Coli
al	*aristaless*
b	*black*
C	*cytosine*
c	*curved*
ca	*claret*
cDNA	complementary DNA
co-IP	co-immunoprecipitation
CS-P	CantonS P-element free
csw	*corkscrew*
cu	*curled*
CyO	Curly of Oster
dab	*disabled*
DER	Drosophila epidermal growth factor receptor
DN	Dominant negative
DNA	deoxyribonucleic acid
dos	daughter of sevenless
DPP	DECAPENTAPLEGIC
Dsor	*downstream suppressor of Raf*
drk	*downstream receptor tyrosine kinase*
e	*ebony*
ECM	extracellular matrix
EGF	epidermal growth factor
EGFR	epidermal growth factor receptor
EMS	ethyl methane sulfonate
ERK	extracellular signal regulated kinase
EY	EYELESS
G	guanine
GDP	guanine diphosphate
GEF	guanine nucleotide exchange factor
GFP	green fluorescent protein
GMR	glass multimer reporter
Grb2	growth factor receptor bound 2
GTP	guanine triphosphate
h	*hairy*
HER	human epidermal growth factor receptor
JNK	Jun N-terminal kinase
MAPK	mitogen activated protein kinase
MAPKK	mitogen activated protein kinase kinase
MEK	mitogen activated or extracellular-regulated kinase kinase
MG	midline glia
NT	Neu transforming
NYPD	Neu tyrosine phosphorylation deficient
pax	*Paxillin*
PCR	polymerase chain reaction
phl	*pole hole*
PI3'K	phosphatidylinositol 3' kinase
pr	*purple*

PBD	phosphotyrosine binding domain
PCD	Programmed Cell Death
PTB	phosphotyrosine binding
pTyr	phosphotyrosine
px	*plexux*
rl	*rolled*
RNA	ribonucleic acid
RTK	receptor tyrosine kinase
ru	*roughoid*
sev	*sevenless*
SH2	Src-homology 2
SHC	src homology 2 domain containing
sos	*son of sevenless*
sp	*speck*
spi	*spitz*
sr	*stripe*
sr	*scarlet*
STAM	Signal transducing adaptor molecule
STAT	Signal-transducer and activator of transcription
T	*thymine*
th	*thread*
toy	*twin of eyeless*
UAS	upstream activating sequence

CONTRIBUTIONS:

Zhong Xiao-Li of Dr. Ana Campos Lab, McMaster University has generated most of the Neu transgenic lines. Data for the Table 2.1 of chapter 2 was generated by Enio Polena and Nasrine Yacoub during their undergraduate research project at the Dr. Jacobs Lab.

CHAPTER 1: INTRODUCTION

1. Introduction

The sophisticated developmental process that gives rise to an adult organism with thousands of cells, as in *Caenohabditis elegans* or tens of trillions of cells, as found in large vertebrates, simply starts with a single fertilized egg (Kalthoff, 1996). Eventually, this single cell gives rise to different tissues, organs, systems, and finally the whole organism. In order to accomplish a flawless developmental process, each and every cell must be able to integrate signals appropriately for growth, differentiation, survival and apoptosis. In other words, individual cells invariably, must be able to recognize environmental cues, process multiple signals and generate appropriate responses (Melicharek et al., 2008; Huang and Rubin, 2000). The signaling molecules that accomplish this sophisticated but intricate function are of various categories: (1) transmembrane receptors to recognize extra-cellular cues, eg. Growth Factors, (2) intracellular proteins to relay and amplify these signals, and (3) effector molecules to convert the signals into the developmental outputs. The underlying molecular mechanisms of these signaling events have been used repeatedly, with context specificity throughout the developmental process (Huang and Rubin, 2000). Defects in signaling pathways have been found as the underlying mechanism of cancer and various types of human diseases (Ramjaun and Downward, 2007; Hunter, 2000).

In eukaryotes, many genes encode for cell surface receptors that receive, process and transmit the extra-cellular cues into the cells. One large family of cell surface receptors has the capability of intrinsic protein tyrosine kinase activity and is appropriately called the Receptor Tyrosine Kinase family (RTKs). RTKs function

through the transfer of γ-phosphate of ATP to the hydroxyl group of tyrosine on target proteins (reviewed by Takeuchi and Ito, 2010; Schlessinger and Lemmon, 2006; Schlessinger, 2000).

The rat-Neu/ErbB2 is a type1 transmembrane receptor tyrosine kinase and a member of the Epidermal Growth Factor Receptor (EGFR) family. ErbB2 is a potent mediator of normal cell growth and development (reviewed in Baselga and Swain, 2009). Neu/ErbB2 amplification or over-expression has been reported in 20-30% of human breast cancers, as well as in subsets of patients with ovarian cancers, gastric carcinoma and salivary gland tumors (Vermeij et al., 2008; Owens et al., 2004; Yaziji et al., 2004; Slamon et al., 1987; Jaehne et al., 1992). The over-expression of Neu is associated with the consequences of an excess-ErbB2-mediated signaling, which drives oncogenic cell survival, proliferation, migration and angiogenesis (Takeuchi and Ito, 2010; Swain and Baselga, 2009; Schlessinger and Lemmon, 2006). This hyper-expression has also been correlated with poor prognosis in both breast and gastric cancers (Swain and Baselga, 2009; Park et al., 2006; Liu et al., 1992; Jaehne et al., 1992; Slamon et al., 1987). However, the precise mechanism of ErbB2 deregulations during cancer development are poorly understood. A clear understanding of the kinase regulation of ErbB2 will enable us better understand the mechanism of signal transduction in normal development and in carcinomas.

1.1 Signaling by trans-membrane Receptor Tyrosine Kinase (RTK)

The RTK family is composed of 59 related cell surface receptors and has been classified based on their primary structure, ligand affinity and induced biological responsive properties (Schlessinger, 2000; Fantl et al., 1993). These membrane spanning cell surface RTKs fall into several subfamilies or categories: (1) the Epidermal Growth Factor Receptors (EGFRs or ErbBs), (2) the Fibroblast Growth Factor Receptors (FGFRs), (3) the Insulin and the Insulin-like Growth Factor Receptors (IRs or IGFR), (4) the Platelet-derived Growth Factor Receptors (PDGFRs), (5) the Vascular Endothelial Growth Factor Receptors (VEGFRs), (6) the Hepatocyte Growth Factor Receptors (HGFRs), and (7) the Nerve Growth Factor Receptors (NGFRs) (Stuttfeld and Ballmer, 2009; Cotton et al., 2008; Mukherjee et al., 2006).

All RTKs are structurally similar and contain 4 domains: (1) an extra-cellular ligand binding domain, (2) a single-pass transmembrane domain, (3) a conserved tyrosine kinase domain, and (4) a regulatory carboxyl-terminal tail harboring several tyrosine autophosphorylation or transphosphorylation sites (Hynes and Stern, 1994). Small organic molecules, such as lipids, carbohydrates, peptides and proteins act as the ligands for RTKs (Swain and Baselga, 2009; Schlessinger and Lemmon, 2006; Schlessinger, 2000). Upon ligand binding, RTKs become active through a lateral dimerization in the plasma membrane (Schlessinger, 2000). The RTK transmembrane dimer interface contains the critical structural information that positions the catalytic domains in such a way that they can phosphorylate each other (Li and Hristova, 2006). The phosphorylated RTKs catalyze the transfer of γ-phosphate of ATP to hydroxyl groups of tyrosines on

target proteins to activate and relay the signals (Fig. 1.1). In the dimer, the kinase domain interaction is asymmetrical, with the amino-terminal lobe of one tyrosine kinase interacting with the carboxyl-terminal lobe of the other (Kuriyan et al., 2006). Apart from the insulin and the insulin-like growth factor receptors, all RTKs exist in monomer-dimer equilibrium in normal, non-malignant cells (Li and Hristova, 2006).

1.2 RTK signaling specificity

The signal competent RTKs contain multiple pTyr residues in the carboxyl terminal to bind specific second messenger or adaptor proteins containing the modular Src homology 2 (SH2) or protein tyrosine binding (PTB) domains (Liu et al., 2006; Schlessinger and Lemmon, 2006; Pawson and Nash, 2000). Second messenger proteins, including kinases, phosphatases or phospholipases induce the signaling 'cascades' and transduce a growth or differentiating signal to the nucleus. Adaptor proteins, on the other hand, act as intermediates linking the activated RTKs with the second messenger proteins (Bradshaw and Waksman, 2002; Schlessinger, 2000). For example, in the Ras-Raf-MAPKinase signaling cascade, adaptor proteins, such as Grb-2 or Shc, associate with activated RTKs through their SH2 domains and further recruit the second messenger protein-guanine nucleotide exchange factor, Son of Sevenless (Sos), through its SH3 domain.

Figure 1.1: Signal Transduction through Receptor Tyrosine Kinases (RTKs). Upon ligand binding, receptor tyrosine kinases aggregate and undergo autophosphorylation. Once a receptor is phosphorylated at tyrosine residues on the cytosolic tail, proteins with SH2 domains such as phospholipase C (PLC) and GRB2 bind to the receptor. The binding of adaptor protein, GRB2 causes the activation of Sos, a guanine-nucleotide release protein to which it binds. The second messenger molecule, Sos then causes the activation of the Ras protein by converting it to the Ras-GTP state from the Ras-GDP state. Activated Ras initiates a cascade of events that ultimately results in the activation of the transcription factors needed for cell growth and metabolism. (Permission of Garret and Grisham, 1998).

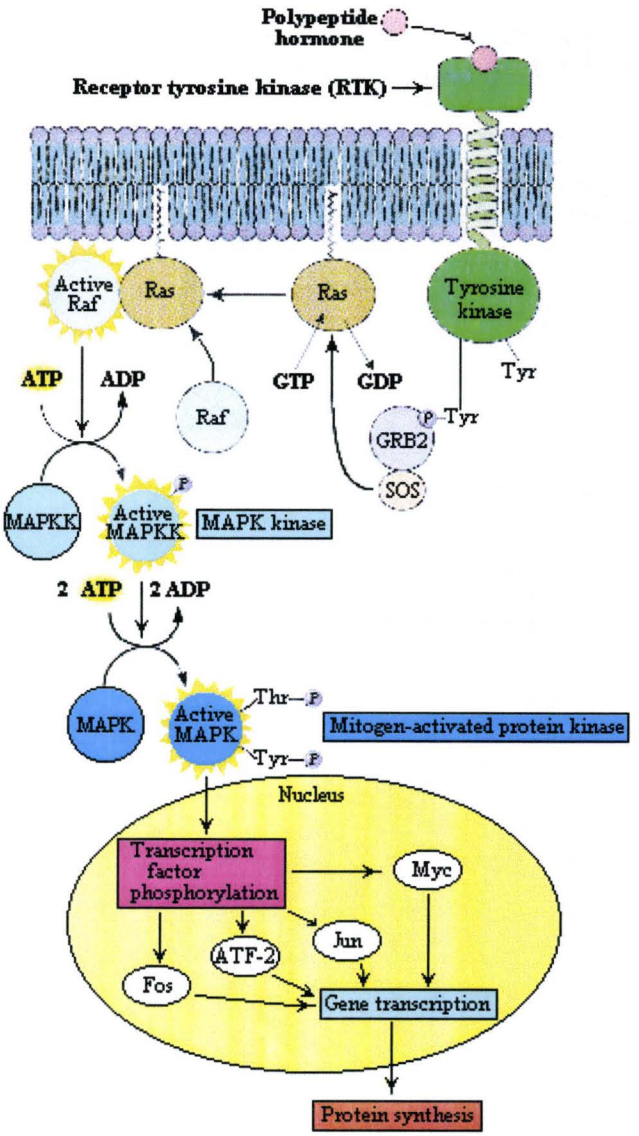
Polypeptide hormone
Receptor tyrosine kinase (RTK)
Active Raf
Ras
Ras
Tyrosine kinase
ATP
ADP
Raf
GTP
GDP
Tyr
GRB2
Tyr
SOS
MAPKK
Active MAPKK
MAPK kinase
2 ATP
2 ADP
MAPK
Active MAPK
Thr—P
Tyr—P
Mitogen-activated protein kinase
Nucleus
Transcription factor phosphorylation
Myc
Jun
ATF-2
Fos
Gene transcription
Protein synthesis

1.2.1 Site specific signaling

A large number of cytoplasmic or membrane bound SH2 domain-containing proteins possess intrinsic enzymatic activities. These activities include Protein Tyrosine Kinase- PTK activity (Src kinase), Protein Tyrosine Phosphatase-PTP activity (Shp2), Phospholipase C activity (PLC-γ), and Ras-GTPase activity (Ras-GAP) (Schlessinger, 2000). The multiple signaling outputs of RTKs primarily depend on their binding capabilities with different SH2-containing signaling and adaptor molecules at different phosphotyrosines (pTyr) on the RTK sites. For example, a site directed mutagenesis study with the platelet-derived growth factor receptor-β (PDGFR-β) found that the tyrosine residue at 1021 (Y1021) and at 740/751 (Y740/751) bind to PLC-γ and phosphatidylinositol-3-OH-kinase (PI-3K) respectively. These sites promote chemotaxis, whereas the tyrosine residue at 771 (Y771) that binds to GTPase activating protein (GAP) mediates suppression of migration (Kundra et al., 1994). In the fibroblast growth factor receptor (FGFR), the site that binds PLC-γ is required for phosphatidylinositol turnover and Ca^{2+} flux but not for mitogenesis (Mohammadi et al., 2002; Peters et al., 1992). Another study with the *Caenorhabditis elegans* epidermal growth factor receptor (EGFR) homologue, LET-23 found that six out of eight potential SH2-binding sites function for viability, vulval differentiation and fertility *in vivo* (Lesa and Sternberg, 1997). Three out of six sites were involved in viability and vulval differentiation. The 4^{th} site induced wild-type fertility, while the 5^{th} one mediated all three above-mentioned LET-23 functions. However, the 6^{th} site mediated tissue specific negative regulation.

Taken together, all these data suggest that the putative SH2 binding sites function in non-equivalent manner *in vivo*.

1.2.2 Tissue and context specific signaling

RTK tissue specificity is regulated by at least two independent factors *in vivo*: (1) by tissue specific effectors and (2) by tissue specific regulators. Depending on the cellular contexts or developmental stages, these effectors and regulators are thought to trigger either activation or repression of gene expression to initiate and control distinct signaling pathways, resulting in different cellular responses (Swain and Baselga, 2009; Roch et al, 2002; Simon, 2002; Schlessinger and Ullrich, 1992). For example, during early embryonic development, FGFR1 is required for cell migration in mesodermal patterning and gastrulation (Sahni et al., 1999). On the other hand, FGFR1 is required for cell proliferation in fibroblasts and for cell survival and differentiation in neuronal cells. Moreover, a novel direct RTK signaling pathway is involved in several types of human cancers and primary tumor cells. For instance, the activated EGF-EGFR complex translocates to the nucleus through the signal transducers and activators of transcription (STAT). A higher level of EGFR was found in the nuclei of cancer and primary tumor cells of skin, breast, bladder, cervix, adrenocorticord, thyroid and oral cavity (Lo et al., 2005; Bourguignon et al., 2002; Marti et al., 2001; Lin et al., 2001; Lipponen and Eskelinen, 1994; Kamio et al., 1990).

1.3 Vertebrate family of EGF receptors (EGFRs)

The vertebrate Epidermal Growth Factor Receptor subfamily has four members: (1) EGFR/ErbB-1, (2) ErbB2/Neu, (3) ErbB3, and (4) ErbB4. These ErbB members share a single-pass transmembrane helix flanked by an extracellular ligand binding domain and a cytoplasmic C-terminal domain that harbours a conserved but not equally functional tyrosine kinase domain (Schlessinger, 2000). The ligands for these ErbB receptors share an EGF-like domain of approximately 60 amino acids and are required and sufficient for the ErbB activation (Barbacci et al., 1995). The ligands that bind to ErbB1/EGFR are: Epidermal Growth Factor (EGF), Heparin binding EGF-like growth factor (HB-EGF), transforming growth factor-α (TGF-α), epiregulin, amphiregulin and betacellulin (reviewed by Ranson, 2004). Neuregulins (NRG) are the ligands for ErbB3 and ErbB4 (Stove and Bracke, 2004). Interestingly, ErbB2 has no reported ligand and ErbB3 lacks intrinsic kinase activity (Fig. 1.2). The functionally distinct ErbB2 and ErbB3 receptors are the preferred heterodimeric partners for other ErbB receptors (Beerli et al., 1995).

ErbB receptors have been implicated in many, perhaps in all, of the fundamental developmental processes, including cell-growth, proliferation, differentiation, survival and migration. The loss of ErbB result in deleterious effects in the embryos of 'knock-out' mice (Riethmacher et al., 1997). For example, ErbB2/ErbB3-deficient mice resulted in a hypoplastic development of the sympathetic nervous system, while ErbB2/ErbB4-deficient mice have malformation of cardiac ventricular trabecules (Britsch et al., 1998; Gassmann et al., 1995; Lee et al., 1995).

Figure 1.2: Key-signaling pathways activated by the ErbB2-ErbB3 hetero-dimers in human cancers. The most widely known and best-characterized Ras signaling pathways include MAPK-ERK, the MAPK-JNK and p38 pathways. Ras-MAPKinase signaling promotes proliferation, while signaling through the PI3K-Akt pathway leads to several cellular end points, such as cell-survival and anti-apoptosis. The kinase domain interaction is asymmetrical. The amino-terminal lobe of one tyrosine kinase interacts with the Carboxyl-terminal of the other. GSK3, glycogen synthase kinase3; NF-B, nuclear factor-B; PDK1, pyruvate dehydrogenase kinase 1; PIP2, phosphatidylinositol biphosphate; PIP3, phosphatidylinositol triphosphate. (Permission of Swain and Baselga, 2009).

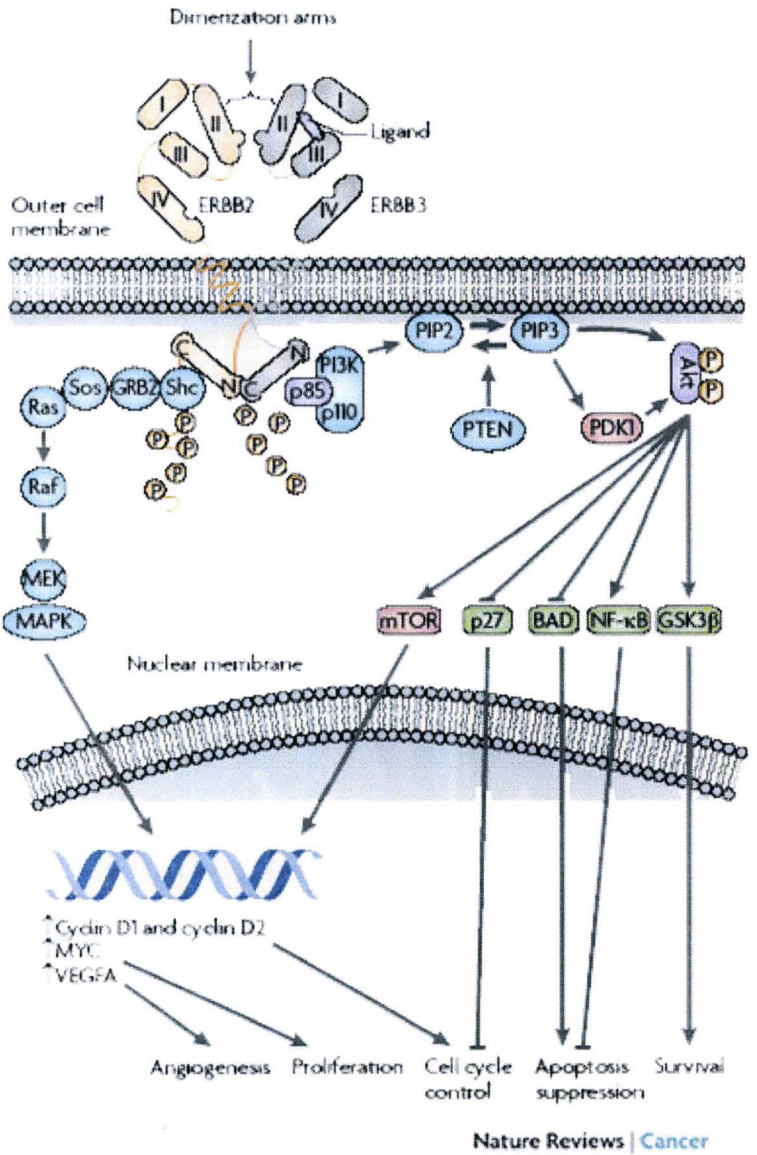
Dimerization arms
Ligand
Outer cell membrane
ERBB2
ERBB3
PIP2
PIP3
PI3K
p85
p110
PTEN
PDK1
AKT
Ras
Sos
GRB2
Shc
Raf
MEK
MAPK
mTOR
p27
BAD
NF-κB
GSK3β
Nuclear membrane
Cyclin D1 and cyclin D2
MYC
VEGFA
Angiogenesis
Proliferation
Cell cycle control
Apoptosis suppression
Survival
Nature Reviews | Cancer

1.4 Signaling by ErbB2/Neu

All RTKs comprise with 4 highly conserved domains (Hynes and Stern, 1994). The deregulated functions of each of these conserved domains have been implicated in various types of cancers, including human breast, lung, and ovarian cancers (Kuriyan et al., 2006; Li and Hristova, 2006). Therefore, in order to better understand the roles of ErbB2 in human carcinomas, it is of prime importance to better understand the structural and functional characteristics of each of these domains.

1.4.1 The extra-cellular domain

Crystal structure analysis has revealed an 'auto-inhibited' domain in the extra-cellular region in EGFR/ErbB1, ErbB3 and ErbB4. In contrast, the oncogenic version of ErbB2, even without a ligand, can transform cells when simply over-expressed (Di Fiore et al, 1987). Four domains (I- IV) in the extra-cellular region, are believed to render this orphan receptor an 'auto-activated' configuration. This constitutive conformation enables the receptor to form signaling-competent hetero or homo-dimers (Citri et al., 2003). Recently, crystal structure analysis revealed that the extra-cellular region of human ErbB2 resembles the extended form of ligand bound *Drosophila*-EGFR (DER) (Alvarado et al., 2009).

1.4.2 The transmembrane span

The transmembrane (TM) domain plays critical roles in RTK activation and in disease development (Li and Hristova, 2006). It is believed that the RTK TM dimer

interface contains the critical structural information that positions the catalytic domains in such a way that they can phosphorylate each other. Therefore, the substitution of the TM

Table 1: Pathogenic/Constitutive active ErbB2 TM Domain Mutations

Rat-ErbB2	Val664Glu	Overactivation of Receptor	Schechter et al., 1984 Bargmann et al., 1986
Rat-ErbB2	Val664Gln	Overactivation of Receptor	Bargmann and Weinberg, 1998
Rat-ErbB2	Val659Gln	Overactivation of Receptor. Oncogenic When introduced into Human ErbB2	Fleishman and Schessinger, 2002
Human ErbB2	Ile654Val	Increased risk of Breast cancers	Frank et al., 2005.

domain of one RTK into another RTK produces an active receptor. For instance, the insertion of the TM domain of activated Neu (NeuT) into the PDGFR-β receptor led to constitutive activation of the chimeric receptor (Bell et al., 2000; Petti et al., 1998).

Mutations in the TM domains are believed to cause receptor over-activation by stabilizing the RTK dimer (Webster and Donoghue, 1996). A point mutation was found in the oncogenic version of the rat homologue of ErbB2 (NeuT). Over activation of this oncogenic receptor was found to be the result of a Val664Glu mutation in its TM domain (Bargmann et al., 1986; Schechter et al., 1984). Several other point mutations in the TM domain were reported to have various oncogenic properties (Table 1). Specially, the Ile654Val mutation in ErbB2 is associated with an increased risk of breast cancers (Frank et al., 2005).

1.4.3 The cytoplasmic domain

The C-terminus docking domain of ErbB2/Neu contains five individual tyrosine (Tyr) phosphorylation sites. Four of these Tyr in rat-NeuT contributed to cell transformation with cultured ratl fibroblasts (Dankort et al., 1997). The transforming ability was attributed to the phosphotyrosines (pTyr) binding with either GRB2 or Shc. However, *in vivo* experiments with genetically modified mice showed that signaling through Grb-2 alone result higher rate of metastasis than signaling through Shc alone (Dankort et al., 2001).

1.5 ErbB2 in tumorigenesis

The downstream signaling pathways and ultimate signaling outputs of the ErbB receptor tyrosine kinases mostly depend on the activating ligand and the hetero-dimer partner (Yarden and Sliwkowski, 2001). The signaling potency of the hetero-dimers is regarded to be stronger than that of homo-dimers. The ErbB hetero-dimers comprising from EGFR, ErbB2 and ErbB3 have been implicated in the development and progression of cancer. However, the role of ErbB4 (HER4) in oncogenesis remains less well defined. Recent studies suggest that this receptor might be involved in signaling for cell growth inhibition rather than proliferation (Feng et al., 2007). The over-expression of ErbB hetero-dimers have been reported in various human cancers, including breast, ovarian, lung and prostrate cancer (reviewed in Baselga and Swain, 2009). However, the ErbB2-ErbB3 hetero-dimers are classified as the most potent oncogenic signaling unit with respect to interaction-strength, ligand-induced tyrosine phosphorylation and downstream

signaling with the combined mitogenic and anti-apoptotic cues (Citri et al., 2003; Tzahar et al., 1996; Pinkas-Kraamarski et al., 1996). In human breast cancer, for instance, the expression of ERBB2 molecules of tumor cells exceeds than that of the normal cells by at least 100 fold and facilitates the formation of hetero-dimers and homo-dimers that ultimately results in tumor cell survival and proliferation (Perez and Baweja, 2008; Yarden and Sliwkwoski, 2001).

The hetero-dimers of the ErbB receptor tyrosine kinases signal through canonical Ras-Raf-MAPK cassettes for tumor cell proliferation and through the PI3K-Akt/PKB pathway for tumor cell survival, apoptosis and programmed cell death suppression (reviewed in Baselga and Swain, 2009; Kuriyan et al., 2006; Li and Hristova, 2006). In normal cells, Akt activation is inhibited by the tumor suppressor PTEN phosphatase, which dephosphorylates Phospatidylinositol-3,4,5-triphosphate (PI3-K). In tumor cells, on the other hand, the activation and phosphorylation of ErbB3 facilitates the transformation of Phosphatidylinositol-4,5-bisphosphate (PIP2) to Phosphatidylinositol 3,4,5-triphosphate (PIP3). PIP3 then recruits the serine-threonine kinase, Akt to the plasma membrane through its Plekstrin homology (PH) domain. Upon phosphorylation by pyruvate dehydrogenase kinase1 (PDK1), the activated Akt directly phosphorylates critical regulators of the cell cycle progression and apoptosis, including P21, P27 and MDM2 (Kumar and Hung, 2005; Li et al., 2002; Zhou et al., 2001).

Akt promotes tumor cell survival by removing cell cycle checkpoints and apoptosis. De-regulated PI3K-Akt pathway contributes to an aggressive type of human breast cancers. Specifically, the phosphorylation of Thr145 of p21, a potent inhibitor

CDK2 (Cyclin dependent Kinase 2) and of Thr157 of p27, another negative G1 regulator, results in p27 cytoplasmic retention and nuclear export. In human breast cancers, cytoplasmic phosphorylated p21 has been associated with anti-apoptotic function, enhanced tumor survival and poor clinical outcomes (Xia et al., 2004; Clark, 2003; Huang et al., 2003; Liang et al., 2002; Shin et al., 2002; Viglietto et al., 2002; Winters et al., 2001; Zhou et al, 2001). Moreover, Akt negatively regulates the tumor suppressor, p53 by phosphorylating at Ser 166/186 of MDM2, which associates with p300 and ultimately degrades p53 (Zhou et al., 2001; Rossig et al., 2001). On the other hand, it has been shown that the failure of RTKs to be appropriately deactivated may be a cause of neoplastic growth (Dikic and Giordano, 2003).

1.6 RTK down regulation

In order to maintain an appropriate level of developmental signaling, the activity of each RTK must be tightly regulated for appropriate attenuation and termination of RTK-mediated signal. The mechanisms through which cells accomplish RTK attenuation include: (1) autoinhibition mediated by the extra-cellular or the catalytic domains, (2) antagonistic ligands, (3) hetero-oligomerization with kinase inactive mutant receptors, (4) inhibition by phosphatases, (5) receptor endocytosis and degradation (Schlessinger, 2003, 2000). Among all, the key mechanism of RTK signal termination represents the involvement of endocytosis and lysosomal degradation (Dikic, 2003).

1.6.1 Endocytosis and RTKs downregulation

Endocytosis controls the amount of receptors available in the plasma membrane, whereas the activated receptor signaling controls endocytosis (Sorkin and von Zastrow, 2009). Endocytosis is stimulated by ligand-induced activation leading to the capture of ligand bound transmembrane proteins into cytoplasmic vesicles (Sadowski et al., 2008; von Zastrow and Sorkin, 2007; Mukherjee et al., 2006). Endocytosis is mediated either by clathrin-dependent (CDE) or clathrin-independent (CIE) mechanism. In clathrin-dependent endocytosis, receptors are recruited to clathrin-coated pits by directly interacting with the clathrin coat adaptor complex, AP2 or by binding to other adaptor proteins, such as Epsin, epidermal growth factor receptor substrate 15 (Eps 15) and Dishevelled (Yu et al., 2007; Brett and Traub 2006; Sorkin, 2004). However, during this internalization process, many signaling receptors, such as EGFR and PDGFR are themselves modified by ubiquitylation (Oved et al., 2006; Marmor and Yaden, 2004). The E3 ubiquitin ligases, such as Casitas B lineage lymphoma (CBL), are recruited to the activated receptor directly or through an intermediate adaptor, such as GRB2 in case of EGFR and MET receptor (Borgne et al., 2005).

The Clathrin-coated pits invaginate inwards and pinch off from the plasma membrane (Fig. 1.3). The formation of cytoplasmic pits requires the GTPase dynamin, such as *Shibire* and *Expanded*, and Endophilin (Chen et al., 2002; Di Camilli et al., 1995). The shredded Clathrin coat is recycled for another round of transport, while the uncoated vesicles fuse together to form new endosomes, or fuse with pre-existing early endosomes (EE), called sorting endosomes. The formation of EE requires the small

Figure 1.3: Mechanism of endocytotic downregulation of RTKs. The figure shows that after internalization clathrin pits are recycled for another round of transport, the uncoated vesicles fuse together to form new endosomes, or fuse with pre-existing early (sorting) endosomes, a process that is partly controlled by the small GTPase Rab5 and its effectors. At the early endosomes, the ubiquitinated RTK is sorted into a 'bilayered' clathrin coat, probably by associating with ubiquitin-binding proteins such as Hrs and STAM. From here receptor-bound ligands are then transported to and degraded in the Rab7 present late endosomes or lysosomes. Intraluminal vesicles with their content are then degraded by lysosomal hydrolases. (Permission of Gould and Lippincott-Schwartz, 2009).

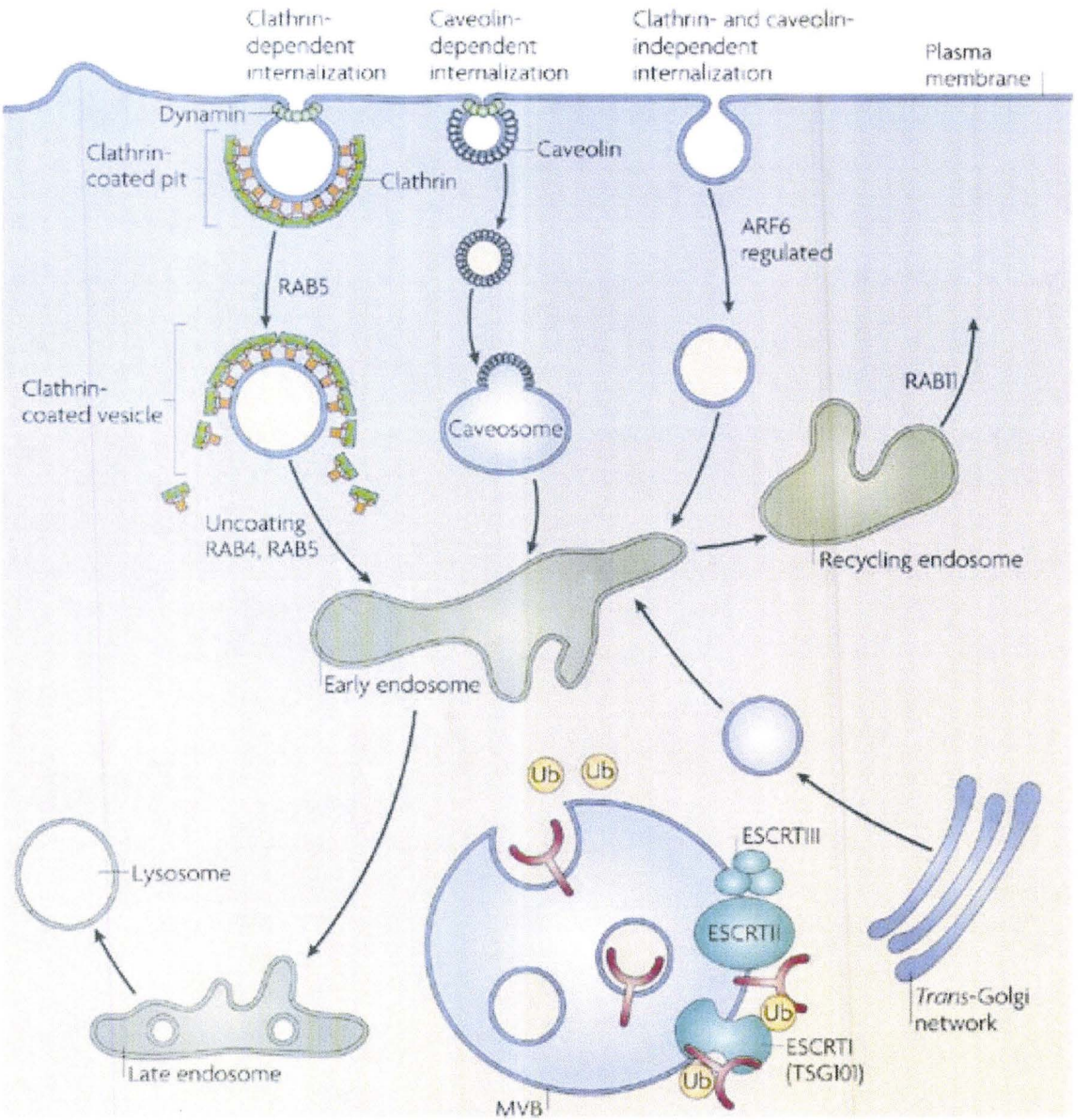

Nature Reviews | Molecular Cell Biology

GTPase, such as Rab5 and its effectors, including Rabaptin-5 and EEA1 (Zerial and McBride, 2001). Internalized receptors either rapidly recycle back to the plasma membrane or remain in the endosome, which mature into multivesicularbodies (MVBs) and late endosomes (LE). At the early endosomes, the ubiquitylated RTK is sorted into a 'bilayered' clathrin coat, probably by associating with ubiquitin-binding proteins such as Hsr and STAM (Raiborg et al., 2009; Bache et al., 2003; Kanazawa et al., 2003; Katzmann et al., 2002).

The recyclable receptors rapidly traffic to the Rab11 containing compartment and recycle back to the plasma membrane in a Rab4 dependent manner (reviewed in Raiborg and Stenmark, 2009; Nickerson et al., 2007). The remaining portions of RTKs are then sorted into intraluminal vesicles of the endosome, in a process mediated by endosomal sorting complex required for transport (ESCRT) (reviewed in Hanson et al., 2009; Raiborg and Stenmark, 2009; Nickerson et al., 2007). The receptor-bound ligands present in the sorting endosomes are then transported to and degraded in the Rab7 containing late endosomes or lysosomes. The intraluminal vesicles, with their contents, are then degraded by lysosomal hydrolases (Bright et al., 2005; Gruenberg and Stenmark, 2004).

Recent studies provide evidence that the endocytic machinery is disrupted in certain types of cancer (Ande et al., 2009). There is a growing list of regulators of RTK downregulation associated with cancers (See Table 2.1 in Result section). For example, mutations in Hip1 (End4/Sla2), c-Cbl and Tsg101 (Subunit of mammalian ESCRT-1) have been identified in human cancers (Gruenberg and Stenmark, 2004; Hyun and Ross, 2004; Shtiegman and Yarden, 2003; Peschard and Park, 2003; Dikic and Giordano, 2003

and Li and Cohen, 1996). Moreover, genes encoding some of the proteins that participate directly in the clathrin-coat formation, during the initial steps of endocytosis, have been identified as targets of chromosomal rearrangements in human haematopoietic malignancies. For example, Eps15 and Endophilin-2 (SH3p8) were fused to ALL1/HRX genes due to chromosomal translocation (Floyd and De Camilli, 1998).

However, there has been very little effort in evaluating these endocytotic components in vivo. *Drosophila* is a good model to genetically evaluate the interaction of various endocytotic components and DER, the EGFR homolog required for multiple roles during eye development.

1.7 Roles of DEgfr during the *Drosophila* development

Drosophila EGFR (DER) functions in almost all fundamental biological processes, such as cell proliferation, differentiation, survival, and apoptosis-suppression (Shilo, 2003). Although humans have 4 ErbB receptor tyrosine kinases, *Drosophila* and *C. elegans* have only one EGF receptor. The *Drosophila* epidermal receptor tyrosine kinase, DER was isolated and cloned in a screen to identify homolog of chicken v-ErbB in the *Drosophila* genome (Livneh et al., 1985). Later, DER was shown to be sufficient to induce ectopic differentiation in the developing eye (Doroquez and Rebay, 2006; Rodrigues et al., 2005; Shilo, 2003; Kumar et al., 2003; Yang an Baker, 2003; Kumar and Moses, 2001; Lesokhin et al., 1999; Kumar et al., 1998). Four activating and one inhibiting ligand have been identified for DER. These ligands include: (1) the Neuregulin: Vein, (2) the TGF- ligands: Spitz, Karen and Gurken, and (3) the repressive

ligand: Argos (Shilo, 2003; Reich and Shilo, 2002; Riese and Stern, 1998; Sawamoto et al., 1996; Schnepp et al., 1996; Schweitzer et al., 1995; Kumar et al., 1995; Freeman, 1994; Sawamoto et al.,1994; Neuman-Silberberg and Schupbach, 1993; Rutledge et al., 1992; Freeman et al., 1992).

DER is reiteratively used throughout the entire developmental process ranging from the adult abdominal dorsoventral patterning, wing vein determination and oogenesis (Shilo, 2005; Shilo, 2003). Vein is necessary for the patterning of the ventral ectoderm and specification of muscle precursors during embryogenesis (Shilo, 2003). The primary DER ligand, Spitz (Spi) is responsible for the DER activation in almost all tissues. For example, Spitz plays roles during the oogenesis, eye development and adult male spermatogenesis (Shilo, 2003). Moreover, DER suppresses apoptosis of midline glia (MG) cell lineages (Settle et al, 2003; Sonnenfeld and Jacobs, 1994) and provides cell proliferation and cell differentiation during eye development (Raz et al., 1991).

1.8 DER in *Drosophila* eye development

The *Drosophila* compound eye is composed of approximately 800-850 repetitive subunits called ommatidia. The ommatidia are arranged symmetrically with respect to the horizontal equator line to form a precise neurocrystalline lattice. Each ommatidium is composed of eight photoreceptors (R1-R8), four lens secreting cone cells, two primary (1°) pigment cells, and a hexagonal lattice of secondary (2°) and tertiary (3°) pigment cells and bristle cells shared by ommatidia (Fig. 1.4) (Wolff and Ready, 1993;

Figure 1.4: The Drosophila eye. (A) Scanning electron micrograph of the adult compound eye. (B) Tangential section and cartoon of the adult eye showing the hexagonal ommatidia and regular pigment cell lattice. The dark-stained light-sensing photoreceptor organelles, or rhabdomeres, are arranged in a trapezoidal pattern. R1-7 are shown in this section; R8 is located at lower section levels. (B, C) Ommatidia are arranged symmetrically with respect to the equator, such that R3 points up in the dorsal half, and points down in the ventral half. (Permission of Doroquez and Rebay, 2006).

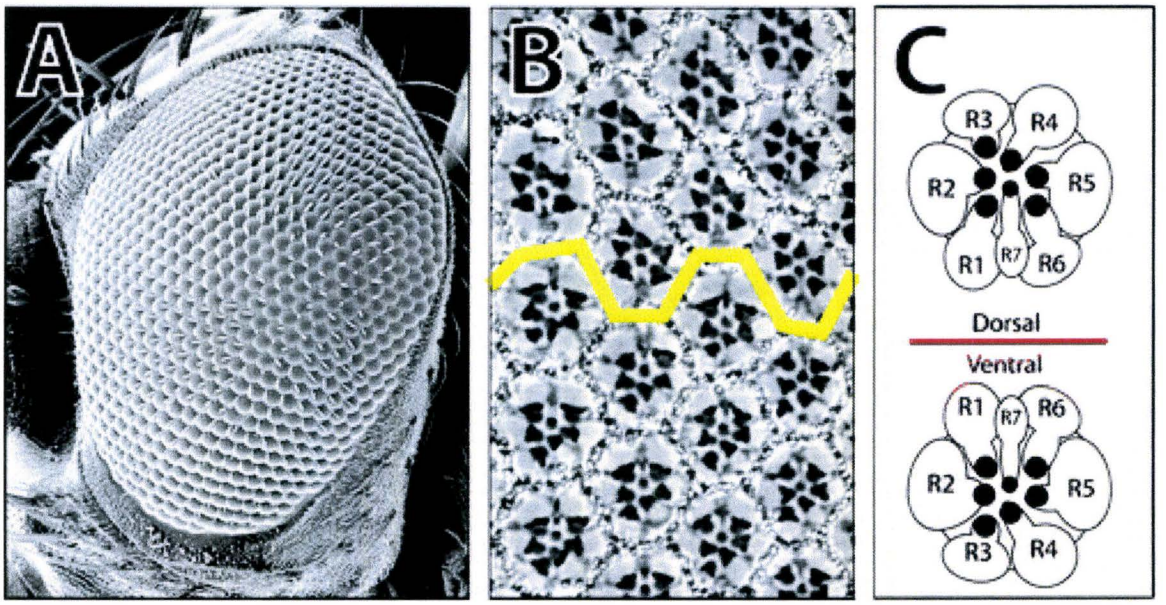
A
B
C
R3
R4
R2
R5
R1
R7
R6
Dorsal
Ventral
R1
R7
R6
R2
R5
R3
R4

Higashijima et al., 1992; Ready et al., 1976). The adult eye structure arises from columnar epithelial primordia, known as the eye-antennal imaginal disc. The disc undergoes extensive proliferation and patterning during larval and pupal stages (Cohen, 1993).

During early larval stages, the disc grows through unpatterned and asynchronous cell division (Wolff and Ready, 1993). At this stage, eye field specification occurs through the action of the retinal determination gene network (RDGN). The components of the RDGN function as master regulators and belong to a group of transcription factors, such as Twin of eyeless (Toy), Eyeless (Ey), Sine Oculis (So), Eyes absent (Eya), Eyegone (Eyg) and Dachshund (Dac) (Silver and Rebay, 2005; Dominguez and Casares, 2005; Pappu and Mardon, 2004). DER was initially thought to be involved in eye field specification. However, a DER independent hypothesis has been proposed (Kenyone et al., 2003). Following eye field specification, cell fate determination and differentiation occurs in a dramatic regulated fashion across the eye imaginal disc. During the late 3rd instar larval stage, an indentation in the eye imaginal disc, called the morphogenetic furrow (MF), is initiated and travels towards the anterior of the disc resulting in waves of cell specification in its wake (Wolff and Ready, 1993).

Cells anterior to the MF proliferate randomly, whereas specified and differentiated cells that comprise the ommatidium are recruited to the posterior of the MF (Wolff and Ready, 1993). In the differentiating cells, DER activates the basic helix-loop-helix (bHLH) transcription factor, Atonal (Ato) (Greenwood and Struhl, 1999; Baker et al., 1996; Jarman et al., 1995; 1994). DER is required (1) before initiation of the MF and

(2) for propagation of new ommatidial columns along the lateral margins of the disc (Kumar and Moses, 2001). Ato expression is then refined at the posterior of the MF to a single cell that gives rise the R8 founder cell (Baker, 2001; Baker et al., 1996; Dokucu et al., 1996; Jarman et al., 1994, 1995;). Ato refinement and restoration to the R8 cell are thought to occur through lateral inhibition by the concerted activities of Notch and the fibrinogen-related dimeric secreted glycoprotein Scabrous (Sca) (Lee et al., 1995; Baker and Zitron, 1995; Baker et al., 1990; Mlodzic et al., 1990).

Initially, DER was proposed to play a role in the specification of R8, as the hypermorphic DER Ellipse mutant (*Elp*) allele showed dramatic changes in ommatidial pre-cluster formation and loss of R8 differentiation (Baker and Rubin, 1989). However, the experiment with the mitotic clones showed that DER null homozygous clones, in comparison with the wildtype one, yielded very small clones but still having some R8 cells developed. This DER independent R8 cell development suggested that DER is required in cell proliferation and/or survival but not in R8 specification (Yang and Baker, 2003; Baonza et al., 2001; Lesokhin et al., 1999; Dominguez et al., 1998; Xu and Rubin, 1993). Following R8 specification or founder cell formation, the pair-wise recruitment of R2/5 and R3/4 is initiated (Ready et al., 1976). The undifferentiated cells that lie between the already differentiated photoreceptors cell clusters (R8, R2/5 and R3/4) return to the cell cycle for a synchronous and terminal cell division, called second mitotic wave (SMW). At this stage, the DER pathway with the cooperation of the cdc25 phosphatase, String (Stg) initiates G2/M transitions and give rise to R1/6, R7, cone and pigment cells (Baker and Yu 2001).

After Second Mitotic Wave, the R7 photoreceptor is the last photoreceptor to be recruited to the ommatidium. It develops through the orchestrated signaling by DER, the Sevenless (Sev) receptor tyrosine kinase and Notch (N). In brief, the R8 photoreceptor cell expresses the membrane bound ligand Bride-of-Sevenless (Boss) that binds to Sev and is transendocytosed into the R7 cell (Cagan et al., 1992; Krammer et al., 1991). This ligand-receptor interaction leads to RTK activation via trans and auto-phosphorylation on tyrosine residues and employs the Ras/MAPK cassettes to control the Sev-mediated R7 development (Gebelein et al., 2004; Rebay and Rubin, 1995; Biggs et al., 1994; Brunner et al., 1994; Olivier et al., 1993; Simon et al., 1993; Dickson et al., 1992; Fortini et al., 1992; Simon et al., 1991). The combined activity of DER and Sev dismantle the repressor activity of the transcription repressor factor- Tramtrack88 (Ttk88) and Yan over the homeodomain transcription factor Prospero (pros), ultimately inducing R7 cell fate (Xu et al., 2000; Kauffmann et al., 1996). The RTK pathway effectors, Pointed (Pnt) and the Ets transcription factor Lozenge (Lz), activate the expression of *prospero* in the R7 determining cell (Xu et al., 2000). The other remaining 4 cells in the cluster take the cone cell fate, which is induced by the *Drosophila* homolog of the vertebrate Pax2 gene, dPax2 through a combinatorial effect of the DER and Notch signaling pathways (Flores et al., 2000; Daga et al., 1996).

Following the R cell and cone cell determination, the pigment and sensory bristles are determined from the pool of undifferentiated cells in the *Drosophila* eye discs. This final stage of ommatidial patterning involves the tight coordination of signaling between cell survival and apoptosis, the programmed cell death (PCD) (Twomey and McCarthy,

2005; Hay et al., 2004; Brachmann and Cagan, 2003; Rusconi et al., 2000; Steller and Grether, 1994). Finally, pigment cells differentiate during the late stage of pupal development. The remaining interommatidial undifferentiated cells then undergo PCD through a combinatorial action of DER and Notch signaling pathway (Hay et al., 1994; Wolff and Ready, 1991; Ready et al., 1976). Failure of PCD results in unnecessary cells that perturb the ommatidial lattice structure leading to a malformed adult eye (Baker et al,, 2001; Rusconi et al., 2000). In another set of experiments, the temperature sensitive Notch (N^{ts}) allele, in restrictive temperature, resulted in supernumerary 2° cells due to the loss of PCD (Cagan and Ready, 1989). DER activation leads to MAPK phosphorylation and downregulation of pro-apoptotic protein Head Involution defective (Hid) and thereby preventing PCD (Bergmann et al., 1998; Kurada and White, 1998). Similarly, loss of DER activity in the interommatidial precursor cell (IPC) resulted in the loss of 2°/3° pigment cells and increased cell death (Miller and Cagan, 1998; Freeman, 1996).

It has been shown that expression of rat-Neu/ErbB2 renders effects similar to the activated *Drosophila*-DER eye phenotype (Settle et al., 2003), suggesting that this vertebrate RTK co-opts endogenous second messengers. Therefore, Drosophila eye development is a suitable genetic model system for studying rat-*Neu* signaling *in vivo*.

1.9 Previous studies with the transgenic Neu

The identification of pTyr outputs of the ErbB receptors is largely established by the data from peptide inhibition, phosphotyrosine labeling and protein co-immunoprecipitation experiments *in vitro* (reviewed by Lemmon 2009; Schlessinger,

2002; Pawson and Nash, 2000). The data from these *in vitro* experiments, therefore, must be validated by functional assessment *in vivo*. *In vivo* experiments reveal more functional distinctions of different pTyr outputs (Sundaram, 2006; Dankort et al., 2001; Lesa and Sternberg, 1997). The structure and function of many SH2/PTB proteins in signaling is conserved in model organisms like *Caenorhabditis elegans* and *Drosophila*. For example, human GRB2 (Growth factor Receptor Binding 2) and *C. elegans* SEM-5 share an identical architecture of SH2 and SH3 domains and 58% amino acid sequence identity (Moghal and Sternberg, 2003; Worby and Margolis, 2000; Stern et al., 1993). It has also been shown that human GRB2 and *Drosophila* Drk (downstream of receptor kinase) can rescue *sem-5* function in *C. elegans* (Olivier et al., 1993; Simon et al., 1993). Moreover, the PTB and SH2 binding properties of *Drosophila*-Shc (Dshc) and mammalian-Shc are highly conserved (Guy et al., 2002; Lai et at., 1995).

The *Drosophila* epidermal growth factor receptor (DEgfr or DER) shares an overall 56% amino acid similarity with the rat-Neu/ErbB2. Sequence analysis between these two RTK receptors have shown that the highly conserved kinase domains account 79%, while the lowest conserved, C-terminal domains, contain 39% amino acid similarity (Settle et al., 2003). A conserved NPEYL motif (Neu-YC and ϕ-DEgfr) was found both in DER and Neu/ErbB2. Moreover, there is sequence conservation surrounding the pTyr at 1028 of ErbB2 (Neu^{YA}) and 1261 of DER (DEgfr-δ) (Fig. 1.5).

A number of studies have taken the advantage of the well-characterized signal transduction pathways in *Drosophila* to screen for proteins that interact with vertebrate

Figure 1.5: Structural comparison of rat Neu and the DEgfr. Neu and the DEgfr show an overall 56% sequence similarity. However, the kinase domain showed the highest 79% amino acid sequence similarity while the docking domain has the least 31% amino acid sequence similarity. Further sequence analysis showed that DEgfr shares an NPEYL sequence with Neu^{YC} (Y1201) and Neu^{YE} (Y1253). The other two protein binding sites have a high degree of conservation (compare DEgfr-δ and Neu^{YA}). (This figure is adapted from Dr. J.R. Jacobs).

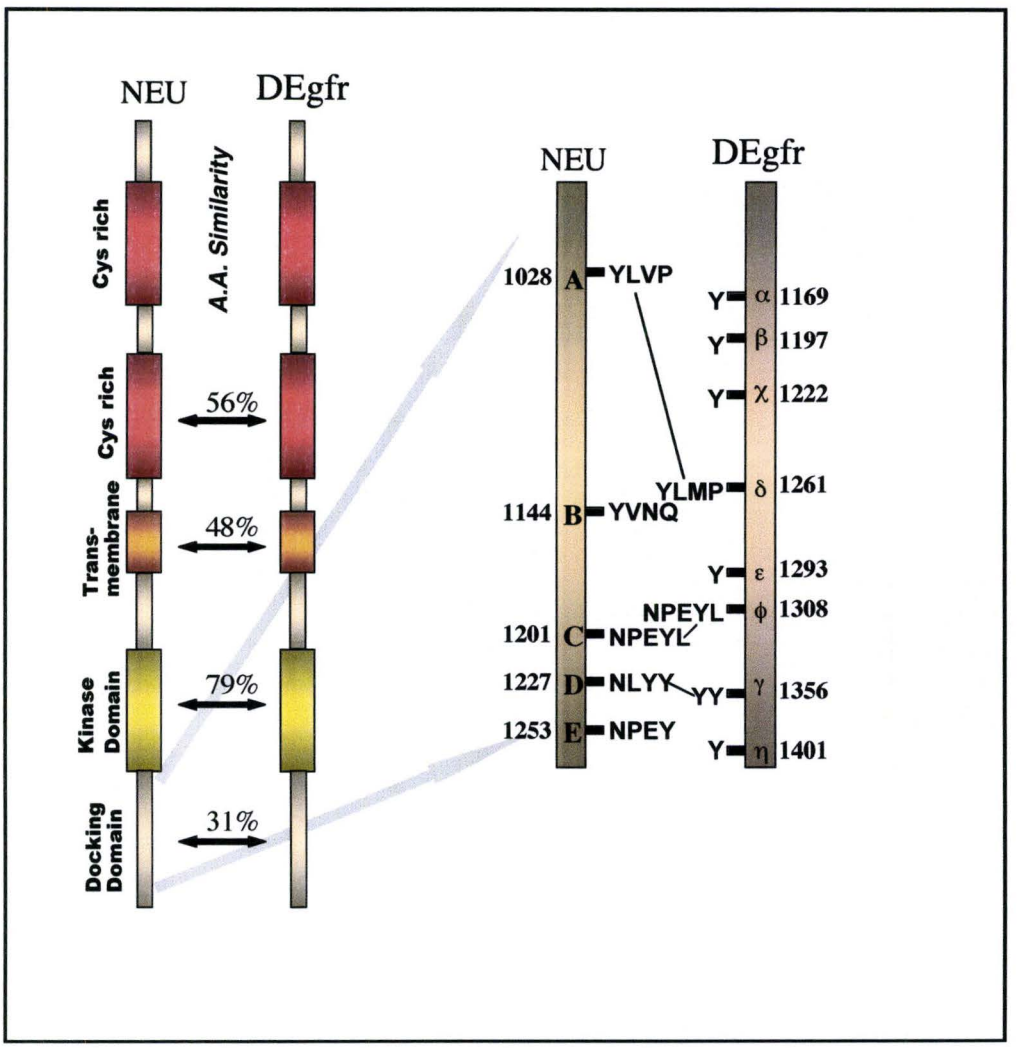
NEU
DEgfr
A.A. Similarity
Cys rich
Cys rich
Trans-membrane
Kinase Domain
Docking Domain
56%
48%
79%
31%
NEU
DEgfr
1028 A YLVP
1144 B YVNQ
1201 C NPEYL
1227 D NLYY
1253 E NPEY
YLMP
YY
Y α 1169
Y β 1197
Y χ 1222
δ 1261
Y ε 1293
NPEYL φ 1308
γ 1356
Y η 1401

transgenes (Jackson et al., 2002; Kazantsev et al., 2002; Rubinsztein, 2002; Bhandari and Shashindra, 2001). For example, human *Adenomatous polyposis coli (hAPC)* was successfully expressed in transgenic *Drosophila* and screened two components of Wnt/Wg signaling pathway (Bhandari and Shashindra, 2001). Apart from signaling conservations among model organisms, fly models have extensively been used not only to study human diseases, such as Alzheimer's, Parkinson's and Huntington but also to discover drugs, including ones targeting human heart diseases (Doumnis et al., 2009; Botella et al., 2009; Iijima and Iijima, 2009; Moloney et al., 2009; Akasaka and Ocorr, 2009; Ocorr et al., 2007; Bier and Bodmer, 2004). Moreover, the targeted misexpression system in *Drosophila*, using the *GAL4*-upstream activating sequence (*GAL4-UAS*) has made this organism more attractive to the geneticists and developmental biologists (Johnston, 2002; Brand and Perrimon, 1993). Using the appropriate 'enhancer-trap' GAL4 line, the misexpression of any particular gene can be done in cell and tissue specific manner (Brand and Perrimon, 1993).

Drosophila is genetically amenable and powerful model organism for efficient identification of signaling pathways *in vivo*. We previously showed that the adaptor binding sites of a vertebrate RTK, such as rat-Neu could successfully signal through the adaptor proteins in *Drosophila* (Settle et al., 2003). We found that activated Neu expression in the midline glia suppressed apoptosis, a similar phenotype seen with the activated *Drosophila* EGFR expression. For this study, a constitutively active *Neu* allele (neu^{NT}) was generated by a Val664Glu mutation at the transmembrane region of the wildtype Neu/ErbB2. By substituting Phenylalanine for Tyrosine at the all known C-

terminal Phosphorylation sites (on Neu^{NT} background), a *Neu* Tyrosine Phosphorylation Deficient (Neu^{NYPD}), was made to evaluate the roles of pTyrs in the docking domain (Dankort et al., 1997). By adding back a single Tyr to each position, multiple Neu 'add-back' alleles were created to functionally identify the outputs of individual pTyr (Fig. 1.6) (Settle et al., 2003; Dankort et al., 1997). Using rat fibroblast as a model, Dankort et al. (1997) showed that four tyrosine-autophosphorylation sites (YB, YC, YD and YE) in the cytoplasmic tail of Neu/ErbB2 could transduce Neu-transforming signals *in vitro*.

Specifically, each functional autophosphorylation site on a constitutively active background, induced by a point mutation at the transmembrane domain, was sufficient to mediate Neu-dependent transformation *in vitro*. Using eye and wing tissues, we have previously shown that the pTyr residues ('add-back' alleles) generated graded phenotypes- suitable for dosage sensitive modifier screen (Settle et al., 2003). By suppressing the ErbB2/Neu induced phenotypes in tissues haplo-sufficient for genes encoding for second messengers and adaptor proteins, we showed that YB, YC and YD required Grb2, Crk and Shc respectively. The requirement of distinct adaptor proteins for distinct pTyr suggested multiple effector pathways to promote transformation *in vitro* (Dankort et al., 1997).

Neu^{YA}, on the other hand, lacked the transforming ability in rat1 fibroblast (Dankort et al., 1997). Another study with 'knock-in mice' showed that YA (Erbb2-Y1028F) mutant could rescue the perinatal lethality in the hemizygous *Erbb2* animals and suggested that YA might provide an inhibitory role in ErbB2 signaling (Chan et al.,

Figure 1.6: Schematic representation of Neu receptor tyrosine kinase alleles. A point mutation (V664E) at the transmembrane domain was induced to generate the constitutive active, Neu^{NT}. Replacing all the tyrosine (Y)residues with phenylalanine (F) generated the Neu phosphorylation deficient, Neu^{NYPD}. In a NYPD background, the restoration of a single tyrosine at a particular residue generated the 'add-back' alleles: Neu^{YA} (1028), Neu^{YB} (1144), Neu^{YC} (1201), Neu^{YD} (1226/1227), and Neu^{YE} (1253).

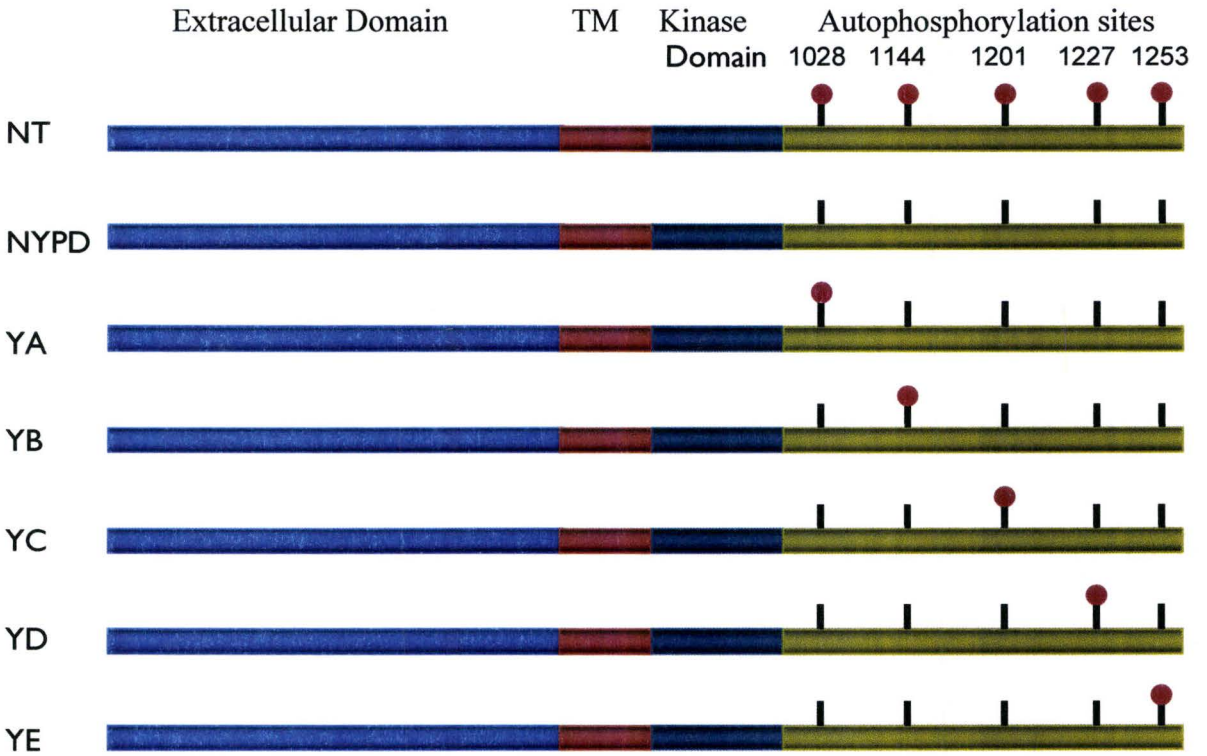
Extracellular Domain
TM
Kinase Domain
Autophosphorylation sites
1028
1144
1201
1227
1253
NT
NYPD
YA
YB
YC
YD
YE

2004). During my M.Sc. studies I found that while expressed in the *Drosophila* eye, Neu^{YA} showed a less strong phenotype than that of Neu^{NYPD} suggesting that Neu^{YA} might have an inhibitory role upon Neu^{NYPD}. Additionally, Neu^{YA} was able to attenuate the signaling outputs from other pTyrs of Neu/ErbB2 (Hossain, 2005: Msc. Thesis).

Therefore, we hypothesized that Neu^{YA} might have an inhibitory role in RTK signaling and may interact with RTK signal attenuating pathways, such as Receptor mediated endocytosis and degradation. The Misexpression of *Neu* 'add-back' alleles generates graded phenotype and is suitable for dosage sensitive modifier genetics. For example, a genetic screen in tissues haplo-sufficient for genes encoding various components of receptor endocytosis and degradation pathways would verify the role of Neu^{YA} or others ('add-back' alleles) in these processes. Moreover, a genome wide modifier screen of 'double add-back' allele, such as Neu^{YAE} would serve to identify gene(s) required for Neu^{YA}, Neu^{YE} and Neu^{NYPD} as well as in signaling in *Drosophila.* Taken together, the candidate gene(s) will not only allow us to verify the role of Neu^{YA} signaling in *Drosophila* but also to decipher the pathways of Neu^{YA}, Neu^{YE} and Neu^{NYPD} function *in vivo.*

1.10 Large scale genetic screening

The short generation time and large number of progeny have made *Drosophila melanogaster* one of the best model systems for performing large-scale genetic screening for mutations that affect a given process. The large-scale genetic screening of Neu^{YA} would identify potentially all the candidates required for Neu^{YA} function in *Drosophila.*

The candidates could therefore, be used to reveal their mammalian homologues and orthologues. Dominant modifier screening is the most commonly used, as it allows the identification of the candidate genes by virtue of enhancement or suppression of the control phenotype in the F1 generation. In this screen, the modifiers specific to only Neu^{YA} will be identified either as the suppressors or enhancers. The YA-specific suppressors and enhancers can be categorized as the positive and negative regulators respectively. In fact, dominant modifier screens were undertaken to identify the novel components of several signal transduction pathways, such as the Ras-MAPKinase 'cascades' and Sevenless signaling components (Dickson et al., 1996; Simon et al., 1993).

On the other hand, the classic screens, involving mutations affecting the genes of a given process, have been used to identify the regulators of various development processes. For instance, forward genetics revealed the genes that control embryo segmentation and nervous system development (Seeger et al., 1993; Nusslein-Volhard and Wieschaus, 1980). Moreover, it is now possible to screen for mutant phenotypes in virtually any cell and at any developmental stage by performing a mosaic clonal screen using the yeast Flp/FRT recombination system to generate mitotic clones. These clonal cells are homozygous for a particular mutagenized chromosome arm (Xu and Rubin, 1993). This scheme is very useful to screen for potential lethal interactions.

The most common mutagens used in *Drosophila* are *P*-elements and chemicals, such as Ethyl Methanesulfonate (EMS). *P*-elements are transposable elements that generate mutations by inserting themselves into the genes (Mullins et al., 1989; O'Hare

and Rubin, 1983). However, they are inefficient mutagens due to the fact that the majority of *Drosophila* genes are predicted to be 'cold spots' for *P*-element insertion. This property makes *P*-elements relatively poor mutagens for saturation screens that set out to identify most of the genes required for a particular process (Spralding et al., 1999; Ashburner et al., 1999). In contrast, chemical mutagens can generate mutations more efficiently and have no bias in causing mutations in different loci (reviewed in Martin et al., 2001). However, it has been estimated that over 66% of *Drosophila* genes are phenotypically silent when mutated to a loss of function and hence would not be possible to be identified in conventional genetic screens (Miklos and Rubin, 1996).

EMS, a mono functional alkylating agent and the mostly used chemical mutagen, produces point mutations by attacking (ethylation) the *O*-6 position of guanine and the *O*-4 position of thymine. This mutation allows mis-pairing with thymine and guanine resulting in G:C to A:T and T:A to C:G transitions respectively (Kreig, 1963). EMS also produces small deletions and occasionally other rearrangements as well. This mutagen works in a concentration dependent manner, meaning that the higher EMS concentration the higher the mutation rate. A higher mutation rate in the X-chromosome would result with higher X-linked lethality. It is established that approximately 30% of X-linked lethality indicates one hit per autosome on average or one hit in 2000 to 5000 for most loci (Roberts, DB, 2003, Drosophila, 2nd edition, Oxford University press, pp 56-57). Primarily, a single hit mutation is aimed to assess the consequences caused by a single gene at a time.

The mutations can be mapped molecularly either by Restriction Fragment Length Polymorphism (RFLP) or Single Nucleotide Polymorphism (SNP) (Jakubowski and Kornfeld, 1999; Saiki et al., 1985). RFLP can map the mutations by the variation of DNA fragment after restriction digestion and is slow and cumbersome as it requires a large amount of sample DNA, probe labeling, DNA fragmentation, electrophoresis, blotting, hybridization, washing, and autoradiography. On the other hand, SNP mapping requires both genetic and molecular techniques to determine the position of the mutations in the recombinant chromosome (Jakubowaski and Kornfeld, 1999). SNP mapping is relatively faster than that of RFLP but is too expensive to be afforded by the most generously funded fly labs. Another approach, called shotgun sequencing had been used by the Human Genome Project (Venter et al., 1996). In brief, DNA is randomly broken into small segments (100 to 1000/2000 bp) and is cloned and sequenced using the chain termination method to obtain the 'reads'. Multiple overlapping reads, obtained from several round of fragmentation and sequencing, are fed into the computer program to assemble them into a continuous sequence (Venter et al., 1996). Shotgun DNA sequencing is may result in some gaps between contigs, as DNA fragment is made randomly. This DNA sequencing is suitable for genome wide sequencing.

However, two complementary approaches have been standard in mapping the point mutations: (1) mapping by meiotic recombination and (2) mapping by deletion mapping. Meiotic recombination involves the recombination of a mutant between two visible markers and can only give a statistical estimate of its position. Deletion mapping, on the other hand, positions the mutation by failing to complement with a particular

deficiency. Various other approaches have been available to refine the location of the gene, such as *P*-mediated male recombination (Chen et al., 1998), and the meiotic recombination between two *P*-elements that flank the region containing the mutation. The existing deficiency kits available at the Bloomington and Harvard stock centre cover almost 85% of the *Drosophila* genome and have made it possible to identify the candidates within a range of 10/20 gene spans. The single gene mutation can finally be verified with the available single gene mutant stocks or RNAi stocks available publicly.

1.11 Thesis objectives and outline

In this study, our specific aim is to determine the role and specificity of Neu^{YA} over RTKs and to identify the signaling pathways through which Neu^{YA} renders it functional entity. Specifically, we asked whether Neu^{YA} could attenuate RTK signaling in *Drosophila*. To test this hypothesis, we genetically tested the Neu^{YA} interactions with several UAS and mutant receptor alleles, including *Drosophila*-EGFR and Sevenless receptor tyrosine kinases. Our data shows that the pTyr at 1028 (YA) partially suppressed the eye phenotypes of DER gain-of-function, Elp^{B1} mutant, Sev-Torso chimera and all the *Neu* 'add-back' alleles, suggesting an inhibitory role in RTK attenuation. Moreover, a dosage sensitive modifier screen of Neu^{YA} for various components of RTK attenuating pathways, such as receptor-mediated endocytosis and lysosomal degradation, was undertaken to understand the potential RTK signaling down regulating mechanisms.

Finally, a dominant modifier screen of 'double add-back' Neu^{YAE} allele was undertaken to reveal the YA specific RTK attenuating components in *Drosophila*. EMS

treated flies were crossed with the *GMR-Neu*^{YAE}*,TM3/D* virgins. We screened over 60,000 F1 progeny either for suppression or enhancement of the rough eye phenotype as compared to control flies. We isolated and mapped several groups of suppressors and enhancers from a pool of 24 complementation groups spanning both the 2nd and 3rd chromosome. Here, we report the result of the genetic screen with first of a kind 'double add-back' *Neu* allele and the identification of the known gene *lilliputian* and several novel *Neu*^{YA} and *Neu*^{NYPD}-interactors in RTK signal attenuation in *Drosophila.*

CHAPTER 2: GENETIC IDENTIFICATION OF NOVEL COMPONENTS OF RECEPTOR TYROSINE KINASE DOWN-REGULATION PATHWAYS IN *DROSOPHILA MELANOGASTER.*

2.1 Introduction:

Neu/ErbB2, the type 1 transmembrane receptor tyrosine kinase (RTK), is a member of the epidermal growth factor receptor (EGFR) family that functions as a potent mediator of normal cell growth and development (reviewed in Takeuchi and Ito, 2010; Swain and Baselga, 2009; Schlessinger and Lemmon, 2006; Schlessinger, 2000). However, Neu/ErbB2 is also amplified and over-expressed in significant fraction of many human carcinomas, including breast and ovarian cancers, gastric carcinoma and salivary gland tumors (Vermeij et al., 2008; Owens et al., 2004; Yaziji et al., 2004; Jaehne et al., 1992; Salmon et al., 1987). ErbB2 amplification is implicated in during early stages of human breast cancers and overexpression is directly correlated with poor disease prognosis in both breast and gastric cancers (Swain and Baselga, 2009; Park et al., 2006; Liu et al., 1992; Yarden and Sliwkowaski, 2001).

Currently, several drugs targeting ErbB2 deregulated signaling in various stages of human cancers, have been in clinical trial either as single or as conjugate drugs (Kiewe et al., 2006; Spector et al., 2005; Franklin et al., 2004; Le et al., 2003; Cho et al., 2003; Izumi et al., 2002; Lane et al., 2002; Citri et al., 2002 and Munster et al., 2002). However, the clinical success has been moderate and also associated with drugs resistance, and side effects, including cardiac dysfunctions with the reduction of the left ventricular ejection fraction (Portera et al., 2008). Therefore, a clear understanding of the signal regulation or deregulation of the receptor molecule, such as ErbB2 is not only important for understanding the mechanism of signal transduction in normal growth and development but also for better drug development.

The vertebrate EGFR family consists of four members: EGFR/ErbB1, ErbB2/Neu, ErbB3 and ErbB4. These ErbB receptors share a common structure with (a) an extra-cellular domain for binding ligands or forming dimers with other ErbB partners, (b) the single-pass transmembrane domain that facilitates stable dimer and multiple phosphotyrosine (pTyr) residues for binding to the second messenger or adaptor molecules through their Src Homology 2 (SH2) or Protein Tyrosine binding (PTB) domains (Schlessinger and Lemmon, 2006; Schlessinger, 2000).

Human EGFR has several known ligands, such as epidermal growth factor (EGF), Heparin binding EGF-like growth factor (HB-EGF), transforming growth factor-α (TGF-α), epiregulin, amphiregulin and betacellulin (reviewed by Stuttfeld and Ballmer, 2009; Cotton et al., 2008; Mukherjee et al., 2006; Rawson, 2004). Neuregulins (NGR), on the other hand, are ligands for ErbB3 and ErbB4 (Stove and Bracke, 2004). However, there is no reported ligand for ErbB2, whereas ErbB3 lacks intrinsic kinase activity. Even without any reported ligand, the X-ray crystal structure analysis of the extra-cellular region of human ErbB2 revealed the resemblance of an extended form of ligand bound, active *Drosophila*-EGFR (DER) (Alvardo et al., 2009). These two functionally distinct receptors, ErbB2 and ErbB3 are the preferred heterodimeric partner for other ErbB receptors (Beerli et al., 1995). In fact, ErbB2-ErbB3 heterodimers are classified as the most potent oncogenic signaling unit with respect to the strength of interaction, ligand induced tyrosine phosphorylation and downstream signaling with combined mitogenic and anti-apoptotic cues (Citri el al., 2003; Tzahar et al., 1996).

So far, currently available drugs targeting ErbB receptors have been designed to attack one or the multiples of the following criteria: (1) inhibition of ligand binding, (2) inhibition of dimer formation, (3) inhibition of kinase activity, (4) destabilization of the receptor itself, and (5) inhibition of downstream signaling components. There has been little effort in exploring and manipulating the potential intrinsic negative signaling of the individual pTyr residue during human cancer development and diseases treatment. It was reported that at least one pTyr residue has negative signaling capability in rat-Neu/ErbB2, in the C. elegans homolog of epidermal growth factor receptor- Let-23, and in the platelet derived growth factor receptor-β (PDGFR-β) (Chan et al., 2004; Lesa and Sternberg, 1997; Dankort et al., 1997). In a study with the rat fibroblast, Dankort et al. (1997) showed that the pTyr residue at 1028 of rat-Neu/ErbB2 suppressed the transforming ability of other pTyr residues *in trans*.

A further study with the 'knock-in mice' showed that YA (Erbb2-Y028F) mutant could rescue the perinatal lethality in the hemizygous ErbB2 animals and suggested that YA might play a role in ErbB2 signaling (Chan et al., 2004). Moreover, Lesa and Sternberg et al. (1997) found that pTyr 1225 of Let-23 mediated tissue specific negative regulation, suggesting potential inhibitory signaling by this pTyr residue. Moreover, the intrinsic negative signaling behaviour of any of these pTyr residues, such as pTyr at 1028 of Neu, can effectively be exploited in downregulating the intrinsic signaling capabilities of the receptors.

Apart from the intrinsic negative signaling capability of the certain pTyr residues, RTK attenuation can also be accomplished any of the followings: (1) autoinhibition

mediated by the extra-cellular or the catalytic domains, (2) antagonistic ligands, (3) hetero-oligomerization with kinase inactive mutant receptors, (4) inhibition by phosphatases, (5) receptor endocytosis and degradation (Schlessinger, 2003, 2000). The key mechanism of RTK signal termination represents the involvement of endocytosis and Lysosomal degradation (Dikic, 2003). Recent studies provide evidence that the endocytotic machinery is disrupted in certain types of cancer (Ande et al., 2009).

This is the first genetic study to explore the potential signaling downregulation of the pTyr residue at 1028 of the oncogenic Neu/ErbB2 using transgenic *Drosophila* as a model. Here we have chosen the *Drosophila* compound eye as a model system to determine the signaling characteristics of pTyr at 1028 (Neu^{YA}) of rat-Neu and evaluate the genetic interactions of known components of RTK signal attenuating pathways, including receptor mediated endocytosis and lysosomal degradation, through which Neu^{YA} might function. *Drosophila* eyes are dispensable and known to require the activation of the only fly homolog of epidermal growth factor receptor, DEgfr or DER. During eye development, DER plays important roles in propagation of the morphogenetic furrow (MF) of the eye imaginal disc, in fate determination of photoreceptor cells (R1-R8) and in apoptosis of undifferentiated cells during final stages of eye development (reviewed in Doroquez and Rebay, 2006).

Using the targeted misexpression system, the GAL4-Upstream Activating Sequence (GAL4-UAS) (Brand and Perrimon, 1993), our lab has shown that individual pTyr residue of rat-ErbB2 can signal through the *Drosophila* adaptor proteins and can generate graded phenotypes (Settle et al., 2003). These graded phenotypes were used to

identify the genetic interactions of various downstream signaling components in an unbiased nature (Settle et al., 2003). Exploiting the advantages of the *Drosophila* model, we sought to determine and evaluate the signaling characteristics of Neu/ErbB2 and the possible mode of function. We evaluated the genetic interactions of various 'add-back' *Neu* and several UAS and mutant receptor alleles, including *Drosophila*-EGFR and Sevenless receptor tyrosine kinases. Specifically, we asked whether pTyr 1028 could affect signaling from heterologous RTKs. We also verified the genetic interactions of various known components of RTK signal attenuating pathways, including receptor mediated endocytosis and lysosomal degradation, through which Neu^{YA} might function. Our data shows that the pTyr at 1028 of *Neu* (Neu^{YA}) partially suppressed the eye phenotypes of DER Ellipse, Elp^{B1} mutant, Sev-Torso chimera and all the *Neu* 'add-back' alleles, suggesting a non-autonomous and inhibitory role in RTK attenuation. Phenotypic suppression of various components of receptor mediated endocytosis and lysosomal degradation suggests that Neu^{YA} renders it signal-attenuating capability, at least partially, through the receptor-mediated endocytosis and lysosomal degradation. However, YA is not required for RTK endocytosis. Therefore, pioneering data from this study sheds light on potential RTK signaling down regulating mechanisms for better drug development against many human cancers, including breast, gastric and ovarian cancers.

2.2 Materials and Methods:

2.2.1 *Drosophila* fly socks

Unless otherwise indicated, *Drosophila melanogaster* fly strains were obtained from Bloomington Stock Centre. All fly lines were stored and crosses were done at room temperature (22-25°C). The wild type Oregon R strain was used in all controls. The following *UAS-DER* lines have been used in this study: *UAS-DER^{wildtype}* (11-9) (Source: N. Baker), *UAS-DER^{ACT}* (Baker and Rubin, 1989), *UAS-DER^{A887T}* (12-4) (Lesokhin et al., 1999), *UAS-DER^{DN}* (Freeman, 1996). The mutants used in this study are as follows: *DER^{WT}*, *DER^{A887T}*, *DER^{ElpB1}*, *DER^{DN}*, *Alpha-adaptin*, *Aux^{D128}*, *Eps-15^{EP2513}*, *Ex^{K12913}*, *Chc^{1}*, *Epsin-like^{03685}*, *Mer^{4}*, *Rab5^{K08232}*, *Hrs^{D28}*, *Rab11^{2JD1}*, *Hk*, *Ept^{2}*, *Eff^{8}*, *Uba1^{s3484}*, *Uba1^{s3484}*, *Cbl^{KG03080}*, *Scribble^{KG04161}*, *Avl*, *Vps^{25}*, *Lgd^{08}*, *14-3-3 epsilon^{S-696}*, *Dor^{8}*, *drk^{10626}*, *Kek1*, *Px*, *Sty5*, *Ebi^{CSS-6}*, *Src^{42A}*, *and Src^{64B}*. *P[UAS-Neu]* expression was regulated by *p[GAL4]* strains, *GMR-GAL4* (Hay et al., 1997) and *C96* (Gustafson and Boulianne, 1996; Stewart et al., 2001). Crosses with *p[GMR-GAL4]* were conducted at 18°C in order to suppress a weak ommatidial defect, which is intrinsic to the stock. On the other hand crosses with *C96* were always conducted at 25°C.

2.2.2 Transgenes: Single 'add-back' alleles

A constitutively active rat-ErbB2 *(Neu^{NT})* was generated by a E664V point mutation in the transmembrane domain (Dankort et al., 1997). Upon the *Neu^{NT}* background, the generation of *Neu* phosphorylation deficient allele or *Neu^{NYPD}* was done by the tyrosine to phenylalanine transition at 1028, 1144, 1201, 1226/1227 and 1253

Tyrosine residues. 'Add-back' alleles were generated upon the NYPD background by restoring tyrosine residue at 1028 (YA), 1144 (YB), 1201(YC), 1226/1227(YD) and 1253 amino acid position (Dankort et al. (1997). By using the Site-Directed (SD) mutagenesis technique (Nickoloff and Deng, 1992), we generated the Neu^{YE} allele by restoring the tyrosine at the 1253 position on the Neu^{NYPD} background. The SD mutagenesis was done according to the manufacturers protocol (Quick-Change XL Site-Directed mutagenesis kit, Stratagene). The *UAS-*Neu^{NYPD} plasmid was amplified by using the mutagenic oligonucleotide pair 5'GCAGAGAACCCTGAGTA**CC**TAGGCCTGGATGTACC3' (forward, ML1977) and 5'GGTACATCCAGGCCTAG**GT**ACTCAGGGTTCTCTGC3' (Backward, ML1978), which will restore tyrosine at the site E (1253). Nucleotides that differ from the Neu^{NYPD} sequence are in bold and underlined. The PCR amplification was performed for 14 cycles of 60s at 94°C, 1 min 40s at 60°C and 30 mins at 68°C. The PCR product was then treated with 1μL *Dpn I* endonuclease and incubated at 37°C for 1 hour to digest the parental DNA template and to select for mutation containing synthesized DNA. 2 μL of the digested product was then used to transform 50 μL of XL10-Gold ultracompetent cells provided with the Mutagenesis kit. 100 μL of the transformed cells (in NZY^{+} broth, see Stratagene's instruction manual, cat# 200517) was spread on the LB Ampicillin agar plate and allowed to grow at 37°C for 16-18 hours. Several well distant colonies were picked up and grown overnight in 14 ml falcon tubes (Corning) supplemented with LB Ampicillin broth medium. The plasmid was prepared separately from all the bacterial samples using the Plasmid Minipreps kit (Qiagen). All the plasmid preparations were then restriction mapped with XhoI (Invitrogen, cat# 15231-012) and

EcoRI (Roche, cat# 703737) restriction enzymes and only a few of the chosen samples which have the right band size revealing proper length and orientation as well, were sent to the Mobix Lab (McMaster University) for sequencing. The sequences were then aligned with Rat mRNA for *Neu* oncogene (p185) encoding an epidermal growth factor receptor-related protein (Accession# X03362, Version X03362.1 gi# 56745). The result was then analyzed and only that sample was considered, which does not have any mutation but the expected tyrosine restoration at the site E (1253).

2.2.3 Sub cloning of cDNA

The generated Neu^{YE} cDNA was subcloned into a fresh *pUAST* vector. 2.4 μg of plasmid DNA and 2.4 μg of pUAST vector were digested separately with 1.5μl of EcoRI at 37°C for 1.5 hours. The digested product from the plasmid DNA was electrophoresed on a 1% agarose gel and 4 kb band was excised and purified using Gel extraction kit (Qiagen, cat.#20021). On the other hand, 2.5 μl of Shrimp Alkaline phosphatase, SAP, (Boheringer, Germany) along with 10X buffer was added to the *pUAST* digestion product for 1 hour at 37°C. Following incubation, SAP was inactivated at 65°C for 15 minutes and the reaction mix was kept in room temperature for additional 30 mins. The concentration of linearized *pUAST* and purified Neu^{YE} cDNA were measured using spectrophotometer at 260 nm. In order to ligate the insert into *pUAST* (Brand and Perrimon, 1993), 500 ng of insert DNA and 100 ng of *pUAST* DNA were mixed along with 3 μl of 5X ligation buffer, 1 μl of T4 ligase (Invitrogen) to make the final volume of 19 μl. The reaction was kept at 14°C overnight. 4μl of ligation mix was used to transform

50µl of DH5-α competent cells according to the manufacturer's specification. Colonies were screened using Minipreps (Qiagen) and EcoRI (Roche). Clones with positive inserts were further digested with XhoI (Invitrogen) to reveal the orientation.

2.2.4 Preparation of DNA constructs for microinjection

DNA extractions were done individually using the endo free plasmid maxi kits (Qiagen). The prepared plasmid DNA size was compared with the High Mass DNA ladder prior to make a 30 µg of sample for microinjection. This sample contains the *pGMR* and helper vector p in a ratio of 5:1. The volume of the sample was then made 100 µL with distilled water followed by precipitation by adding additional 10µL of 3M sodium acetate. After precipitation, 250µL of absolute cold ethanol was added and kept in –80°C for 15 minutes before spinning at 13000 rpm for 15 minutes at 4°C. Following a rewash with 70% ethanol, the pellet was dried for 10-15 minutes in room temperature and resuspended in 50µL of injection buffer (10mm Tris-Hcl [ph7.5], 0.1 mm EDTA, 100 mm NaCl, 30µM spermine and 70µM spermidine).

2.2.5 DNA microinjection

Except for Neu^{YB}, Zhong Xiao-Li of Dr. Campos Lab, McMaster University, did all other microinjections according to the standard protocol as described by (Spradling, 1986). Microinjection of pUAST constructs was performed on yw^{-} embryos. The embryos were collected on an apple juice agar plate attached to a fly house made of 100 ml plastic beaker (Nalgene) with tiny holes to allow airflow. In order to encourage the

flies to lay eggs, a bit of yeast paste was added onto the solidified apple juice agar plates. Fly houses were set up and maintained at 25°C and the plates were changed at every thirty minutes so that early stages embryos can be collected and injected before the pole cell formation. After 5 minutes decorionation with 50% bleach solution, embryos were collected in a nitex sieve chamber. Then approximately 30-35 embryos were lined up on a double-sided adhesive tape attached on a standard glass slide within a 20 minutes time limit. The embryos were then placed on Anhydrous Calcium Sulfate bed (W.A. Hammond Company product # 23001) in a desiccator. After appropriate desiccation, embryos were covered with a thick layer of halocarbon oil (Halocarbon®). Injection was performed under a Leica inverted microscope (Leica, Germany). Needles were pulled from 100X1 mm Borosil glass capillary tubes (FHC) and were broken by gently touching the side of the glass slide. Approximately 2-3 μL of the desired DNA construct was loaded into the glass needle using a Hamilton 26 gauge needle (Fisher Scientific, cat.# 14-813-1). A tiny amount (a barely visible bubble) of DNA construct was injected into the posterior of the embryos. Injected embryos were kept in a Petri dish containing a wet paper towel to provide necessary moisture to the embryos. The embryos were then kept at 18°C for 48 hours and the surviving embryos (usually crawled out from the oil) were transferred to yeast agar food vials at 25°C until they eclosed. Individual flies were then crossed with *yw*⁻ adults and the F1 generation was screened for eye pigmentation. Flies with the eye pigmentation were crossed again with *yw*⁻ adults and the purified stocks were balanced and p-element insertion was mapped by crossing (individual stock) with various marked balancers.

2.2.6 Wings mounting and light microscopy

Flies were anesthetized by keeping them at -20°C for 5-10 minutes. The anesthetized flies were then dehydrated in ethanol gradient (50%, 70%, 90%, 95% and 100%). Wings were clipped by using a wing clippers scissor (F.S.T 91500-09, Germany) and were kept in methyl salicylate prior to mounting. Wings were then mounted in D.P.X *Neu*tral mounting medium (Aldrich) on frosted glass slides (Corning) using 24X24 mm cover slips. The slides were then stored or photographed through a Nikon SMZ1500 microscope and a Nikon digital camera (Nikon Coolpix990). The photographs were then stored directly on a Mac OS X (version 10.2.8) computer and prepared for figures by Adobe Photoshop® version7.0.

2.2.7 Immunohistochemistry and Confocal microscopy

Embryos of particular stages of development from appropriate crosses set in a 100 ml plastic beaker (Nalgene) covered with solidified apple juice agar and tiny bit of yeast paste were collected, decorinated and fixed. Standard immunohistochemistry techniques, as described by Patel (1994), were followed. In brief, the fixed embryos were incubated in primary antibody and 10% normal goat serum (NGS). The primary monoclonal antibody, such as anti-GFP and anti-phosphotyrosine (Upstate, NY) were used at 1: 600 and 1: 300 dilutions respectively. After primary staining, embryos were incubated in fluorescent secondary antibody (Alexa 488 and Alexa 594: Molecular Probes) at a dilution of 1:300. Embryos were visualized by Leica SP5 Confocal microscope and images of single sections or projections were processed using ImageJ and Photoshop.

Intensity of pTyr immunofluoresence was calculated with Photoshop, as averaged intensity from randomly selected cells (Supplement 2.9).

2.2.8 Environmental electron microscopy:

Adult flies, from the appropriate crosses, were anesthetized by keeping them at -20°C for at least 5 minutes. At least 5 adult females from the appropriate genotype were mounted on the centre of the stand covered with homogenously mixed white glue and charcoal. The fly eyes were viewed, photographed at 100X, 150X, and 300X or sometime at X800 at 3.0 Torr of a Philips Environmental Scanning Electron Microscope and images were saved in the Hard disk of a Philips computer as TIF files. The images were finally processed with Adobe Photoshop® Version 7.

2.3 Results:

2.3.1 *Neu*^{YA} suppressed eye phenotypes rendered by other 'add-back' Neu alleles.

Neu^{YA} lacks transforming ability in rat1 fibroblast cell cultures and reduces transforming potential of other Neu alleles *in cis*, suggesting a negative role in RTK signaling (Dankort et al., 1997). We have previously shown that the adaptor binding sites of rat-Neu/ErbB2 oncogene could successfully signal through the adaptor proteins in *Drosophila* (Settle et al., 2003). Using several 'add-back' alleles, we also showed that *Neu* misexpression resulted in ectopic veins and wing deltas formation and wing margin loss (Hossain, 2005: MSc. Thesis; Supplement 2.1). Having these graded phenotypes handy, we asked whether the suggested negative role of *Neu*^{YA} could be verified *in vivo*. Specifically, can *Neu*^{YA} suppress the phenotypes induced by other 'add-back' *Neu* alleles? To test this hypothesis, we used the Drosophila eye tissue specific *GMR-GAL4* driven misexpression system.

GMR-GAL4 driven misexpression of *Neu*^{YA} resulted in a nearly wild type eye surface with usual ommatidial size, shape and arrangement. The bristles were uniformly distributed on the eye surface (Fig. 2.1 A). In contrast, the *Neu* phosphorylation deficient allele- lacking all pTyr, *Neu*^{NYPD} showed a weak phenotype in regards to ommatidial size, shape and bristle arrangement. A flattened ommatidial outer surface was characteristic to *Neu*^{NYPD} (Fig. 2.1 C). We examined whether *Neu*^{YA} could suppress the *Neu*^{NYPD} eye phenotypes *in vivo*. Co-expression of both *Neu*^{YA} and *Neu*^{NYPD} was closer to wildtype in regards to ommatidial size and shape, bristles arrangement, and eye roughness (Fig. 2.1

Figure 2.1: *Neu*^{YA} suppresses eye phenotypes induced by other *Neu* alleles. (A-D) The *p[GMR-GAL4]* driven misexpression system at 18°C. The bristles and ommatidial facets in control, *p[GMR-GAL4]* flies are regularly arranged and spaced with smooth outer eye surface appearance (A). *Neu*^{YA} shows a mild eye surface-roughness phenotype (B). *Neu*^{NYPD} shows irregularly spaced bristles with randomly distributed groups of 2 or 3 bristles. Variation in ommatidial size makes the outer eye surface coarse (C). However, co-expression of *Neu*^{NYPD} and *Neu*^{YA} shows more uniform ommatidial sizes and bristles distribution making the outer eye surface smoother and similar to control flies (D). (E-P) Mis-expression of various *Neu* alleles was accomplished by using the *p[sev-GAL4]* driver. Mild eye roughness phenotypes were observed in *Neu*^{YA} (F). Double dosages of *UAS*-sequence, in *UAS-Neu*^{YA}*,sev-GAL4/UAS-GFP* adults, have little or no effect on the rough-eye phenotypes (Compare E and F). However, *Neu* 'add-back' alleles, *in trans* with *Neu*^{YA}, showed a range of suppression of eye phenotypes of the particular allele (compare G and H for *Neu*^{YB}, I and J for *Neu*^{YC}, K and L *Neu*^{YD}, M and N for *Neu*^{YE} and O and P for *Neu*^{NT}).

All images were taken at X300 magnification on an Environmental Scanning Electron Microscope (ESEM). Transgenes are indicated at the top right of each panel. Scale bar indicates 150 μm.

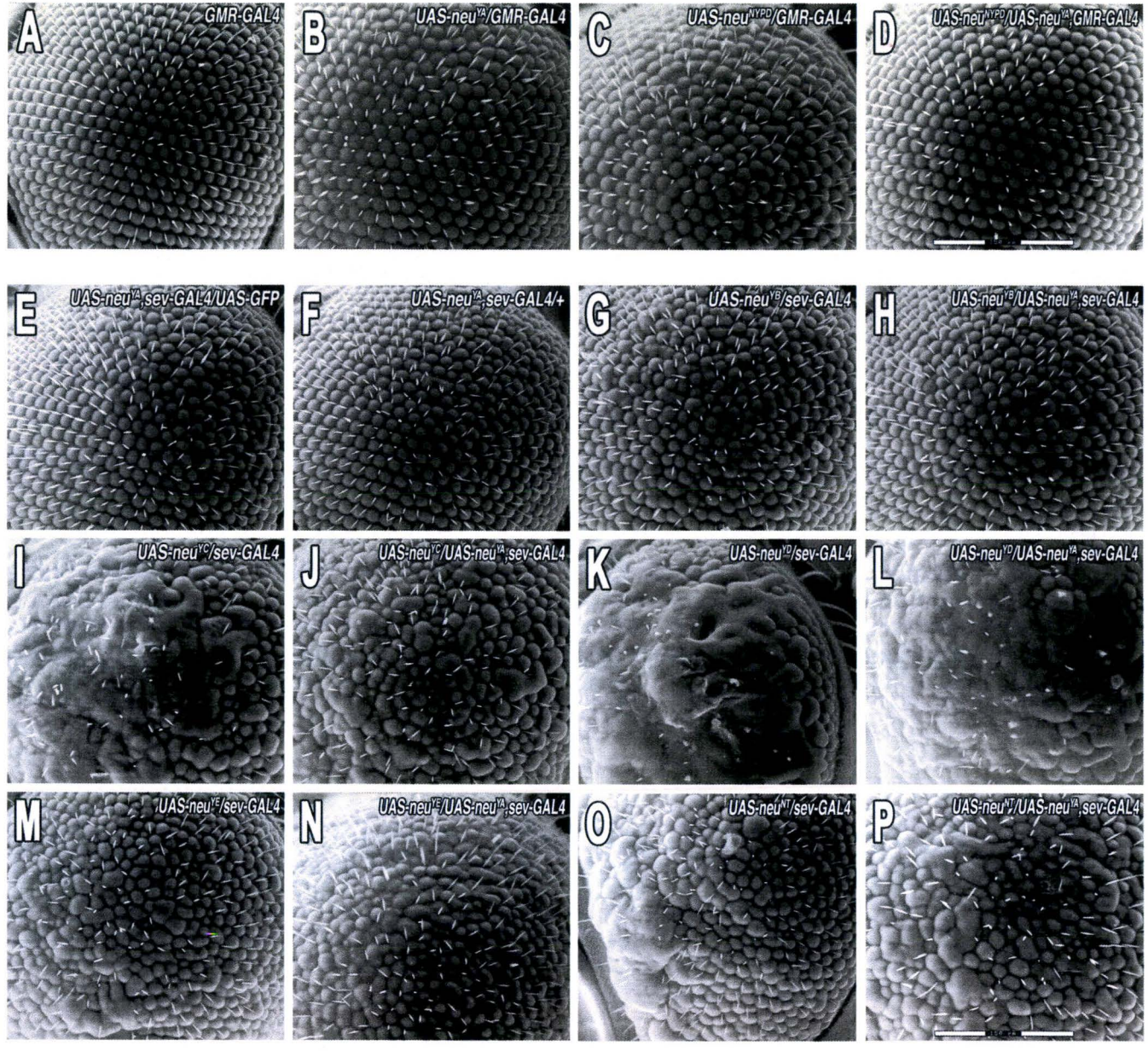
A
GMR-GAL4
B
UAS-neu^YA/GMR-GAL4
C
UAS-neu^NYPD/GMR-GAL4
D
UAS-neu^NYPD/UAS-neu^YA;GMR-GAL4
E
UAS-neu^YA,sev-GAL4/UAS-GFP
F
UAS-neu^YA,sev-GAL4/+
G
UAS-neu^YB/sev-GAL4
H
UAS-neu^YB/UAS-neu^YA,sev-GAL4
I
UAS-neu^YC/sev-GAL4
J
UAS-neu^YC/UAS-neu^YA,sev-GAL4
K
UAS-neu^YD/sev-GAL4
L
UAS-neu^YD/UAS-neu^YA,sev-GAL4
M
UAS-neu^YE/sev-GAL4
N
UAS-neu^YE/UAS-neu^YA,sev-GAL4
O
UAS-neu^NT/sev-GAL4
P
UAS-neu^NT/UAS-neu^YA,sev-GAL4

D). The misexpression data with the *Drosophila* wing tissues also showed a phenotypic suppression of Neu^{NYPD} by co-expression of Neu^{YA} (Supplement 2.2, Panel I and J).

We then asked whether Neu^{YA} could suppress the phenotypes rendered by the other 'add-back' *Neu* alleles. Since the *p[GMR-GAL4]* driver has intrinsic phenotypes at room temperature and the misexpression is associated with lethality of Neu^{YC} and Neu^{NT} alleles (Supplement 2.3), we used the *p[sev-GAL4]* driven misexpression. Neu^{YA} partially suppressed the eye phenotypes of other alleles *in trans* (Fig. 2.1 E-P). However, a complete suppression of eye phenotypes of any of the *Neu* alleles was not seen.

2.3.2 Neu^{YA} attenuates signaling from the endogenous *Drosophila*-EGFR (DER):

The experiments with *Neu* 'add-back' alleles establish that Neu^{YA} can act in trans, but doesn't establish whether this action is restricted to *Neu*. Since DER is the only known vertebrate orthologue of ErbB family member in *Drosophila* we asked whether Neu^{YA} might suppress DER misexpression phenotypes. To test this hypothesis, we mis-expressed several *UAS-DER* alleles, including a wildtype *DER* (DER^{WT}), two gain-of-function DER^{A887T} and DER^{ACT}, and a dominant negative DER^{DN} allele in *Drosophila* eye tissue using *sev-GAL4* driver. Mis-expression of these *DER* alleles resulted with rough-eye phenotypes (Fig. 2.2 I). The DER^{DN} resulted in significantly reduced eye size with severely rough-eye surface and dense bristles (Fig. 2.2 G). Neu^{YA}, *in trans*, partially restored the wildtype eye size of the DER^{DN} allele (Fig. 2.2 H). On the other hand, Neu^{YA} showed a mild or no suppression of rough eye phenotypes with the gain-of-function

Figure 2.2: *Neu^{YA}* selectively suppresses the *UAS-DER* (DEgfr)- induced eye phenotypes. Expression of wild type *Drosophila*-EGF receptor (*DER^{WT}*) in the eye with *p[sev-GAL4]* driver resulted in a rough eye with reduced ommatidial facet and bristles (A). The rough eye phenotypes were unchanged in *UAS-DER^{WT}/ UAS-Neu^{YA},sev-GAL4* (A, B), in *UAS-DER^{ACT}/ UAS-Neu^{YA},sev-GAL4* (C, D) and *UAS-DER^{A887T}/ UAS-Neu^{YA},sev-GAL4* (E, F). However, *Neu^{YA}* shows a partial rescue of wildtype eye sizes with increased ommatidial number in both *DER^{ACT}* and *DER^{DN}* (H). Images were taken at X150 magnifications on an ESEM. Transgenes are indicated on the top right of each panel. Bar indicates 300 μm.

The bar graphs show the total ommatidial counts in the respective genotype (I). The ommatidial numbers have been averaged at least from 3 adult female eyes of each genotype. Standard error bars are shown. The paired *t*-test results (*p*-values) are shown in Supplement 2.5 and Supplement 2.6.

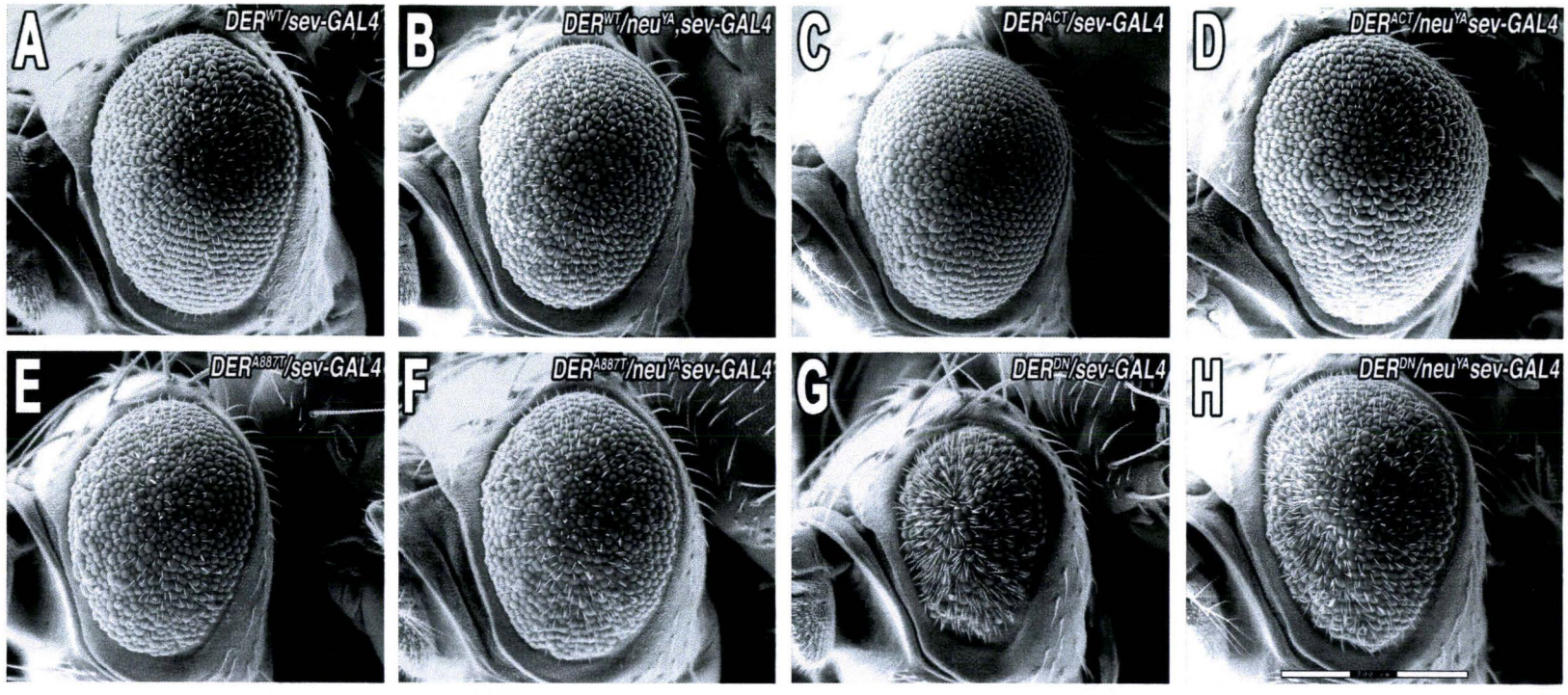
A
DER^WT/sev-GAL4
B
DER^WT/neu^YA,sev-GAL4
C
DER^ACT/sev-GAL4
D
DER^ACT/neu^YA sev-GAL4
E
DER^A887T/sev-GAL4
F
DER^A887T/neu^YA sev-GAL4
G
DER^DN/sev-GAL4
H
DER^DN/neu^YA sev-GAL4

(I)

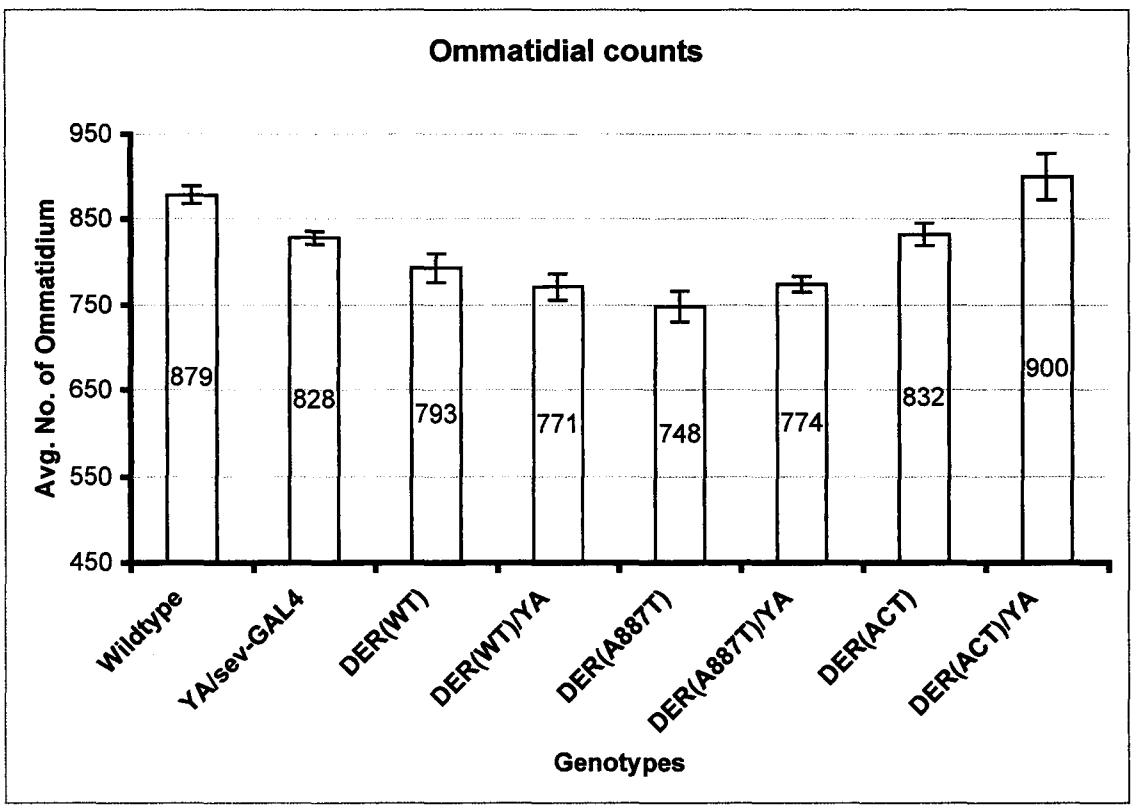
Ommatidial counts
Avg. No. of Ommatidium
950
850
750
650
550
450
879
828
793
771
748
774
832
900
Wildtype
YA/sev-GAL4
DER(WT)
DER(WT)/YA
DER(A887T)
DER(A887T)/YA
DER(ACT)
DER(ACT)/YA
Genotypes

alleles, DER^{ACT} (2.2 C, D) and DER^{A887T} (Fig. 2.2 D and F).

However, the ommatidial count in DER^{ACT}/Neu^{YA} heterozygote increased significantly (*p*-value 0.0245) (Fig. 2.2 I). A higher number of smaller ommatidial facets accounted for the increased ommatidial count in the heterozygote. Here we hypothesize that Neu^{YA} might reduce the hyperactive DER signaling closer to a normal level, which is required for proper cell proliferation and survival (Lesokhin et al., 1999; Dominiguez et al., 1998; Baker and Rubin, 1989).

It is believed that the RTK TM dimer interface contains the critical structural information that positions the catalytic domains in such a way that they can phosphorylate each other. A point mutation was found in the oncogenic version of this domain in rat-*ErbB2* (Neu^{NT}) (Bargmann et al., 1986; Schechter et al., 1984). Over activity of this oncogenic receptor was attributed to a Val664Glu transformation in the TM domain. Since all the 'add-back' *Neu* alleles- used in this study, contain a point mutation at the transmembrane region, Neu^{YA} might exerts its suppressive role by forming a heterodimer with the other *Neu* alleles, and reducing it activity. The point mutation (A887T) at the intracellular kinase domain of DER^{ACT} allele was accounted for increased activity due to increased homo-dimerization (Lesokhin et al., 1999). Neu^{YA} may prevent DER^{ACT} from forming homo-dimers, resulting in reduced activity and increased ommatidial count. On the other hand, the hypoactive DER^{DN} contains a normal extracellular and transmembrane domain and a truncated C-terminal domain. YA could prevent DER^{DN} from dimerizing with endogenous *DER* or clear it from cell surface.

2.3.3 *Neu*^{YA} attenuates the signaling from other Receptor Tyrosine Kinases (RTKs) *in vivo.*

Next, we asked whether the *Neu*^{YA} suppression was only observed with GAL4 mediated over expression or not. To test this hypothesis, we tested the genetic interactions of *Neu*^{YA} with several RTK alleles, including EGFR gain-of function allele, *Elp*^{B1} and a Sevenless-Torso chimera. The Sev-Torso chimeric proteins comprised of the extracellular domain of Sevenless (sev) and cytoplasmic domain of Torso gene and was placed under the control of sev-enhancer/promoter, creating *p[sev-Sev-Torso]* flies. The sev-enhancer/promoter expresses the chimera in the presumptive R7 cell and four non-neuronal cone-cells that ultimately take the R7-cell fate. The production of ectopic R7 cells disrupts the interior eye morphology and causes rough eyes in appearance (Karim et al., 1993). In a study with cultured COS-7 cell lines and transgenic *Drosophila*, it has been demonstrated that Torso RTK activates Extracellular signal Regulated Kinase (Erk) signaling through a small G protein, Rap1 in a Ras-independent manner (Mirsha et al., 2005). The *sev-GAL4* driven misexpressed *Neu*^{YA} significantly rescued the eye sizes and ommatidial counts of *p[sev-Sev-Torso] in trans*, suggesting reduced signaling from the chimera (Fig. 2.3).

The gain-of-function DER mutant allele, *Elp*^{B1} is a spontaneous point mutation at the intracellular kinase domain, which results in a lower ommatidial count and rough eye phenotype (Fig. 2.3). However, superimposed expression of *Neu*^{YA} in *Elp*^{B1}*/UAS-Neu*^{YA}, *sev-GAL4* flies partially rescued the ommatidial number (Fig. 2.3 I). This partial rescue of ommatidial count was also seen with the *UAS-DER*^{ACT} allele (Fig. 2.2). Together, these

Figure 2.3: *Neu*^{YA} suppresses eye phenotypes induced by two unrelated Receptor Tyrosine Kinases (RTKs). (A-C) The genetic interaction of *Neu*^{YA} with the gain-of-function DER Ellipse-mutant, *Elp*^{B1}. In control, *p[sev-GAL4]* flies, the bristles and ommatidia are regularly spaced and arranged, resulting in a smooth eye surface (A). *Elp*^{B1} shows smaller eye with relatively coarse eye surface phenotypes (B). However, the eye rough-eye phenotypes were unchanged in *Elp*^{B1}/*Neu*^{YA} adults (C). *Neu*^{YA} on the other hand, significantly (p value 0.0082) increased ommatidial counts in *Elp*^{B1} *in trans* (I). (D-F) The genetic interaction of the Sevenless-Torso (Sev-Torso) chimeric protein. The chimera was expressed under the control of sevenless promoter/enhancer (*sev*) resulting in rough-eye surface with smaller eye size possibly due to fewer cluster formation at the posterior of morphogenetic furrow, where sevenless is first expressed during *Drosophila* eye development (D). However, *Neu*^{YA}, *in trans,* significantly (*p*-value 0.0062) increased the ommatidial counts in the chimera (compare D and F). Images were taken at X150 magnifications on an ESEM. Transgenes are indicated on the top right of each panel. Bar indicates 300 μm.

The bar graphs show the total ommatidial counts in the respective genotype (G). The ommatidial numbers have been averaged at least from 3 adult female eyes of each genotype. Standard error bars are shown. The paired *t*-test results (*p*-values) are shown in Supplement 2.7 and Supplement 2.8.

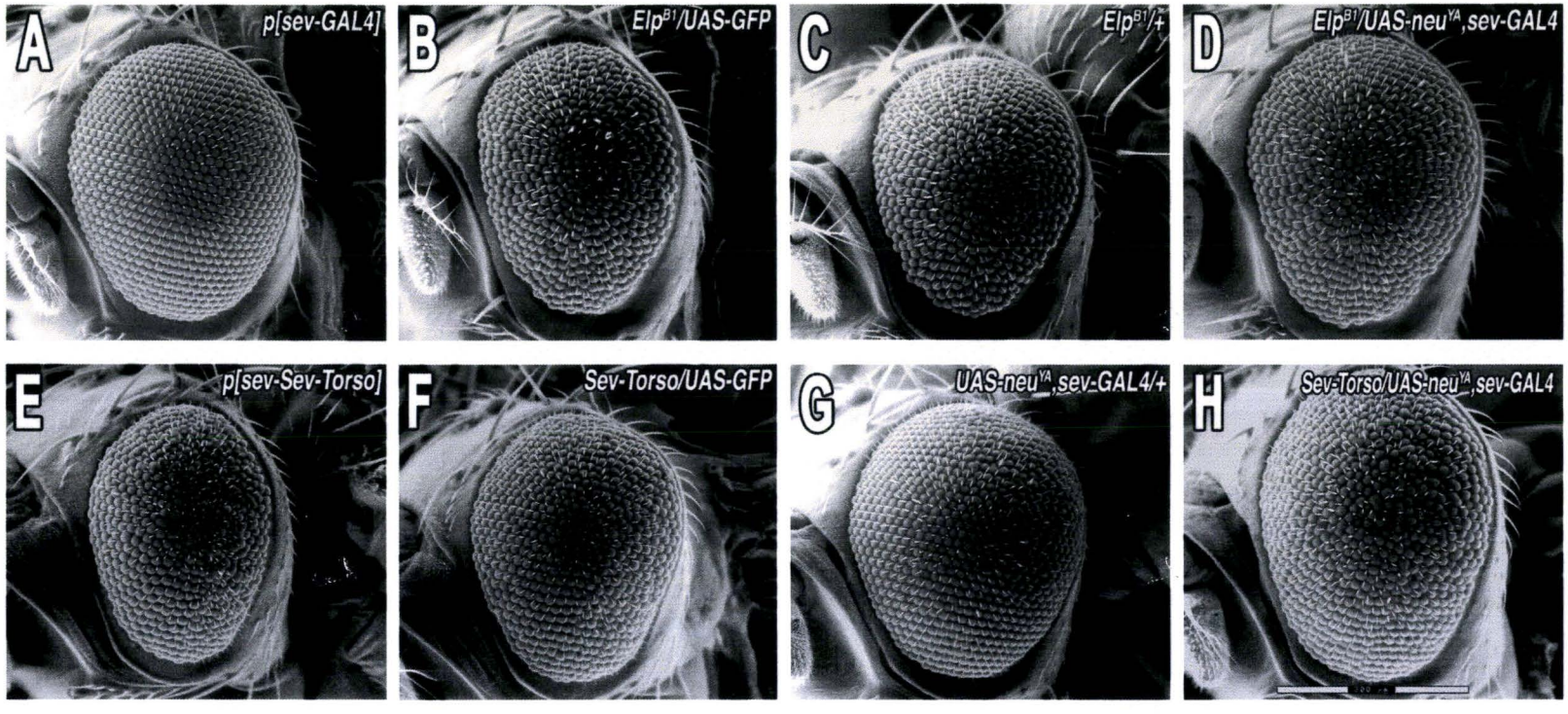
A
p[sev-GAL4]
B
Elp^B1/UAS-GFP
C
Elp^B1/+
D
Elp^B1/UAS-neu^YA,sev-GAL4
E
p[sev-Sev-Torso]
F
Sev-Torso/UAS-GFP
G
UAS-neu^YA,sev-GAL4/+
H
Sev-Torso/UAS-neu^YA,sev-GAL4

(G)

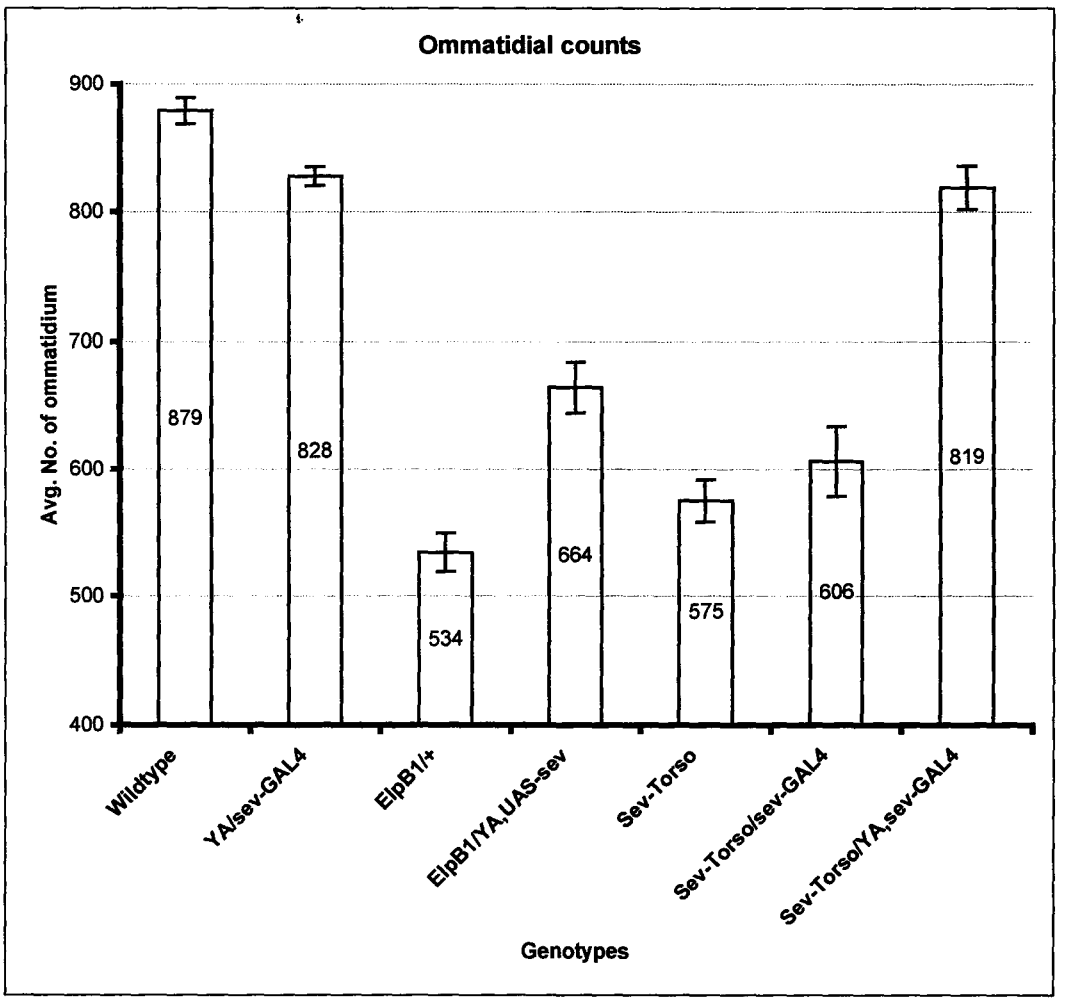
Ommatidial counts
Avg. No. of ommatidium
900
800
700
600
500
400
879
828
534
664
575
606
819
Wildtype
YA/sev-GAL4
ElpB1/+
ElpB1/YA,UAS-sev
Sev-Torso
Sev-Torso/sev-GAL4
Sev-Torso/YA,sev-GAL4
Genotypes

results demonstrated that the signal attenuating capability of Neu^{YA} is not specific to misexpression experiments alone. Neu^{YA} attenuates signaling at least from two unrelated Receptor Tyrosine kinases, such as EGFR and Sevenless.

2.3.4 Neu^{YA} attenuates the phosphorylation levels *in vivo.*

Next, we hypothesized that the Neu^{YA} receptor tyrosine kinase might downregulate the other *Neu* alleles or the other RTKs by reducing tyrosine phosphorylation levels. In order to test this hypothesis, we examined the phosphorylation levels of various *Neu* 'add-back' alleles either with *I-76-D-GAL4* (GAL4 in epidermal Stripes) or *Twist-GAL4* driver. *Twist-GAL4* driver expresses the genes of interest in the presumptive mesoderm, in ventral region during the stage 5-6 of the developing embryos, while *Stripe-GAL4* expresses the particular gene of interest in ectodermal stripes during the late (Stage 12-13) embryonic development (Chen et al., 1998). Phosphorylation levels were then assessed using the anti-pTyr antibody (Fig. 2.4) (Ganguli et al., 2005). In Neu^{YE}, most of the cells at the dorso-ventral epidermis showed higher level of phosphorylation. On the other hand, in Neu^{YA} most of the cells had minimal level of phosphorylation (Fig. 2.4; Supplement 2.9).

This phosphorylation level corresponds to the phenotypic levels as seen in adult animals. For example, the higher level of phosphorylation resulted in more severe eye phenotype in Neu^{YE} adults (Fig. 2.1). However, the Neu^{YA} adults showed lower phosphorylation level and relatively milder eye phenotype as seen in Fig. 2.1. Expectedly, Neu^{YA} reduced the phosphorylation in Neu^{YE} /Neu^{YA} heterozygote, suggesting

Figure 2.4: *Neu*^{YA} downregulates the phosphorylation level of the other 'add-back' *Neu* alleles. The I-76-D GAL4 driver (GAL4 in epidermal Stripes) expresses the gene of interest (*UAS-GFP*) as a transversal stripe in the ectoderm during the stage 13-14 of developing embryos. A number of cells of the epidermis show higher, while the others (surrounding cells) show minimal level of GFP expression (A). The phosphorylation level in control (wild type) embryo is at a minimal level (B). The mis-expressed *Neu*^{YE} embryos show higher levels of phosphorylation in many of the epidermal cells at the ventral boundary (C), while only a few cells show similar level of phosphorylation in *Neu*^{YA} (D). However, a reduced level of phosphorylation is evident in *Neu*^{YE}/*Neu*^{YA} heterozygote (E). Finally, a higher phosphorylation level than that of *Neu*^{YA} is seen in *Neu*^{NYPD} (F).

All Images were taken at 63X lens and 5.62X magnification on a Leica confocal microscopy. Scale bar indicates 5 μm. (See Supplement 2.9 for signaling intensity and Supplement 2.10 for data with another driver, *Twist-GAL4*).

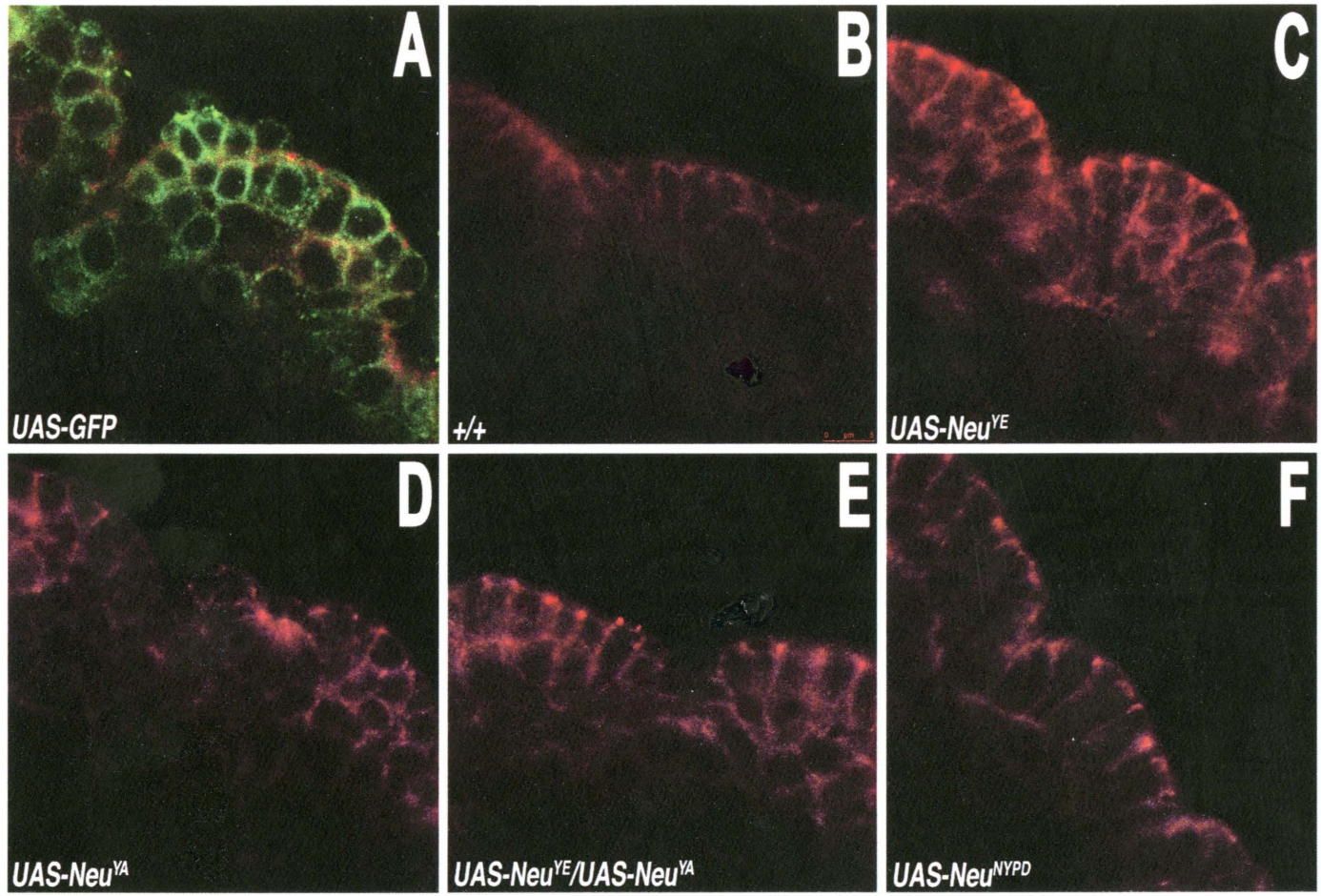
A
UAS-GFP
B
+/+
C
UAS-Neu^YE
D
UAS-Neu^YA
E
UAS-Neu^YE/UAS-Neu^YA
F
UAS-Neu^NYPD

a reduced phosphorylation as the mechanism of signal attenuation. This result is consistent with the data from the mammary cell lines, where ^{YA} mutant (having all the pTyr sites, except YA) showed higher phosphorylation levels than that of either YE-mutant or YE 'add-back' alleles (only YE present) (Kim et al., 2005). Moreover, a higher level of phosphorylation in NYPD verifies our hypothesis that Neu^{YA} might have an inhibitory role upon the Neu^{NYPD} background as suggested by our phenotypic data (Fig. 2.1).

2.3.5 Partial suppression of Neu^{YA} signaling through receptor mediated endocytosis.

Receptor endocytosis controls the number of receptors available in the plasma membrane, and RTK signaling can regulate endocytosis (Sorkin and Zastrow, 2009). When not binding ligand, most EGFRs reside on the cell surface while basal levels of receptors are internalized by endocytosis (Herbs et al., 1994). If endocytosis attenuates receptor signaling, during impaired endocytosis the cell will accumulate Neu^{YA}, resulting in increased rough-eye phenotype. To address this, we verified the genetic interactions of Neu^{YA}, Neu^{YE}, Neu^{YC}, and Neu^{YAE} with various loss-of-function alleles of endocytosis pathway (Fig. 2.5 and Table-2.1). To our surprise, mutations in most of the endocytosis pathway components, including alpha-adaptin, Epidermal Growth factor Receptor Substrate clone 15 (*Eps15*), and Clathrin Heavy Chain (*Chc*) enhanced signaling from Neu alleles without requiring the presence of Neu^{YA} (Table-2.1). All these above-mentioned endocytosis pathway components also enhanced the rough-eye phenotype of

Figure 2.5: *Neu*^{YA} plays a positive role in receptor recycling and lysosomal degradation. *Neu*^{YA}, mis-expressed with the *sev-GAL4* driver, shows variation of ommatidial sizes and randomly distributed pair of bristles resulting in mild rough-eye surface phenotypes (A). A single copy of an amorphic allele of the endocytotic pathway component, expanded (*ex*) almost completely suppressed the rough-eye phenotype of *Neu*^{YA} in trans (compare A and B). However, the ubiquitylation pathway components, Casitas B-Lineage Lymphoma (*cbl*) enhanced the rough-eye phenotype induced by *Neu*^{YA} (C). The negative RTK regulator, *Sprouty* (*Spry*) partially suppressed the rough-eye phenotype of *Neu*^{YA} (D).

Images were taken at X300 magnification on an ESEM and genotypes are indicated on the top right of each panel. Bar indicates 150 μm. See Supplement 2.11 for other RTK regulators' data.

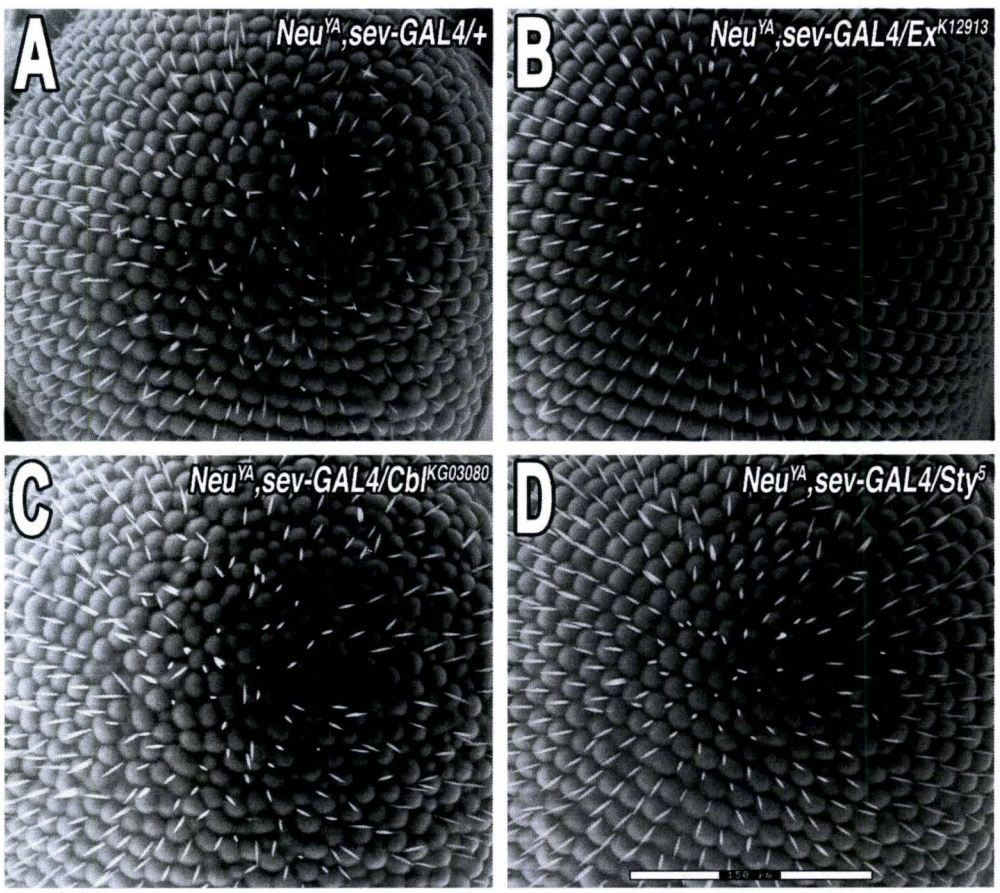
A
Neu^YA,sev-GAL4/+
B
Neu^YA,sev-GAL4/Ex^K12913
C
Neu^YA,sev-GAL4/Cbl^KG03080
D
Neu^YA,sev-GAL4/Sty^5
150 µm

Table 2.1: The summary of the dosage sensitive modifier screen. The interactions of the amorphic alleles of the genes that act in endocytosis, receptor recycling, receptor trafficking and lysosomal degradation were evaluated with various *Neu* alleles. All haplosufficiencies enhanced phenotypes generated Neu^{YE}, Neu^{YC}, and Neu^{YAE} in a YA-independent manner. However, haplosufficiencies of genes involved in receptor recycling and lysosomal targeting suppressed Neu^{YA} phenotype, suggesting a positive role in receptor recycling and receptor trafficking to the lysosomal degradation pathway. Neu^{YAE} was expressed under control of Glass Multimer Reporter (*GMR*), while all other *Neu* alleles were mis-expressed with *sev-GAL4* driver. E- enhancement, S- suppression, N/S- No or weak suppression. See Supplement 2.11 for other RTK regulators' data.

Table 2.1: Summary data of *Neu*^{YA} interactions with various components of receptor mediated endocytotic pathway.

Alleles		*Neu* Modification			Roles in RTKs Regulation	Mammalian relatives	References
		YA	*YE*	*YAE*			
Endocytosis:							
Alpha-adaptin	Alpha-adaptin	N	E	E	Formation of intracellular transport vesicle and/or Selection of cargo for entry into vesicle.	Alpha-adaptin 2 (AP2)	Boehm and Bonificiano, 2001.
Eps-15^{EP2513}	Epidermal Growth Factor Receptor Substrate Clone 15	N	E	E	Link signaling receptors to a clathrin coat. Plays role in the assembly of clathrin-coated pits.	Eps-15	Brett and Traub, 2006.
Ex^{K12913}	Expanded	S	E	S	Expanded functions cooperatively with Merlin to modulate receptor Endocytosis.	Expanded	Boedigheimer, MJ et al.,1997.
Chc^{1}	Clathrin Heavy chain	N	E	E	Formation of invaginated pits on the plasma membrane and subsequent budding of vesicles.	---	Bazinet et al., 1993.
Mer^{4}	Merlin	E	E	E	Merlin and Expanded function cooperatively to modulate receptor endocytosis and signaling.	Neurofibromatosis 2 (NF2)	Maitra S et al., 2006.
Recycling:							
Rab5^{K08232}	Rab5	S	E	E	Small GTPase that plays a key role in the early endocytotic pathway.	Rab5	Zerial M. and McBride H, 2001.
Hrs^{D28}	Hepatocyte Growth Factor regulated tyrosine kinase substrate	N/S	E	E	Hrs regulates endosome membrane invagination. Plays role in receptors sorting in intraluminal vescicles.	Hrs	Lloyd TE et al., 2002.
Rab11^{2JD1}	Rab11	S	E	E	Small GTPase that plays a key role In the early endocytotic pathway regulation. Rab11 regulates recycling through the pericentriolar recycling endosome.	Rab11	Sonnichsen, 2000.
Ubiquitylation:							
Eff^{8}	Effet	N	E	E	Functions as E1 Ubiquitin protein	E1 ubiquitin Protein	Flauvarque et al., 2001.
Uba1^{05642}	Ubiquitin Activating enzyme.	E	N	E	Encodes Ubiquitin Activating Enzyme, E1. Controls Apoptosis autonomously and Tissue growth non-autonomously.	Ubiquitin Activating enzyme (E1 enzyme)	Lee TV, 2008.
Uba1^{s3484}	Ubiquitin Activating enzyme.	N	E	E	Encodes Ubiquitin Activating Enzyme, E1. Controls Apoptosis autonomously and Tissue growth non-autonomously.	Ubiquitin Activating enzyme (E1 enzyme)	Lee TV, 2008.
Cbl^{KG03080}	Casitas B-Lineage Lymphoma	E	E	E	Functions as an E3 ligase, and catalyse the formation of a covalent bond between ubiquitin and Cbl's protein substrates- typically a receptor tyrosine kinase.	Cbl	Traub, 2006.
Scrib^{KG04161}	Scribble	E	E	E	Functions in Ubiquitin-mediated degradation.	hScribble	Takizawa S et al., 2006.
Lysosomal degradation:							
Vps^{25}	Vacuolar Protein Sorting	S	E	E	Involved in Golgi to Lysosome trafficking.	Sec1p	Pevsner J et al., 1999.
Ept^{2}	Erupted	N/S	E	E	Encodes components of Endosomal sorting complex required for transport (ESCRT).	---	Giebel and Wodarz et al., 2006.

Neu^{YAE}, suggesting a YA-independent mechanism. Moreover, Expanded (*ex*) suppressed the rough-eye phenotype of Neu^{YA} and Neu^{YAE}, yet enhanced the eye phenotype of Neu^{YC}.

The receptor recycling pathway components, such as Hepatocyte Growth Factor Regulated tyrosine kinase substrate (*Hrs*), *Rab5* and *Rab11* and the lysosomal degradation pathway components, including Vacuolar Protein Sorting (*vps*) and Erupted (*Ept*) suppressed the rough-eye phenotype of Neu^{YA}, while enhanced the eye phenotypes of both Neu^{YE} and Neu^{YAE} (Table 2.1). The enhancement of Neu^{YE} and Neu^{YAE} rough-eye phenotypes suggest a YA-independent mechanism in receptor recycling and lysosomal degradation. However, the suppression of Neu^{YA} rough-eye phenotype indicates that during impaired receptor recycling and/or lysosomal degradation, cells may up-regulate a novel mechanism in attenuating signaling from a negative RTK potential, such as Neu^{YA}.

As protein degradation attenuates signaling, it was expected that the loss-of-function alleles of the ubiquitylation pathways would enhance the phenotypes of Neu^{YA} allele. Indeed, all the ubiquitylation pathway components, including Effet (*eff*), Ubiquitin activating enzyme (*uba*), *Cbl* and Scrib enhanced the phenotypes of Neu^{YA}, Neu^{YE}, Neu^{YC}, and Neu^{YAE} (Table 2.1). We also verified the genetic interactions of various known positive and negative regulators of RTK signaling components with various *Neu* alleles, including Neu^{YA}, Neu^{YE} and Neu^{YAE}. However, a haplosufficiency for *Sprouty*, encoding the membrane bound phosphoprotein that inhibits growth factor signaling, partially suppressed the Neu^{YA} rough-eye phenotype (Fig. 5D), while enhanced the eye phenotype of all other tested *Neu* alleles. The partial phenotypic suppression of Neu^{YA} by *Sprouty* suggests that these two molecules work in a similar pathway to attenuate RTK signaling

in *Drosophila* (Supplement 2.11).

2.3.6 Neu^{YA} is insensitive to altered function of Jun/STAT and AKT/PKB pathway.

In various human carcinomas, such as breast cancer, the hyperactive receptor heterodimers, such as EGFR and ErbB2 receptors employ the canonical Ras-Raf-MAPK cassettes for tumor cells proliferation. The deregulated PI3K-Akt/PKB pathway is employed for tumor cell survival, suppression of apoptosis and programmed cell death. On the other hand, deregulated JAK/STAT pathway has been reported for novel direct translocation of the receptors to the nucleus (Craven et al., 2003; Baselga and Norton, 2002; Bromberg et al., 1999; Bacus et al., 1996; Sporn and Todaro, 1980). We showed earlier that Neu^{YA} inhibits RTK signaling *in vivo*. Therefore, we hypothesized that the pTyr residue at 1028 or Neu^{YA} would be insensitive to the context specific signaling pathways, such as PI3K-Akt and JAK-STAT.

In order to address this, we verified the genetic interactions of several components of both PI3K-Akt and JAK-STAT pathways with various *Neu* alleles, including Neu^{YA}, Neu^{YB}, Neu^{YE}, and Neu^{YAE}. Neu^{YA} was insensitive to a haplosufficiency in amorphic alleles of the Akt, hopscotch (HOP), Janus kinase (JAK) and STAT pathways (Fig. 2.6). However, these pathway components enhanced the eye phenotypes in by both Neu^{YE} (Fig. 2.6) and Neu^{YB} (data not shown). These data suggest that the individual pTyr residue employs multiple signaling pathways depending on the context specific manners. In other words, a particular pTyr residue signals through a specific cascade during normal growth

Figure 2.6. *Neu*^{YA} function is insensitive to altered function of Jun/STAT and AKT/PKB pathways. The *sev-GAL4* driven misexpression of *Neu*^{YA} resulted in mild eye roughness phenotypes due to variation in sizes and bristle distribution (A). *Neu*^{YE} also showed similar level of eye roughness phenotype with reduced number of bristles (F). *Neu*^{YA} revealed no genetic interaction with various altered alleles of AKT/PKB pathway components, including *AKT*^{EY10012} (B) and *Hopscotch* (C). Moreover, the Jun/STAT pathway components, such as *Janus kinase* (D) and *STAT*^{06346} (E) had no genetic effect (suppression or enhancement) on the *Neu*^{YA} eye phenotype. However, the eye phenotype of *Neu*^{YE} was significantly enhanced in *AKT*^{EY10012} (G), *Hopscotch* (H), *Janus kinase* (I) and *STAT*^{06346} (J).

Images were taken at X800 magnification on an ESEM and genotypes are indicated on the top right of each panel. Bar indicates 50 μm.

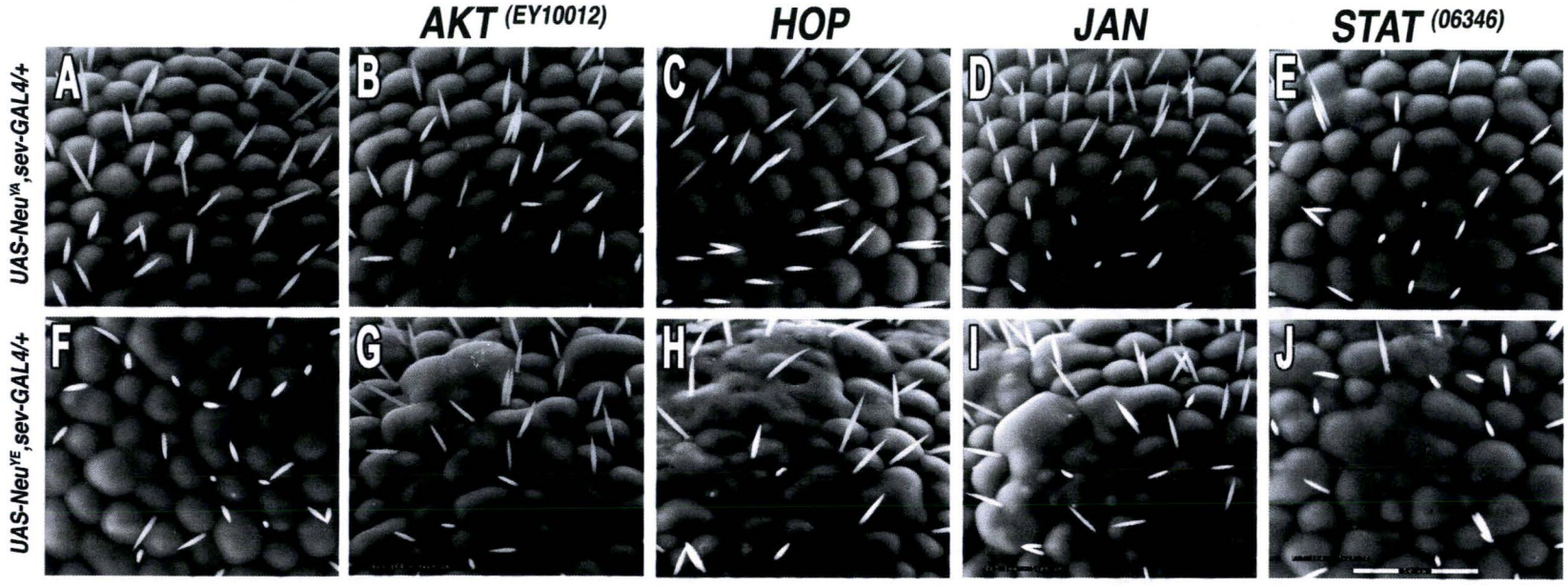
AKT (EY10012)
HOP
JAN
STAT (06346)
UAS-Neu^YA,sev-GAL4/+
UAS-Neu^YE,sev-GAL4/+
A
B
C
D
E
F
G
H
I
J

and development, whereas the same pTyr residue may employ additional signaling pathways during cancer development and metastasis.

2.4 Discussion:

Dankort et al. (1997) showed that a single amino acid substitution from tyrosine to phenylalanine at the 1028 site (Y1028F) of a constitutively active *Neu* allele showed consistent increase in transforming ability. However, restoration of the tyrosine residue at the 1028 site (Y1028) of a tyrosine phosphorylation deficient (NYPD) mutant blocked transformation of cultured fibroblasts. The other four out of five individual pTyr of activated Neu, the rat homologue of ErbB2, contributed individually to transform cultured fibroblasts indicating that tyrosine the 1028 site negatively modulates ErbB2 activity. In a genetic study with LET-23, a *C. elegans* EGFR homologue (Lesa and Sternberg, 1997) and in another site-directed mutagenesis study with *Drosophila* Torso (Tor) receptor tyrosine kinase (Perrimon et al., 1985) have found at least one specific phosphorylation site that was responsible for negative or down regulation of RTK signaling.

Misexpression of *Neu/ErbB2* in *Drosophila* using various GAL4 drivers showed the convincing result that the specific phosphorylation sites could act positively and negatively (Hossain, 2005: Masters thesis). We showed that Neu^{NYPD} mis-expression in the wings resulted in a thicker mass of wing vein deltas than that of Neu^{YA} (Supplement 2.1). The reduced level of phenotypes in Neu^{YA} signaling may reflect the inhibitory feedback of YA upon the NYPD signal. All of these data tempted us to determine the role and specificity of Neu^{YA} over other RTKs and to identify the signaling pathways through which Neu^{YA} renders it functional entity.

It has been previously shown that activated mammalian *Neu/ErbB2* generates phenotypes in transgenic *Drosophila* comparable to overactivation of endogenous DEgfr pathway (Settle et al., 2003). For example, *Neu* suppresses apoptosis in the MG lineage, generates rough eye phenotypes and expands the domains of wing veins, all characterized by DEgfr (DER) hypermorphic alleles (Settle et al., 2003; Lanoue and Jacobs, 1999; Sturtevant and Bier, 1995; Baker and Rubin, 1989). *In vivo* experiments reveal more functional distinctions of different pTyr outputs and genetic analysis is an efficient means of identifying signaling pathways (Bhandari and Shashindra, 2001; Dankort et al., 2001; Lesa and Sternberg, 1997). In fact, due to the conserved structural and functional nature of RTK signaling in metazoans, the mammalian rat-*Neu* (ErbB2) could successfully signal through the adaptor proteins in *Drosophila* (Settle et al., 2003). Therefore, *Drosophila* is a suitable genetic model organism to decipher the role and mechanism of Neu^{YA} in RTK signaling downregulation *in vivo*. This study is significant for better understanding of RTKs down regulation, a possible targeting mechanism for developing future cancer therapeutics.

2.4.1 Neu^{YA} renders inhibitory role in RTK signaling

In order to understand *Neu* signaling in *Drosophila*, we mis-expressed various 'add-back' *Neu* alleles in both wing and eye tissues. This mis-expression system generated a range of phenotypes both in wing and eye tissues and Neu^{NT} proved to be the most responsive (Fig. 1 and supplement 2.1). Our data is consistent, as Neu^{NT} also resulted in the highest transforming ability in Rat1 fibroblasts cell cultures (Dankort et

al., 1997). Moreover, our lab previously showed that Neu^{YD} and Neu^{NT} are the most penetrant in both Midline Glia (MG) and wing tissues (Settle et al., 2003). Although it lacks all Tyr phosphorylation sites, Neu^{NYPD} generated both wing and eye phenotypes (Fig. 2.1 and Supplement 2.1, Supplement 2.3) and retained transforming potential in mammals (Dankort et al., 2001). It has been demonstrated that in Neu^{NYPD} a pTyr residue in the kinase domain can transmit signal through binding with the mediator of ErbB2-driven cell motility, Memo (Marone et al., 2004).

While verifying the findings of Settle et al. (2003), Neu^{YA} misexpression generated both eye and wing phenotypes but milder than that of Neu^{NYPD} (Fig. 2.1; Supplement 2.3). Neu^{YA} also showed less phenotypic penetrance in the wing tissues than that of eye tissues (compare Fig. 2.1 and Supplement 2.1). In a cell culture study, Dankort el al. (1997) showed that Neu^{YA} lacked transforming potential, suggesting an inhibitory role in RTK signaling (Dankort et al., 2001; Dankort et al., 1997). The reduced level of phenotypes in Neu^{YA} signaling may reflect the inhibitory feedback of YA upon the NYPD signal. Using 'knock-in' mouse as a model, Chan et al. (2004) found that a single amino acid substitution at the 1028 (YA) site (ErbB2-Y1028F) of *Neu* resulted in increased ErbB2 protein expression levels as compared to the level of proteins in embryos expressing the ErbB2 cDNA, the Y1144F (YB site) cDNA or the Y1227F (YD site) cDNA alleles. This elevated ErbB2 protein expression by Y1028F mutant suggests that the tyrosine at 1028 (Y1028) has inhibitory roles in ErbB levels, possibly affecting lifetime of the proteins. Therefore, a suppression of other RTK phenotypes while *in trans* with Neu^{YA} may reflect similar negative regulation.

While mis-expressed, Neu^{YA} significantly suppressed the phenotypes induced by the other 'add-back' *Neu* alleles both in the eye (Fig. 2.1) and wing tissues *in trans* (Supplement 2.3). Experiments with the Rat1 fibroblast showed that addition of site A to the *NT-YB* allele (YAB) virtually abolished the transforming activity (Dankort et al., 1997). However, the complete suppression of phenotypes of the other alleles *in trans* with the Neu^{YA} was neither seen in the eye nor in the wing tissues. This could be due to the involvement of different adaptor signaling pathway with different signaling strength of these pTyr residues, where YA may correspond to the weakest signaling profile.

2.4.2 Neu^{YA} may inhibit RTK during normal growth and development and cancer metastasis

In a mouse model, Chan et al. (2004) found that the ErbB2 Y1028F allele resulted with increased ErbB2 protein levels. Elevated ErbB2 level modestly affected the EGFR protein levels. However, the protein expression level of other ErbB members, such as ErbB3 and ErbB4, were unaffected. This could be due to the lacking of kinase domain in ErbB3 and differential requirement of ligand for ErbB4. Since DER is the only known ErbB family member in *Drosophila*, we thought that Neu^{YA} might affect DER expression level. In the developing eye, DER is required for late ommatidial development. DER plays important roles in R8-photoreceptor maintenance, induction of all cells following the R8/founder cell, cell-proliferation, survival and ommatidial rotation (Roignant and Triesman, 2009; Braid and Verheyen, 2008; Rodriguez et al., 2005).

DER mis-expression resulted in eye phenotypes ranging from a rough eye surface

to a severely reduced eye size in an allele specific manner (Fig. 2.2). Therefore, if there was an inhibitory role in RTK signaling, Neu^{YA} would reduce the DER protein expression level in *Drosophila* and eventually suppress these allele specific phenotypes *in trans*. Neu^{YA} expression resulted in suppression of reduced-eye phenotypes in the $UAS\text{-}DER^{DN}/Neu^{YA}$ adults. Furthermore, a moderate increase of ommatidial count was observed with either $UAS\text{-}DER^{ACT}$ or Ellipse mutant, Elp^{B1} alleles *in trans* with Neu^{YA}. The hypermorphic $UAS\text{-}DER^{ACT}$ or Ellipse B1 mutant, Elp^{B1} is the type1 protein characterized with a single substitution of Ala887Thr in the intracellular kinase domain (Lesokhin et al., 1999). This A887T mutation showed increased ligand-independent autophosphorylation and MAP kinase activation in *Drosophila* cells, resulting in increased RTK activity (Lesokhin et al., 1999). On the other hand, the transmembrane region of *Neu* receptors have revealed a conserved, site-specific Val-Glu-Gly tri-peptide (VEG) domain and is responsible for transformation and signal transduction of wildtype *Neu* Receptor (Burke et al., 1997). Loss or mis-localization of this domain greatly reduces the tendency for *Neu* receptors to dimerize. It is possible that Neu^{YA} forms heterodimers with the DER alleles, at least with $UAS\text{-}DER^{ACT}$ and $UAS\text{-}DER^{DN}$ alleles. This physical interaction can be verified by co-expressing the DER^{DN} allele with the chimera having the above-mentioned domains from the DER^{DN} plus the intracellular Neu^{YA} kinase domain could test this hypothesis. Similarly, a chimera with extracellular and transmembrane *Neu* with the intracellular DER^{ACT} allele will generate phenotypes similar to DER^{ACT}, which could be suppressed by the co-expression with Neu^{YA}.

Surprisingly, Neu^{YA} did neither suppress the rough-eye phenotypes nor the total

ommatidial counts in either *UAS-DER^{A887T}* or *DER^{A887T}* mutant alleles. A similar lack of suppression was found in heterozygotes of *Neu^{YA}* and *UAS-DER^{A887T}* when mis-expressed in the wing tissue (data not shown). However, *Neu^{YA}* partially rescued the total ommatidial number in *Elp^{Bl}* mutants (Fig. 2.3 I). Taken together, it is possible that *Neu^{YA}* works in heterodimers in independent manner.

2.4.3 *Neu^{YA}* may favour receptor recycling and degradation

In recent years, RTK signal attenuating steps, such as receptor dephosphorylation and degradation, effector/substrate depletion, ligand stimulation and endocytotic trafficking have seen much attention (Sorkin and Zastrow, 2009; Wiley, 2003). In resting state, most EGFRs reside on the cell surface while a basal level of receptors is internalized by endocytosis (Herbst et al., 1994). Ligand stimulation enhances the internalization of activated receptors through the clathrin-coated pits. Depending on the cell type, the internalized EGFRs may be trafficked to the plasma membrane or to be transported to the endoplasmic reticulum and Golgi for reprocessing or to the late endosome and then onto lysosome for degradation (Ceresa, 2006). It is increasingly clear that receptor signaling regulates the endocytosis and endocytosis has many effects on signal transduction (Sorkin and Zastrow, 2009). Therefore, it is understandable that during endocytosis, the recycling of the receptors to the plasma membrane or the degradation by lysosomes can be signal-attenuating factors in receptor activity.

The dosage sensitive modifier screen showed the involvement of receptor-mediated endocytosis, receptor recycling to the plasma membrane and lysosomal

degradation in a YA-independent mechanism. On the other hand, among all the tested RTK modulators, only Sprouty mutant suppressed the Neu^{YA} rough-eye phenotype (Fig. 2.5, Supplement 2.11). The negative feed back regulator of RTK signaling, Sprouty, in association with hepatocyte growth factor-regulated tyrosine kinase substrate (Hrs), interferes with the trafficking of activated receptor tyrosine kinase specifically at the step of progression from early to late endosome (Kim et al., 2007). As endocytic trafficking is also being regarded as the means of intracellular signal propagation (Sorkin et al., 2002), the impediment of RTKs at the early endosome would attenuate their signaling. On the other hand, among the *Neu* alleles, only the Neu^{YA} rough-eye phenotype was suppressed by the receptor recycling pathway components, such as *Hrs*, *Rab5* and *Rab11* and the lysosomal degradation pathway components, including *vps* and *Ept* (Table 2.1, Fig. 2.5, Supplement 2.11).

The study with C2C12 murine myoblasts and MIAPaCa-2 human pancreatic tumor cells found that in presence of human Sprouty 2 (hSpry2), almost 60-70% of the ligand-bound EGFR remained localized to the early endosome, within 2 hour of EGF stimulation (Kim et al., 2007). In contrast, in absence of hSpry2, 60-70 % of the EGFR were found at the late endosome, as early as within 30 min of EGF stimulation. Taken together, it is possible that if endocytosis, receptor recycling, or lysosomal degradation is impaired or endosomal trafficking from early-to-late endosome is blocked, cells may up-regulate a YA-attenuating signaling mechanism that requires the involvement of Sprouty and Hrs, at least partially. During impaired endocytosis or blocked endosomal trafficking, Neu^{YA} may attenuate the RTK signaling by facilitating the removal of the internalized

signal-competent receptors from the early endosome to the plasma membrane in a rab11 dependent mechanism or by facilitating lysosomal degradation of the already internalized (in late endosome) receptors.

2.4.4 *Neu*^{YA} may not take part in cancer metastasis and in drug resistance

EGFR signaling pathways have been implicated in human tumorigenesis, tumor proliferation, progression and therapeutic resistance (Carven et al., 2003; Baselga and Norton, 2002; Bromberg et al., 1999; Bacus et al., 1996; Sporn and Torado, 1980). The ultimate signaling outputs and downstream signaling pathways of the ErbB2 receptor tyrosine kinases mostly depend on the activating ligand and the heterodimer partner (Yarden and Sliwkowski, 2001). The over-expression of ErbB heterodimers have been reported in various human cancers, including breast, ovarian, lung and prostrate cancer (reviewed in Baselga and Swain, 2009). In human breast cancer, for instance, the tumor cells exceed at least by 100 fold the expression of ERBB2 molecules over that of normal cells. This increased expression facilitates the formation of heterodimers and homodimers that ultimately results in tumor cell survival and proliferation (Perez and Baweja, 2008; Yarden and Sliwkwoski, 2001). The heterodimers of the ErbB receptor tyrosine kinases signal through the canonical Ras-Raf-MAPK cassettes for tumor cell proliferation and through deregulated PI3K-Akt/PKB pathway for tumor cell survival, apoptosis and programmed cell death suppression (Li et al., 2002).

In normal breast cells, Akt signaling is hypoactive due to low expression levels of EGFR/HER2 and/or existence of functional PTEN, the tumor suppressor phosphatase

that dephosphorylates the Phospatidylinositol-3,4,5-triphosphate (PI3-K). However, in tumor cells, the activation and phosphorylation of the heterodimeric partner, such as ErbB3, facilitates the recruitment of the Phosphatidyl-inositol 3' kinase (PI3-K). The recruitment occurs directly or indirectly through the adaptor proteins, such as Grb-Sos (son of sevenless)-Ras complexes. Ultimately these events recruit the serine-threonine kinase, Akt to the plasma membrane through its Plekstrin homology (PH) domain (Sergina and Moasser, 2007).

Upon phosphorylation by pyruvate dehydrogenase kinase1 (PDK1), the activated Akt directly phosphorylates critical regulators of the cell cycle progression and apoptosis (Kumar and Hung, 2005; Li et al., 2002; Zho et al., 2001, 2001). Akt promotes tumor cell survival by removing cell cycle checkpoints and apoptosis. Specifically, the phosphorylation of Thr157 of p27, another negative G1 regulator, results in p27 cytoplasmic retention and nuclear export (Xia et al., 2004; Clark, 2003; Huang et al., 2003; Liang et al., 2002; Shin et al., 2002; Viglietto et al., 2002; Zho et al, 2001; Winters et al., 2001). Moreover, Akt negatively regulates the tumor suppressor gene p53 by phosphorylating at Ser 166/186 of MDM2, which associates with p300 and ultimately degrades p53 (Zhou et al., 2001; Rossig et al., 2001). Together, de-regulated PI3K-Akt and JAK/STAT pathways contributed to an aggressive type of human breast cancers. It is possible that most of the pTyr residues (YB, YC, YD and YE) of Neu/ErbB2 play some roles during cancer metastasis and drug resistance. However, the pTyr residue at the 1028 of oncogenic rat-*Neu*/ErbB2 is likely to be insensitive to cancer metastasis and drug resistance, as none of the JAK/STAT and PI3'K/PKB pathway components were

sensitive to Neu^{YA}.

2.5 Conclusion:

This is the first detailed genetic study revealing the mechanistic system of any particular signal attenuating pTyr residue of receptor tyrosine kinase *in vivo*. Our misexpression data shows that Neu^{YA} suppressed the rough-eye phenotypes of all other 'add-back' *Neu* alleles. This phenotypic suppression may be due to the signal attenuating capability of Neu^{YA} by forming a heterodimer with other alleles. The data with the various mis-expressed and mutants DER alleles suggest that Neu^{YA} may prevent DER, at least, DER^{DN} allele from forming dimers with the endogenous DER or may remove them from the cell surface through an unknown mechanism. The genetics suggest that for signal attenuation, *Neu* requires endocytosis but do not act in a YA-dependent manner. Furthermore, the dosage sensitive modifier screen suggests that during impaired endocytosis, receptor recycling, and/or lysosomal degradation, cells may up-regulate a novel mechanism in attenuating YA-signaling that involves the negative RTK regulator, Sprouty and the hepatocyte growth factor regulated tyrosine kinase substrate, Hrs.

2.6 Future research:

A better understanding of the signal attenuation mechanism of Neu^{YA} will help us better understand human cancer, which is caused by the overactivation of RTKs. The identification of novel components of YA signaling pathway may lead us to design better drugs with better clinical success. The double 'add-back' *Neu* allele, particularly Neu^{YAE}

will allow us to study them in homozygous in various tissues, such as wings, eyes and MG cells. A genome wide large-scale genetic screen of Neu^{YAE}, for instance, will serve multiple purposes in this regard. Specifically, this screen will identify mutants that not only enhance or suppress Neu^{YA} phenotypes but also other 'add-back' *Neu* alleles, such as Neu^{YE} and Neu^{NYPD} immediately. The Neu^{YA} specific candidates will reveal genes required for the repression of RTK signaling in *Drosophila*. Afterwards, the mammalian ortholog of these candidates will help reveal the signaling pathways that can be utilized for targeting better drug development with a view to attaining higher clinical success in cancer treatment.

CHAPTER 3: GENETIC IDENTIFICATION OF NOVEL COMPONENTS OF RECEPTOR TYROSINE KINASE DOWN-REGULATION PATHWAYS IN *DROSOPHILA MELANOGASTER.*

3.1 Introduction:

The type 1 transmembrane receptor tyrosine kinase (RTK), Neu/ErbB2 is a member of the Epidermal Growth Factor Receptor (EGFR) family that functions as a potent mediator of normal cell growth and development (reviewed in Takeuchi and Ito, 2010; Swain and Baselga, 2009; Schlessinger and Lemmon, 2006). However, Neu amplification is implicated in the early stages of human breast and ovarian cancers and its overexpression is directly correlated with poor disease prognosis in several human cancers, including breast and ovarian cancers, gastric carcinoma and salivary gland tumors (Swain and Baselga, 2009; Vermeij et al., 2008; Park et al., 2006; Owens et al., 2004; Yaziji et al., 2004). At least one pTyr residue in Neu, Let-23 and PDGFR-β receptor tyrosine kinase was reported to have negative signaling capability (Chan et al., 2004; Lesa and Sternberg, 1997 and Dankort et al., 1997). The intrinsic negative signaling behavior of any of these pTyr residues, such as pTyr at 1028 of Neu (neu^{YA}) has yet to be fully exploited with a view to identifying novel targets for better cancer treatment.

Using the targeted misexpression system, the *GAL4*-Upstream Activating Sequence (*GAL4-UAS*) (Brand and Perrimon, 1993), our lab has shown that individual pTyr residues of rat-ErbB2 can signal through the *Drosophila* adaptor proteins and can generate graded phenotypes (Settle et al., 2003). These graded phenotypes were used to identify the genetic interactions of various downstream signaling components in an unbiased nature (Settle et al., 2003). In chapter 2, we genetically explored the potential signaling downregulation of the pTyr residue at 1028 of the oncogenic Neu/ErbB2. Using

Drosophila compound eye as a model, we determined the signaling characteristics of pTyr at 1028 (Neu^{YA}) of rat-Neu and examined the genetic interactions of known components of RTK signal attenuating pathways, including receptor mediated endocytosis, receptor recycling to the plasma membrane, and lysosomal degradation, through which Neu^{YA} might function. Our data suggests that the pTyr at 1028 of Neu renders it signal-attenuating capability, at least partially, through the trafficking-dependent alteration in early or late endosomal compartment, and through lysosomal degradation. Our additional genetic data showed that Neu^{YA}, unlike all other Tyr phosphorylation residues in the C-terminus domain of rat-Neu/ErbB2, is possibly regulated by the *Sprouty*, a negative feedback regulator of RTK signaling pathway. Collectively, Neu^{YA} may involve a novel RTK-signal attenuation pathway, at least in *Drosophila.*

To identify components of the Neu^{YA} in RTK signaling attenuation pathway, a genome-wide dominant modifier screen was undertaken. EMS treated flies were crossed with the *GMR-*Neu^{YAE}*,TM3/D* virgins and over 60,000 F1 progeny were screened either for suppression or enhancement of the rough-eye phenotype as compared to control flies. We isolated and mapped several groups of suppressors and enhancers from a pool of 24 complementation groups spanning both the 2^{nd} and 3^{rd} chromosome. One complementation group of suppressors was identified as the known gene *lilliputian.* Additionally, using deficiency mapping several other complementation groups of enhancers were narrowed down to certain regions uncovering 10-30 genes, not previously

known to the receptor tyrosine kinase signaling pathways. Collectively, here we report several novel neu^{YA} interactors in RTK signal attenuation in *Drosophila*.

3.2 Materials and Methods:

3.2.1 *Drosophila* Fly Socks

All fly strains were obtained either from the Bloomington Stock Centre (for mutants and Deficiency stocks) or Vienna Stock center (RNAi lines). Flies were stored at room temperature (22-25°C) in polypropylene shell vials (Fisher Scientific, AS 519) and the crosses were done in16X100 mm glass culture tubes (Fisher Scientific) supplemented with a sucrose-yeast agar food medium and capped with rayon rope (Fisher Scientific, APS205). The wild type Oregon R strain was used in all control experiments. Microinjection of *p[UAS]* and *p[GMR]* element was performed on yellow white$^-$ (*yw*$^-$) or on the embryos from the *yw*$^-$*; +/+; +/+* X *yw*$^-$*; Sco/CyO; D/TM3* crosses respectively (see below). *p[UAS-neu]* expression was regulated by *p[GAL4]* strains, GMR-GAL4 (Hay et al., 1997) and sev-GAL4.

3.2.2 Transgenes:

'Single Add-Back' Alleles

The generation of constitutively active rat *ErbB2* (Neu^{NT}), a mutant form of the *neu* gene, has a E664V point mutation in the transmembrane domain (Dankort et al., 1997). Upon the Neu^{NT} background, the generation of Neu phosphorylation deficient allele or Neu^{NYPD} was done by a tyrosine to phenylalanine transition at Y1028, Y1144, Y1201, Y1227 and Y1253 amino acid residues. The 'add-back' alleles were made by restoring tyrosine residue at the1028 (YA), 1144 (YB), 1201(YC) and 1227(YD) amino acid position of Neu^{NYPD} (Dankort et al., 1997).

'Double Add-Back' Alleles

'Double add-back' alleles were generated using the Site-Directed Mutagenesis technique (Nickoloff and Deng, 1992). We used the Quick-Change XL Site-Directed mutagenesis kit (Stratagene) according to the manufacturers protocol. In brief, we restored the tyrosine at the 1028 position upon the Neu^{YB}, Neu^{YC}, Neu^{YD} and Neu^{YE} to generate Neu^{YAB}, Neu^{YAC}, Neu^{YAD} and Neu^{YAE} respectively. The mutagenic oligonucleotide primer pair was 5'GGTAGACGCTGAAGAGT**A**TCTGGTGCCCCAG3' (Forward, ML 2538) and 5'CTGGGGCACCAGA**T**ACTCTTCAGCGTCTACC3' (Backward, ML 2539). The nucleotide that has been changed to restore tyrosine at the 1028 position (YA) is shown bold and underlined. The PCR amplification was performed for 14 cycles of 60s at 94°C, 1 min 40 sec at 60°C and 30 mins at 68°C. The PCR product was then treated with 1μL *Dpn I* endonuclease and incubated at 37°C for 1 hour to digest the parental DNA template and to select for mutation containing synthesized DNA. 2 μL of the digested product was then used to transform 50 μL of XL10-Gold ultracompetent cells provided with the Mutagenesis kit. 100 μL of the transformed cells in NZY^{+} broth was spread on the LB Ampicillin agar plate and allowed to grow at 37°C for 16-18 hours. Several well distant colonies were picked up and grown overnight in 14 ml falcon tubes (Corning) supplemented with LB Ampicillin broth medium. The plasmid was prepared separately from all the bacterial samples using the Plasmid Minipreps kit (Qiagen). All the plasmid preparations were then restriction mapped with XhoI (Invitrogen) an EcoRI (Roche) restriction enzymes to identify clones with the right band size to reveal the proper length and orientation. These plasmids were sent to the Mobix Lab (McMaster

University) for sequencing. The sequences were then aligned with Rat mRNA for *Neu* oncogene (p185) encoding an epidermal growth factor receptor-related protein (Accession # X03362, Version- X03362.1 gi # 56745).

3.2.3 Sub Cloning of cDNA

The newly made 'double add-back' alleles were subcloned into a fresh *pGMR* vector (A gift from Dr. Therrien). 2.4 μg of plasmid DNA and 2.4 μg of *pGMR* vector were digested separately with 1.5μl of EcoRI at 37°C for 1.5 hours. The digested product from the plasmid DNA was electrophoresed on a 1% agarose gel and 4 KB band was excised and purified using Gel extraction kit (Qiagen). On the other hand, 2.5 μl of Shrimp Alkaline phosphatase, SAP, (Boheringer, Germany) along with 10X buffer was added to the *pGMR* digestion product for 1 hour at 37°C. Following incubation, SAP was inactivated at 65°C for 15 minutes and the reaction mix was kept in room temperature for additional 30 mins. The concentration of linearized *pGMR* and purified Neu (double add-back alleles) cDNA were measured using spectrophotometer at 260 nm.

In order to ligate the insert into *pGMR* vector, 500 ng of insert DNA and 100 ng of *pGMR* DNA were mixed along with 3 μl of 5X ligation buffer, 1 μl of T4 ligase (Invitrogen) to make the final volume of 19 μl. The reaction was kept at 14°C overnight. 4μl of ligation mix was used to transform 50μl of DH5α competent cells according to the manufacturer's specification. Colonies were screened using Minipreps (Qiagen) and EcoRI (Roche) for proper band size. Clones with positive inserts were further digested

with XhoI (Invitrogen) to reveal the orientation. For this study we only generated the *Neu*^{YAE} transgenic *Drosophila* as follows.

3.2.4 Preparation of DNA Constructs For Microinjection

DNA extraction was done individually using the endo free plasmid maxi kits (Qiagen). The prepared plasmid DNA size was compared with the High Mass DNA ladder prior to make a 30 μg of sample for microinjection. This sample contains the *pGMR* and helper vector p in a ratio of 5:1. The volume of the sample was then made 100 μL with distilled water followed by precipitation by adding additional 10μL of 3M sodium acetate. After precipitation, 250μL of absolute and cold ethanol was added and kept in –80°C for 15 minutes before spinning at 13000 rpm for 15 minutes at 4°C. Following a rewash with 70% ethanol, the pellet was dried for 10-15 minutes in room temperature and resuspended in 50μL of injection buffer (10mM Tris-Hcl [pH7.5], 0.1 mM EDTA, 100 mM NaCl, 30μM spermine and 70μM spermidine).

3.2.5 DNA Microinjection

Microinjection of *pGMR* constructs was performed on the embryos from the *yw*$^{-}$; +/+; +/+ X *yw*$^{-}$*; Sco/CyO; D/TM3* crosses according to the standard protocol as described by Spradling (1986). The embryos were collected on an apple juice agar plate attached to a fly house made of 100 ml plastic beaker (Nalgene) with tiny holes to allow airflow. In order to encourage the flies to lay eggs, a bit of yeast paste was added onto the solidified apple juice agar plates. Fly houses were set up and maintained at 25°C and the plates

were changed at every thirty minutes so that early stages embryos can be collected and injected before the pole cell formation. After 5 minutes decorionation with 50% bleach solution, embryos were collected in a nitex sieve chamber. Then approximately 30-35 embryos were lined up on a double-sided adhesive tape attached on a standard glass slide within a 20 minute time limit. The embryos were then placed on Anhydrous Calcium Sulfate bed (W.A. Hammond Company) in a dessicator. After appropriate dessication, embryos were covered with a thick layer of halocarbon oil (Halocarbon®). Injection was performed under a Leica inverted microscope (Leica, Germany). Needles were pulled from 100X1 mm Borosil glass capillary tubes (FHC) and were broken by gently touching the side of the glass slide. Approximately 2-3 μL of the desired DNA construct was loaded into the glass needle using a Hamilton 26 gauge needle (Fisher Scientific). A tiny amount (approximately $1/10^{th}$ volume of the embryo) of DNA construct was injected into the posterior of the embryos. Injected embryos were kept in a Petri dish containing a wet paper towel to provide necessary moisture to the embryos. The embryos were then kept at 18°C for 48 hours and the surviving embryos (usually crawled out from the oil) were transferred to yeast agar food vials at 25°C until they eclosed. Individual flies were then crossed with *yw*⁻ adults and the F1 generation was screened for eye pigmentation. Flies with the eye pigmentation were crossed again with *yw*⁻ adults and the purified stocks were balanced and p-element insertion was mapped by crossing (individual stock) with various marked balancers. Specifically, for this study the working stocks were made with the flies with genotypes of (a) *yw*⁻; *GMR-Neu*^{YAE}/+; +/+ (b) *yw*⁻; +/+; *GMR-Neu*^{YAE}/+ (c) *yw*⁻; +/*CyO,GMR-Neu*^{YAE}; +/+ and (d) *yw*⁻; +/+; +/*TM3,GMR-Neu*^{YAE}.

3.2.6 Large-Scale Genetic Screening:

EMS Mutagenesis

For the large-scale mutagenesis study, we used the 2nd and 3rd chromosome isogenized wiltype Oregon R males and followed the standard EMS mutagenesis scheme (Lewis and Bacher, 1968). In brief, approximately 150 males of 3-4 days old were collected in each of at least 4 empty polystyrene vials (Fisher Scientific) at 12 pm and were starved for 5 hours to make them thirsty. At 4:30 pm of the same day, a neutralizing solution was made in a plastic container by adding 0.5 gm of thioglycolic acid (Sigma) in a 100 ml of 4% NaOH solution. In addition a 25 ml of 1% sucrose solution was made in a 50 ml centrifuge tube (Corning). In the mean time, 2 pieces of 7X1.5 cm of no.1 whatman filter paper (Whatman®, cat. # 1001-125), were attached separately to the inside walls of each vial with adhesive tape. The vial was then properly capped with rayon rope (Fisher Scientific). From this point all the preparations were done into the fume hood assigned for EMS uses. At 5 pm 66 μL of Ethyl methane sulfonate (EMS) (Sigma, EC # 200-536-7) was gently dispensed into the sucrose solution by using a 1-c.c syringe (Becton Dickinson & C0. cat. # 309604) with 22-gauge needle (Becton Dickinson & Co., cat. #. 305156). The needle was then immediately filled with neutralizing solution and discarded into that plastic container containing neutralizing solutions. By using another 10 c.c syringe with 22-gauge needle, EMS and sucrose solution was mixed gently but thoroughly for 6-7 times. This syringe was also neutralized and discarded into the neutralizing solution containing plastic container. Afterwards, 0.5 ml of EMS mix was

added onto the two filter paper stripes attached to the inside walls of the capped polystyrene vial by using another fresh 1 cc syringe with 22 g needle. Then the thirsty flies were transferred to the vials treated with EMS and kept in the fume hood for overnight. At 11 am the next morning the EMS fed flies were transferred to vials containing yeast sucrose agar fly food. At least 3 times of transfer at 1-hour interval were done to make sure that no EMS was left on the vials that would be carried to the fly pushing room. All the vials including the EMS treated and the one with fly food were neutralized and discarded as mentioned earlier. Approximately 100 out of the initially started 150 males were available for the crosses. Then 4-5 EMS treated males were crossed with 10-15 virgins of *p[GMR-neu^{YAE}],TM3/D* flies in each polystyrene vial containing standard fly food supplemented with a tiny yeast paste labeled numerically. In order to obtain the maximum numbers of progeny, the flies from each numerically labeled vial were transferred to a new vial with food at least 2 times for the next two days and 3 times for the 3rd and 4th days. At this time each vial was labeled alphabetically and starting with the numerical number assigned earlier. For example, each transfer from the original vial number 1 and 2 were labeled as 1a, 1b, 1c, 1d .... and 2a, 2b, 2c and 2d .... respectively.

3.2.7 Modifier Screening And Linkage Analysis

The progeny from these crosses (F1) were observed to score the eye phenotype enhancement or suppression (Fig. 3.1). Individual F1 progeny that either suppressed or enhanced the rough eye phenotypes of the both eyes as compared to the *GMR-*

neu^{YAE},TM3/D flies, were backcrossed to *GMR-neu^{YAE},TM3/D* parental flies. The F2 progeny was rescored for suppression and enhancement for both eyes. Individual F2 progeny (usually males) were mated pair-wise to *yw^{-}; +/+; GMR-neu^{YAE},TM3/D* and *yw^{-}; GMR-neu^{YAE},CyO/Sco; +/+* flies. If the F3 generation shows modifiers only in females, the modifier mutation was thought to have linkage to the X-Chromosome. On the other hand, if half of CyO flies in F3 generation carried modifiers, they were assigned to have linkage to the 2nd chromosome. However, if all the stubble (TM3) flies in the F3 generation carried modifiers, they were mapped to the 3rd chromosome. Using of *GMR-neu^{YAE},CyO/Sco* or *GMR-neu^{YAE},TM3/D* flies in F2 crosses will ease balancing the stock if the mutation is linked to the 2nd or in the 3rd chromosome respectively. The homozygous lethal modifiers were always maintained the stocks as a heterozygote with the *CyO,GMR-Neu^{YAE}* or *TM3,GMR-Neu^{YAE}* balancer chromosome.

3.2.8 *Neu* Specificity And Lethal Complementation Tests

The balanced modifiers were tested for the genetic interactions with various Neu alleles, including *Neu^{YA}*, *Neu^{YB}* and *Neu^{YE}*. The modifiers, usually males were crossed with the *UAS-Neu^{YA},sev-GAL4/CyO*, *UAS-Neu^{YB},sev-GAL4/CyO* and *UAS-Neu^{YE},sev-GAL4/CyO* female in pair-wise. The progeny were tested for the enhancement, suppression or non-modification of the rough eye phenotypes in the CyO+ flies and were documented. On the other hand, the complementation test was carried out by crossing each modifier to the every other of the same chromosome in pair-wise. For example, the balanced 2nd chromosome modifier, *2E01(modifier1)/CyO,GMR-Neu^{YAE}* was crossed with

2E02(modifier2)/CyO,GMR-Neu^{YAE} fly. The modifiers were assigned allelic if they failed to complement each other for lethality.

3.2.9 Meiotic Recombination And Deficiency Mapping

The modifiers were initially mapped by the meiotic recombination mapping for the 2nd and 3rd chromosome. A female heterozygous for the chromosome bearing the mutation and for the marker chromosome, such as *al[1] dp[ov1] b[1] pr[1] c[1] px[1] sp[1]* and *ru[1] h[1] th[1] st[1] cu[1] sr[1] e[s] ca[1]* for the second and third chromosome respectively was generated. This heterozygote female was then crossed *en masse* with the *al[1] dp[ov1] b[1] pr[1]* ***Bl****[1] c[1] px[1] sp[1]/CyO* and *ru[1] h[1] th[1] st[1] cu[1] sr[1] e[s]* ***Pr****[1] ca[1]/TM6B, Bri[1]* for 2nd and 3rd chromosome recombination respectively. The flies from each cross were changed to a new vial at least 2 times for the first two days and at least 3 times for the 3rd and 4th day after setting the crosses to get the maximum number of progeny. The flies from a single recombination were crossed back to the control, *D/TM3,GMR-Neu*^{YAE} flies for the presence of modifiers in that particular recombinant. A relative position of the mutation between two adjacent markers was determination after calculating the recombination rates and proportion of different recombinants with a progeny size of approximately 1500 flies.

After determining the relative position of the modifiers between two adjacent markers, we employed the deficiency mapping to gain a more precise mapping of the mutation. A deficiency chromosome must fail to complement the lethality of the modifier to be considered to uncover the cytological position of the mutation.

3.2.10 Gene Mapping And Verifications

After mapping the mutation with the smallest deficiency spanning only 10 to 20 genes, we verified the mutations with the entire gene or the selective gene mutations of the deficiency-uncovering region. However, for the deficiency regions with unavailable single gene mutation in the publicly available stock centres, we employed the RNAi technique for the 'knock down' of a particular gene to be verified with particular modifiers. The identified genes were then verified at least for Neu and DER specificity. For example, the Neu^{YA} specific candidates were crossed as *UAS-RNAi* (candidate gene) *X UAS-* Neu^{YA}, *sev-GAL4.*

3.2.11 Environmental Electron Microscopy

Adult flies, from the appropriate crosses, were anesthetized by keeping them at the freezer chamber for at least 5 minutes. At least 5 female adult flies from the appropriate genotypes were mounted on the centre of the stand covered with homogenously mixed white glue and charcoal. The fly eyes were viewed, photographed at150X, 300X and occasionally at X800 at 3.0 Torr of a Philips Environmental Scanning Electron Microscope and images were saved in the Hard disk of a Philips computer as TIF files. The images were finally processed with Adobe Photoshop® Version 7.5.

3.3 Results:

3.3.1 Isolation of dominant modifiers (suppressors and enhancers) of *GMR-Neu^{YAE}*

Drosophila EGFR is the ortholog of mammalian Neu/ErbB2. We considered that genes encoding the general factors involved in DER or transgenic Neu/ErbB2 signal transduction are expected to function during multiple signaling events (as redundant genes) at various stages of development. Mutations in these genes are expected to be homozygous lethal and would not be recovered in a conventional F_2 eye phenotype screen. Therefore, in order to identify the components of the mammalian ErbB2 signal transduction pathway in *Drosophila*, we carried out an F1 screen for dominant suppressors and enhancers of an activated *Neu^{YAE}* allele. This activated *Neu* allele was introduced into flies by *p*-element mediated transformation and was expressed under the control of the Glass Multimer Reporter (*GMR*)-enhancer/promoter (*GMR-Neu^{YAE}*). The *p[GMR]* expression vector contains a pentamer of binding sites for the GLASS transcription factor derived from the Rh1 promoter and TATA box sequences from the *Drosophila* hsp70 promoter (Hay et al., 1997). Sequences placed downstream of these sites are transcribed in a similar pattern to *glass* expression, in and posterior to the morphogenetic furrow (MF) during larval and pupal eye development (Ellis et al., 1993). At this stage the ommatidial formation begins and the cells in the imaginal discs respond to differentiate, proliferate, or die (Wolff and Ready, 1993). Therefore, the severely reduced and rough-eye phonotype of *GMR-Neu^{YAE}* flies is likely due to the combination of malfunctioning differentiation, proliferation and cell death. At the cellular level, the rough-eye phenotype may be attributed by improper number of photoreceptor and cone

cells. This phenotype is suitable for the identification of both suppressor and enhancer mutations and provides a suitable sensitized background for a genetic modifier screen (Bach et al., 2003; Therrien et al., 2000; Simon et al., 1991).

A mutation induced by the EMS in one of the two copies present in the diploid genome, should alter the signaling strength and modify the rough-eye phenotype of *GMR- NEU^{YAE}* either positively or negatively. For example, a mutation in one copy of a positively acting downstream gene should reduce signaling strength sufficiently to suppress the *GMR-Neu^{YAE}* rough-eye phenotype. In contrast, a mutation in one copy of the negatively acting downstream gene is expected to increase the signaling strength and therefore, should enhance the *GMR-Neu^{YAE}* rough eye phenotype. In other words, a mutation in a YA specific (but not NYPD or YE) positive regulator will suppress the *Neu^{YA}* rough-eye phenotypes; where as mutations in negative regulator will enhance the rough-eye phenotypes. However, The identification of these mutations in the F1 generation is critical, as many of these genes will be required at earlier stages of development and loss of both copies or homozygous mutation is expected to cause lethality.

Based on the scheme outlined in Fig. 3.1, we screened 61,241 progeny in the F1 generation to score the enhancement or suppression of the *GMR-Neu^{YAE}* rough-eye phenotype. A total of 856 (1.39%) modifiers were isolated in the F1 generation and 195 (22.8%) of them bred to the F2 generation (Table 3.1). The suppressors were scored by looking for reduced blistering and ommatidial fusions, as well as the reappearance of the

Figure 3.1: Mutagenesis Scheme for the enhancers and suppressors of the *GMR-Neu^{YAE}* eye phenotype. A cross scheme is shown for the screen of the sex chromosome and autosomes for dominant modifiers of the *GMR-Neu^{YAE}* rough eye phenotype. EMS treated OregonR males, isogenized for the 2nd and 3rd chromosomes were mated to *+/+; +/+; TM3[sb], GMR-Neu^{YAE}/D* flies. The F1 male and female *TM3[sb]* progeny were scored for altered eye roughness as compared to the parental flies. The individual modifier (either male of female) was backcrossed to the parental flies and was rescored for suppression and enhancement for both eyes. Males from this F2 progeny were mated pair-wise to *yw^{-}; +/+; GMR-Neu^{YAE},TM3/D* and *yw^{-}; +/+; GMR-Neu^{YAE},CyO/Sco; +/+* flies. If the F3 generation shows modifiers only in females, the modifier mutation was thought to have linkage to the X-Chromosome. On the other hand, if half of *CyO* or all *TM3[sb]* flies in the F3 generation carried modifiers were thought to have linkage to the 2nd and 3rd chromosome respectively. See materials and methods for information about the transgenic allele construction and subsequent *Neu* verification, complementation tests and gene mapping.

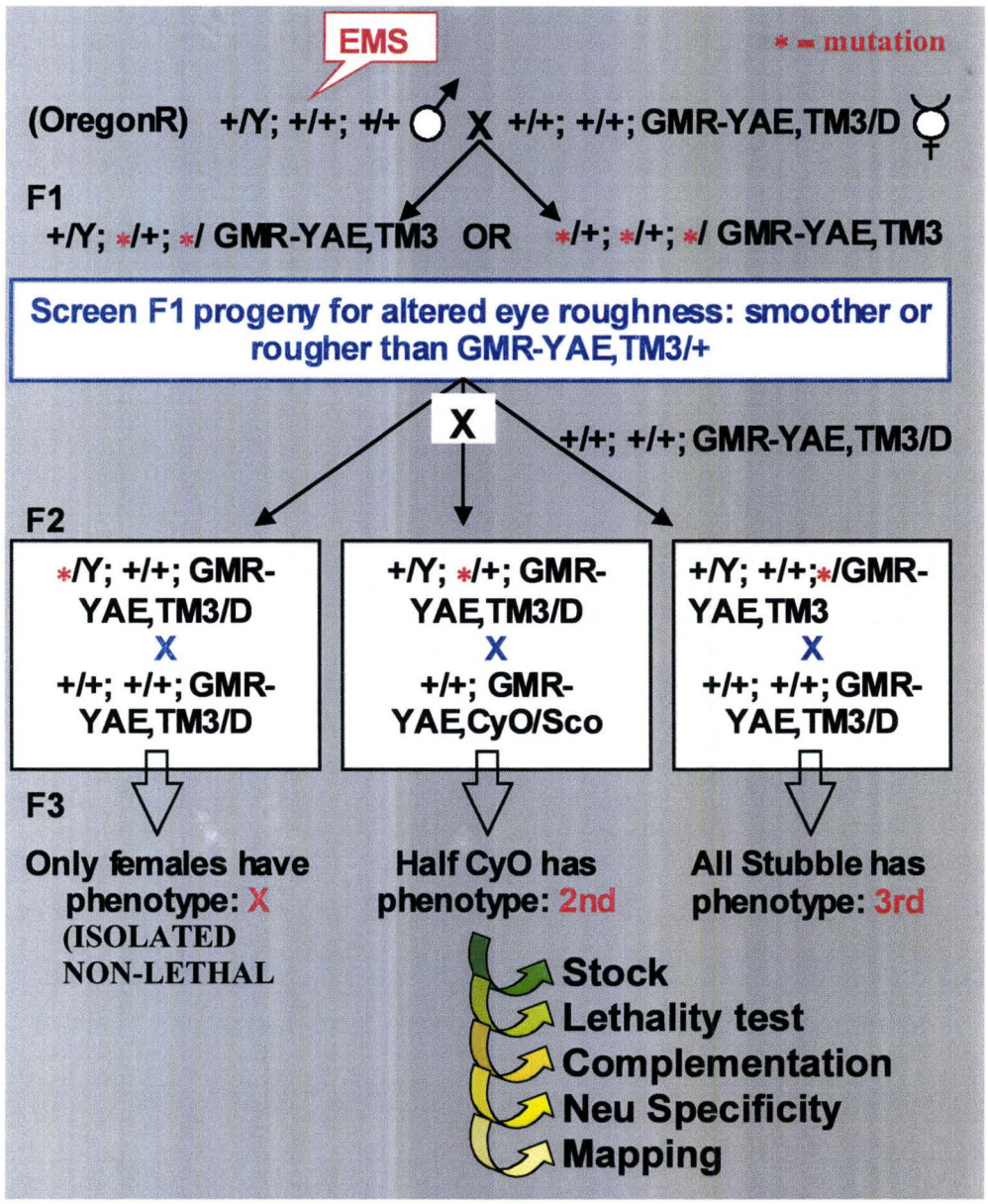
EMS
* = mutation
(OregonR) +/Y; +/+; +/+ X +/+; +/+; GMR-YAE,TM3/D
F1
+/Y; */+; */ GMR-YAE,TM3 OR */+; */+; */ GMR-YAE,TM3
Screen F1 progeny for altered eye roughness: smoother or rougher than GMR-YAE,TM3/+
X
+/+; +/+; GMR-YAE,TM3/D
F2
*/Y; +/+; GMR-YAE,TM3/D X +/+; +/+; GMR-YAE,TM3/D
+/Y; */+; GMR-YAE,TM3/D X +/+; GMR-YAE,CyO/Sco
+/Y; +/+;*/GMR-YAE,TM3 X +/+; +/+; GMR-YAE,TM3/D
F3
Only females have phenotype: X (ISOLATED NON-LETHAL
Half CyO has phenotype: 2nd
All Stubble has phenotype: 3rd
Stock
Lethality test
Complementation
Neu Specificity
Mapping

Table 3.1: Summary of mutagenesis screening.

Total F1 Progeny Screened	F1 Modifiers			F2 Modifiers			YA/YE Specificity	
	Enhancer	Suppressor	Total	Enhancer	Suppressor	Total	Specific	Non-specific
61, 241	498	348	856	**105**	**90**	**195**	**60**	**135**

Figure 3.2: Isolating dominant modifiers. We have performed a genetic screen to isolate modifiers of the *GMR-Neu^{YAE},TM3* rough eye phenotype (A, B). EMS treated OregonR males (A) were crossed with *GMR-Neu^{YAE},TM3/D* virgins (B). The F1 progeny were screened either for suppression (C) or enhancement (D) compared to the rough eye phenotype in control flies (B). In order to identify the modifiers specific to either *Neu^{YA}* or *Neu^{YE}* or to both, all modifiers were tested against *Neu^{YA}*, *Neu^{YB}* and *Neu^{YE}*. Modifiers showing any genetic interaction with *Neu^{YB}* (either by suppression or enhancement) didn't comprise our screening criteria and were discarded (Data not shown). On the other hand, modifiers specific to either *Neu^{YA}* or *Neu^{YE}* or to both were studied further. For example, the suppressor, 3S05 was *Neu^{YA}* specific as the modifiers specifically suppressed the rough-eye phenotype induced by the *Neu^{YA}* (compare E, F and H, I). However, the 3E03 enhancer was identified specific to *Neu^{YE}*, as it specifically enhanced the rough-eye phenotypes induced by the *Neu^{YE}* only (compare E, G and H, J). The photographs were taken at X150 (A-D) and X800 (E-J) magnification using an ESEM. The genotypes are indicated at the top right of each panel. Bar indicated 50 μm. Also see Supplement 3.3, Supplement 3.4 for more modifiers and Supplement 3.5, and Supplement 3.6 for complete *Neu*-allele verification.

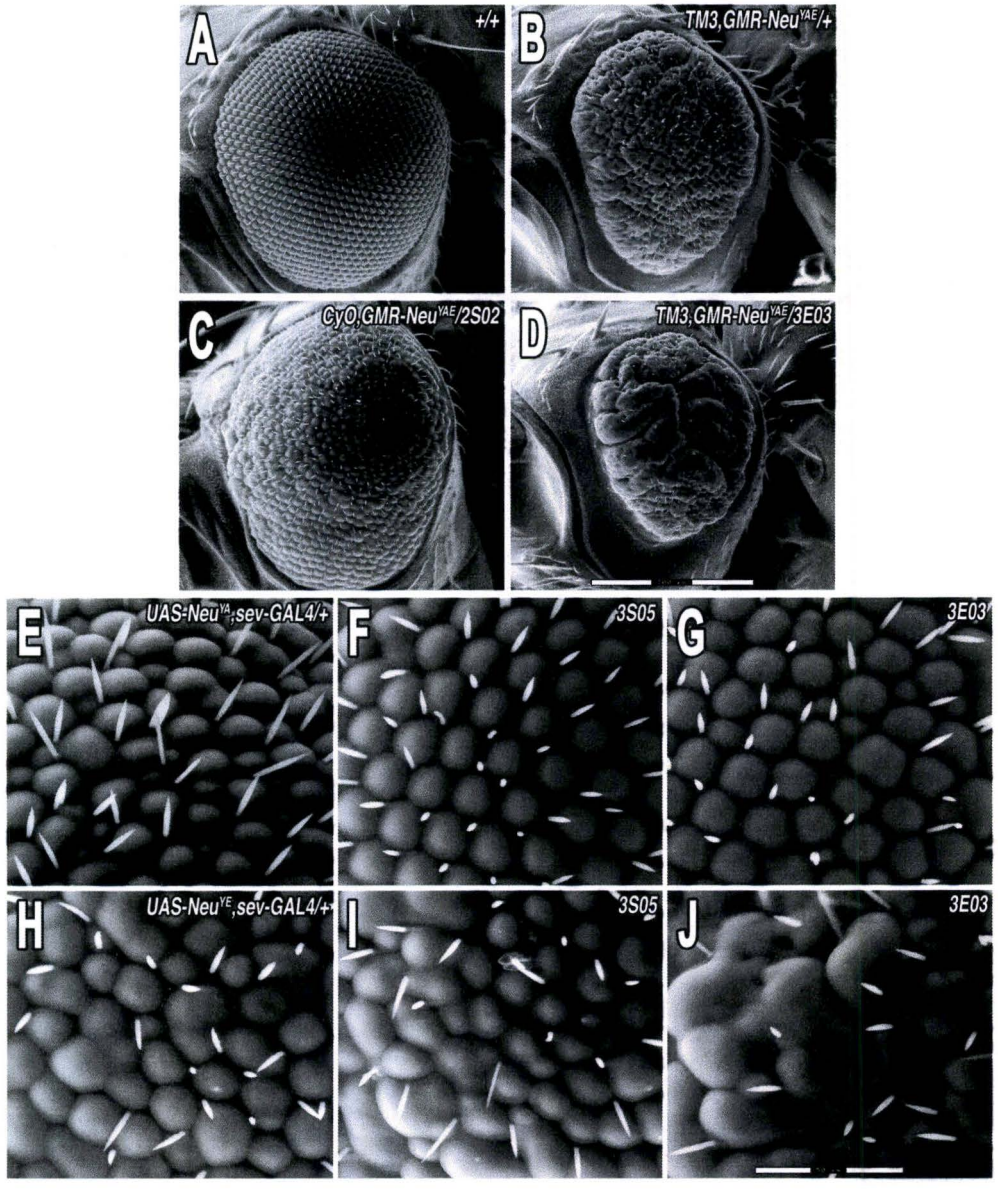
A
+/+
B
TM3,GMR-Neu^YAE/+
C
CyO,GMR-Neu^YAE/2S02
D
TM3,GMR-Neu^YAE/3E03
E
UAS-Neu^YA;sev-GAL4/+
F
3S05
G
3E03
H
UAS-Neu^YE;sev-GAL4/+
I
3S05
J
3E03

straight ommatidial rows and eye sizes. Enhancers were scored by looking for an increased in eye roughness or reduced eye size (Fig. 3.2). The modifiers showed a wide range of eye-phenotypes either as a suppressor or as an enhancer (Supplement 3.5 and Supplement 3.6). Depending on the genetic interaction with various 'add-back' *Neu* alleles, these modifiers were categorized based on the *Neu* specificity (see Materials and methods). Out of the 195 dominant modifiers in the F_2 generation, 60 (30.8%) were specific to either Neu^{YA} or Neu^{YE} or to both (Table 3.2). As predicted many of the dominant modifier genes were recessive lethal, a significant number of enhancers and a few suppressors were homozygous viable with no apparent phenotypes. For this study we continued characterizing only the homozygous lethal modifiers specific either to Neu^{YA} or Neu^{YE} only. The chromosomal linkage of these dominant modifiers were performed as outlined in Fig. 3.1 and balanced stocks were established as the modifiers (m) /CyO,*GMR-*Neu^{YAE} or modifiers (m)/TM3, *GMR-*Neu^{YAE}.

3.3.2 Neu specific modifiers comprised 24 complementation groups

A lethal complementation test was used to identify possible allelism between the modifiers. The complementation test was carried out by performing pair-wise crosses of all the *Neu* specific mutants on a particular chromosome. Most of the *Drosophila* genes (almost 60%) are considered to be redundant and will not result in an obvious phenotype or of lethality even though genes were 'knocked-out' (Adams et al., 2000). We expected that many of the *Neu* specific modifiers, were unlikely to result in a homozygous mutant

Table 3.2: Complementation groups phenotypically linked to YA or YE.

All alleles						All Complementation Groups		
Modifier	**Homozygous Lethal and Neu Specificity**			**Homozygous Viable**	**Linkage to Chromosome**			
	YA	**YE**	**YA/YE**			**YA**	**YE**	**YA/YE**
Suppressors	4	2	3	6	2nd Chromosome	13	7	4
Enhancers	5	3	5	7				
Suppressors	3	2	4	1	3rd Chromosome			
Enhancers	8	4	3	0				
Total	**20**	**11**	**15**	**14**		**24**		

Data based on total 60 *Neu*-specific modifiers reported in Table 3.1.

Table 3.3: Summary of the genetic interactions of the 2nd chromosome modifers.

Complementation Group	Members/alleles	Approximate cytological location	Neu Modification/Specificity YA	YB	YE
Enhancers:					
2E01	**2E01, 2E11, 2E12**	**47E3;48B2**	**-/0**	**0**	**0**
2E02	2E02	38B5-B9;52D3-D7	--	0	0
2E03	**2E03**	**55A1;55C3**	**--**	**0**	**0**
2E04	2E04	24F4-25A1;34D1-D1	--	0	0
2E05	2E05	38B5-B9;52D3-D7	0	0	++
2E07	2E07	24F4-25A1;34D1-D1	+	0	++
2E09	**2E09, 2E10**	**55A1;55C3**	**+**	**0**	**++**
2E13	2E13	38B5-B9;52D3-D7	+	0	0
2E14	2E14	38B5-B9;52D3-D7	+	0	0
Suppressors:					
2S02	**2S02, 2S04, 2S05, 2S06, 2S07**	**23C1-2;23E1-2**	**--**	**0**	**0**
2S03	2S03	38B5-B9;52D3-D7	0	0	-
2S08	2S08	38B5-B9;52D3-D7	0	0	+
2S10	2S10	38B5-B9;52D3-D7	0	0	0

+: Enhancement, -: Suppression, 0: Non-interaction, Modifiers in **bold** have been studied further. Data based on 20 out of total 22 2nd chromosome modifiers reported in table 3.2.

Table 3.4: Summary of the genetic interactions of the 3rd chromosome modifers.

Complementation Group	Members/alleles	Approximate cytological location	Neu Modification/Specificity YA	YB	YE
Enhancers:					
3E01	**3E01, 3E03, 3E10**	**75A4;75A5**	**--**	**0**	**++**
3E04	**3E04, 3E05**	**75A6-7;76C1-2**	**--**	**0**	**0**
3E06	**3E06**	**74B2;74D2**	**-**	**0**	**0**
3E08	3E08	93C7-D1;99C2-C2	--	0	0
Suppressors:					
3S02	3S02	86D3-D4;90E4-F1	0	0	--
3S03	3S03, 3S05, 3S11, 3S12	66D10-D10;72D1-D1	--	0	0
3S04	3S04	75A6-7;76C1-2	++	0	0
3S06	3S06	75A6-7;76C1-2	++	0	0
3S09	3S09	86D3-D4;90E4-F1	+	0	+
3S10	3S10	72D1-D1;73A1-A3	0	0	++
3S13	3S13	72D1-D1;73A1-A3	0	0	--

-: Suppression, +: Enhancement, 0: Non-interaction, Modifiers in **bold** have been studied further. Data based on 17 out of total 24 3rd chromosome modifiers reported in table 3.2.

phenotype. Although these redundant genes can be of interest in Neu/ErbB2 signaling, it may be very difficult to identify and study their functions. For this reason, we decided to pursue only those genes corresponding to the complementation groups that could be identified in a timely manner. Therefore, we tested each modifier-containing chromosome for homozygous lethality in an otherwise wildtype background. Basically, if the homozygous lethality is due to the modifier, the members of the same complementation group will be allelic. As such, the modifiers, which failed to complement each other for lethality, were assigned in the same group. A total of 24 complementation groups were isolated from the *Neu* specific alleles (Table 3.2, 3.3, 3.4; Supplement 3.5 and Supplement 3.6). The 2nd chromosome modifiers constituted three larger complementation groups having at least 3 members in the same group. All these *Neu* specific modifiers were mapped individually by employing meiotic recombination mapping for the 2nd and 3rd chromosome depending on the chromosomal linkage analysis done earlier.

Meiotic recombination mapping identified the modifiers spanning the entire chromosomal arms of both the 2nd and the 3rd chromosome (Fig. 3.3). However, the largest complementation group comprised of five suppressors (2S02, 2S04, 2S05, 2S06 and 2S07) mapped between the recessive marker *al* and *dp* or between the cytological region of 21C1 and 24F4 (Fig. 3.3; Panel A1). The 2E01 enhancer complementation group (2E01, 2E11 and 2E12) mapped between the marker *pr* (38B5-B9) and *c* (52D3-D7), while the 2E09 complementation group (2E09 and 2E10) mapped between the marker *c* (52D3-D7) and *px* (58E4-E8). On the 3rd chromosome 17 modifiers (enhancers

Figure 3.3: Schematic representation of the relative mapping positions of the modifiers. The positions of the modifiers were determined by the meiotic recombination followed by large chromosomal deficiency mapping. For this study, our efforts were concentrated mapping only the allelic enhancers (multiple members in the same complementation group). However, an allelic group of five suppressors in the 2nd chromosome was also mapped for the validation of the mapping scheme. The map position of the allelic groups was also determined the non-complement for lethality of the modifiers with the deleted chromosome region uncovering the estimated region. The cytological locations of several non-complementing deficiencies are shown. Panel A1 shows the 2nd chromosome modifiers spanning both chromosomal arms. Out of 12 complementation groups, we selected only one allelic group from the suppressors (2S02, 2S04, 2S05, 2S06 and 2S07) and two allelic groups from enhancers (2E01, 2E11, 2E12 and 2E09, 2E10) to map out. On the other hand, Panel B1 shows the relative positions of the 3rd chromosome modifiers. Here out of 12, only 3 enhancer groups have been selected for further mapping. See text for detail description. Supplement 3.7 shows the standard calculation methods for the determination of a rough position of a modifier between two visible markers.

A1: Meiotic recombination mapping of 2nd Chromosome modifiers (not to the scale).

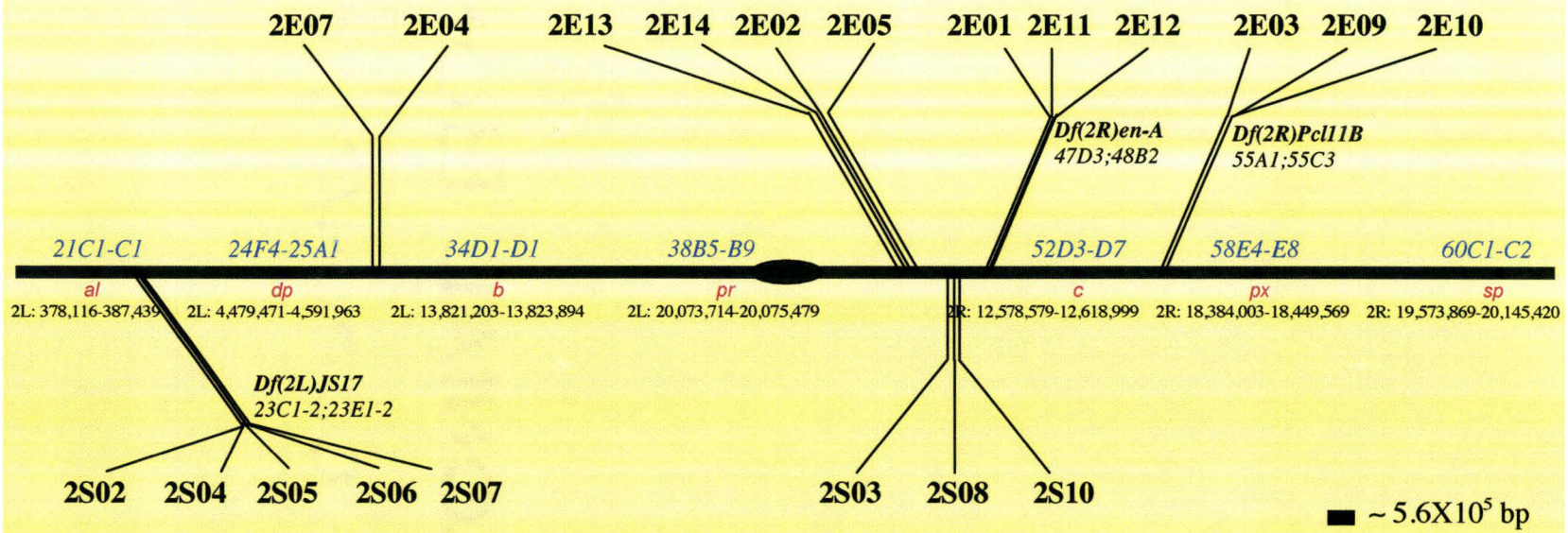

B1: Meiotic recombination mapping of 3rd Chromosome modifiers (not to the scale).

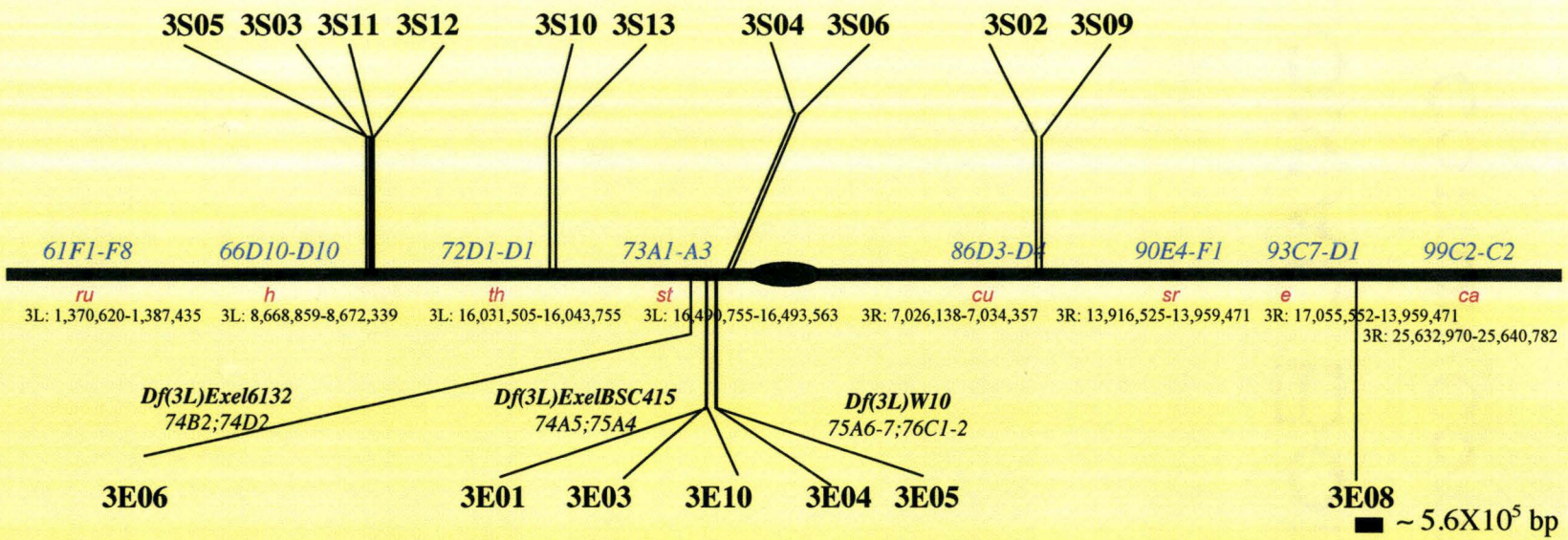

and suppressors) comprised 12 complementation groups, three of them having at least 2 members in them (Fig. 3.3; Panel B1). The largest complementation group comprised with 3 enhancers (3E01, 3E03, and 3E10) mapped between the markers *st* (73A3-A3) and *cu* (86D3-D4). On the other hand, one complementation group containing 4 suppressors (3S03, 3S04, 3S11 and 3S12) mapped between *h* (66D10-D10) and *th* (72D1-D1). In this study, we continued further mapping of the 3-enhancer group mapped between the *st* (73A3-A3) and *cu* (86D3-D4) markers. In this study, we report the mapping of the 2S02, 2E01 and 3E01 complementation group. However, the homozygous viable modifiers (enhancers or suppressors) were not studied further in this report. Even though almost 500 deficiency lines were used, I did not find a Df for 2S03, 2S08, 2S10, 2E02, 2E04, 2E05, 2E13, 2E14, 3S02, 3S03, 3S04, 3S05, 3S06, 3S09, 3S11, 3S12, 3S13, and 3E08.

3.3.3 Meiotic recombination and deficiency mapping showed relative map position of the modifiers

As mentioned earlier, here we only continued mapping the complementation groups constituting of at least two modifiers. In other word, we only mapped the modifiers with more than 1 allele. After determining the relative position of the modifiers between two adjacent markers by using meiotic recombination mapping as shown earlier, we employed deficiency mapping to gain a more precise position of the mutations. The map position of the complementation groups was determined by the non-complement for lethality of the group members of the modifiers *in trans* with deleted chromosomal region uncovering the region. On the 2nd chromosome, deficiency mapping identified the

complementation group 2S02, 2E01 and 2E09 to be non-complemented by Df(2L)JS17, Df(2R)en-A and Df(2R)Pcl11B respectively (Fig. 3.3, Panel A1).

On the 3rd chromosome the 3E01, 3E04 and 3E06 complementation groups were identified to be non-complemented by Df(3L)BSC415, Df(3L)W10, and Df(3L)Exel6132 and respectively (Fig. 3.3, Panel B1). Due to having required Df stock, we mapped the 3rd chromosome complementation group, 3E06 even though it has a single member in them (Fig. 3.3 Panel B1). After mapping the mutations with larger deleted segment, for more precise mapping, we used smaller deficiencies, uncovering the entire deleted regions identified earlier. The smaller deficiency usually uncovered regions ranging from10-30 predicted genes.

3.3.4 Identification of the 2nd chromosome 2S02 suppressor group as *lilliputian*

The 2S02 complementation group has 5 members. These allelic mutants initially failed to complement for lethality with the Deficiencies Df(2L)C144, Df(2L)JS17 and Df(2L)*Lilli*[K05431] respectively. On the other hand, this group was complemented for lethality (viable over) with Df(2L)N6, Rbp9[B], Df(2L)Rrp1 and Df(2L)CG9643 (Fig. 3.4). Therefore, we postulated that these modifiers are to be allelic to *Lilliputian*. *lilli* is a gene within Df(2L)C144 and has been identified as a dominant suppressor of ectopic phenotypes in at least 10 screens (Anderson et al. 2005; Luschnig et al. 2004; Li and Li 2003; Su et al. 2001; Li et al. 2000; Rebay et al. 2000; Greaves et al. 1999; Neufeld et al. 1998; Dickson et al. 1996; Perrimon et al. 1996). A study done by Su et al. (2001) identified the *Lilliputian* gene in the 23C1 segment by failing to complement the

Figure 3.4: Deficiency mapping of the 2S02 complementation group. Schematic representation of the cytological region 23C-D. The cytological locations of several deficiencies are shown. The deficiency lines indicated by the red lines denote the non-complementation for lethality with the modifiers of the 2S02 complementation group. A *lilli*$^{A17\text{-}2}$ mutation also non-complemented for the lethality verifying the 2S02 suppressors are to be *Lilliputian.*

Title: Deficiency mapping of the 2S02-suppressor complementation group.

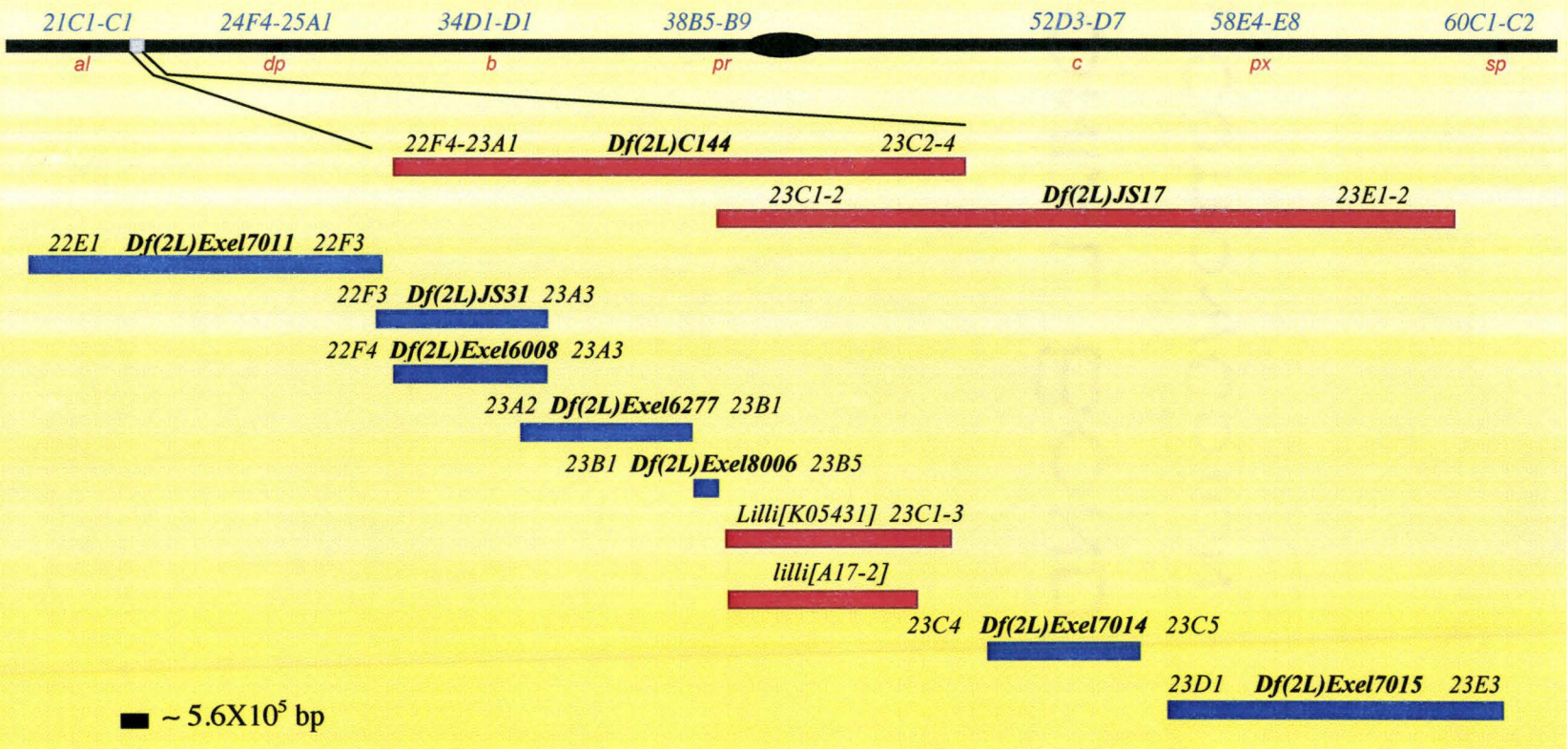

mutations with the same deleted region used in our study. *Lilliputian* was also identified in two other screens for Ras/Mitogen-activated protein kinase (MAPK) signal transduction pathway components. First, *Lilli*putian was identified as a suppressor of gain-of-function phenotypes of *seven in absentia* (SS2-1; Newfeld et al., 1998). Secondly, a screen for gain-of-function phenotypes of *yan* also identified *Lilli* as a suppressor (SY2-1; Rebay et al., 2000).

The complementation tests showed that all of our modifiers failed to complement both the *lilli* deficient line Df(2L) *lilli*[K05431] and a $lilli^{A17\text{-}2}$ lethal mutation allele (Fig. 3.4). Therefore, we conclude that these 5 modifiers are allelic to *lilli*. *lilli* is known to have interactions with various pathways, such as the Ras, Dpp/TGF-β and ecdysteroid pathways (Hasson and Paroush, 2006; Sundaram, 2005; Su et al., 2001).

3.3.5 *Lilliputian* modifies the phenotype induced by the Sevenless (Sev) receptor tyrosine kinase

The *lilli* gene is required for normal cytoskeleton organization, cell size determination, and embryo segmentation. It genetically interacts with each of the Wnt, AKT, and EGFR pathways (Gu and Nelson 2003; Su et al., 2001; Tang et al., 2001; Wittwer et al., 2001). To verify the genetic interactions of *lilli* with the Neu^{YA}-interacting receptor tyrosine kinases, such as *Drosophila*-DER and Sevenless tyrosine kinase, we made heterozygotes of $lilli^{A17\text{-}2}$ mutations with various other *Neu* 'add-back' alleles (Fig. 3.5). The 2S02 complementation group was originally identified as a Neu^{YA} specific suppressor. In consistent with our earlier data, $lilli^{A17\text{-}2}$ showed no genetic interaction with

Figure 3.5: *lilli* mutant shows suppression of the Sev-Torso chimeric eye phenotype. In heterozygote with the control flies, *lilli*$^{A17\text{-}2}$ mutant shows eye phenotype suppression with the *Neu*^{YA} (compare A and B) and with the *Neu*^{NYPD} (compare G and H), while no genetic interaction with the *Neu*^{YB} (compare C and D) and *Neu*^{YE} (compare E and F). This NYPD specific suppressor also showed genetic interaction with the Sev-Torso chimeric signaling allele, while suppressing the rough eye phenotype (compare K and L). However, *lilli*$^{A17\text{-}2}$ mutant was insensitive to the *Drosophila* endogenous EGFR Ellipse-mutant, *Elp*^{B1}, showing no genetic interaction (compare I and J). Images were taken at X800 magnification on an ESEM (also see supplement 3.8 for other magnifications). Transgenes are indicated on the top right of each panel. Bar indicated 50 μm.

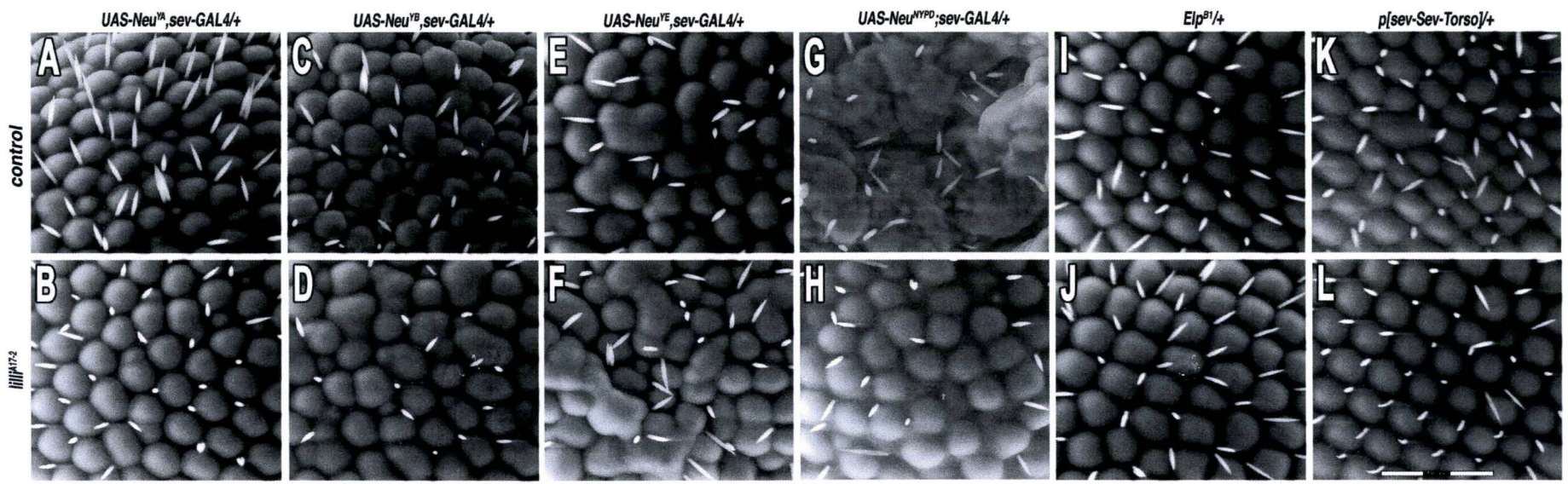
UAS-Neu^YA,sev-GAL4/+
UAS-Neu^YB,sev-GAL4/+
UAS-Neu^YE,sev-GAL4/+
UAS-Neu^NYPD;sev-GAL4/+
Elp^B1/+
p[sev-Sev-Torso]/+
control
Ik17-2
A
B
C
D
E
F
G
H
I
J
K
L

misexpressed Neu^{YB} and Neu^{YE}. Moreover, the gain-of-function DER mutant allele, Elp^{B1} was phenotypically insensitive to $lilli^{A17-2}$. However, $lilli^{A17-2}$ mutant completely suppressed the rough eye phenotypes of Sev-Torso chimera (Supplement 3.8). It has been reported that in *lilli* mutant clones, normal eye cell-fate specification is not disrupted but the photoreceptor rhabdomeres are smaller in size than those of wild-type rhabdomeres (Tang et al. 2001; Wittwer et al. 2001). A reduced signaling output in *Sev-Torso/lilli* heterozygote may result in the suppression of rough eye phenotype, as seen in Sev-Torso chimeric flies due to supernumerary R7 photoreceptor (Karim et al., 1996). Lack of interaction between $lilli^{A17-2}$ and Elp^{B1} may be due to the involvement of a parallel signaling pathway to EGFR signaling cascade during the *Drosophila* eye development. In fact, *lilli* was shown to function in the Dpp/TGF-β signaling pathway in parallel to the EGFR signaling during the dorsal ventral boundary formation in the developing *Drosophila* wing (Bejarano et al., 2008).

3.3.6 Identification of the 2nd chromosome 2E01 group as potential of being *CG7777*

In this study, our target is to identify the genes that negatively regulate the Neu^{YA} signaling. As such, we put much of our effort in mapping YA-specific enhancers isolated from this large-scale genetic screen. We have identified at least 3 complementation groups with more than one member (Fig. 3.3; Table 3.4 and 3.5). Moreover, having the available deficiency lines due to close proximity to the 3E01 enhancer groups, we have

Table 3.5: Summary of Deficiency Screening.

Bloomington Deficiency stock	Symbol	Effect	Break points	Gene identified	Verified with (or be verified)	Total alleles identified
1567	Df(2L)JS17	Su	23C1-2;23E1-2	Lilliputian (lilli)	Gene mutation allele	5 *(2S02, 2S04 2S05. 2S06, 2S07)*
1142	Df(2R)en-B	En	47E3;48B2	CG7777	P-element mutation allele	3 *(2E01, 2E11 2E12)*
25719	Df(2R)BSC231	En	47F8;48B6	----	Gene mutation allele	2
9413	Df(2R)ED3636	En	55B8;55E3	----	---	2
24919	Df(3L)BSC415	En	74A5;75A4	----	---	2
7611	Df(3L)Exel6132	En	74B2;74D2	----	---	2

Su: Suppression, En: Enhancement

Figure 3.6: Deficiency mapping of the 2E01-enhancers complementation group. Schematic representation of the cytological region 47D3-48B2. The cytological locations of several deficiencies are shown. The deficiency lines indicated by the red lines denote the non-complementation for lethality with the modifiers of the 2E01 complementation group. A *P*-element insert at the CG7777 locus non-complemented for the lethality, verifying the 2E01 enhancers are to be the *Drosophila* homolog of mammalian Aqaporin 4 (AQP4).

Title: Deficiency mapping of the 2E01-enhancer complementation group

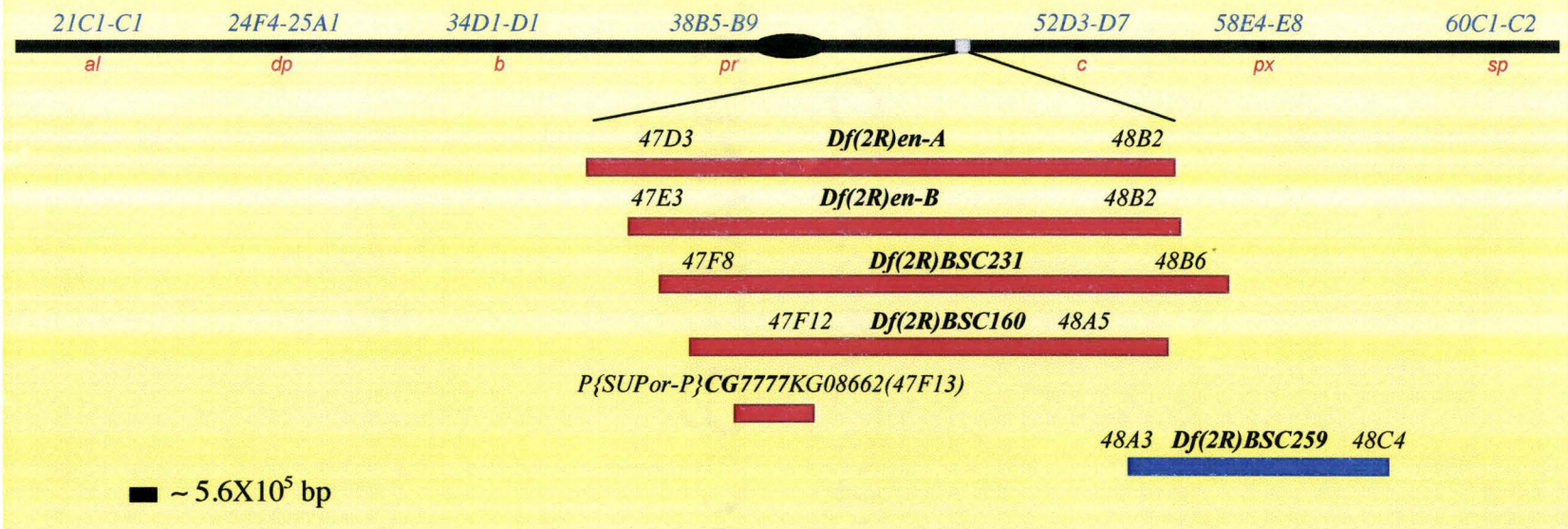

also been trying to map the 3E06 and 3E04 complementation groups. On the 2nd chromosome, 2E01 complementation group comprised of 3 members, including 2E01, 2E11 and 2E12. These allelic mutants failed to complement for the lethality with Deficiencies Df(2R)en-A, Df(2R)en-B, Df(2R)BSC231and Df(2R)BSC160. On the other hand, these allelic chromosomes complemented with (viable over) Df(2R)BSC259 (Fig. 3.6). The smallest deleted region, Df(2R)BSC160 uncovers 8 genes, including *CG30026, CG34054, CG7763, CG7777, CG33472, E(Pc), inv* and *CG30034*. Due to the unavailability of the mutant alleles for each of these loci, we failed to verify all the candidates in this region.

However, we ruled out *E(Pc)* and *inv* as the potential candidates, since both of these mutants complemented with all of our 2E01-enhancers. Interestingly, 2E01 enhancers were lethal over the *P*-element insert at the loci CG7777, (P{SUPor-P}CG7777KG08662). The *P*-element insert in CG7777 selectively enhanced the rough eye phenotypes of Neu^{YA} (Fig. 3.8). Originally identified as a Neu^{YA} specific, the 2E01 enhancer group showed no genetic interaction with Neu^{YB}, while a weak interaction with Neu^{YE} (Fig. 3.7). However, a strong phenotypic enhancement was shown in the $Elp^{B1}/CG7777^{KG08662}$ heterozygote. At this point we cannot conclude that the candidate gene is to be the *CG7777*, as there is no available *CG7777* deficiency or mutant line in the public stock centres. Further screen with the RNAi transgenic lines of *CG7777* gene and other members of that region is worth doing to identify the bonafide candidate. In case of unavailable RNAi transgenes or gene mutation in public stock centres, the molecularly

Figure 3.7: *Neu* specificity of the 2E01-enhancer complementation group. The 2E01-enhancers showed a dual specificity with Neu^{YA} as a suppressor (compare A and D), where as with Neu^{YE} as an enhancer (compare C and F). However, the enhancers didn't show any genetic interaction with the Neu^{YB} (compare B and E).

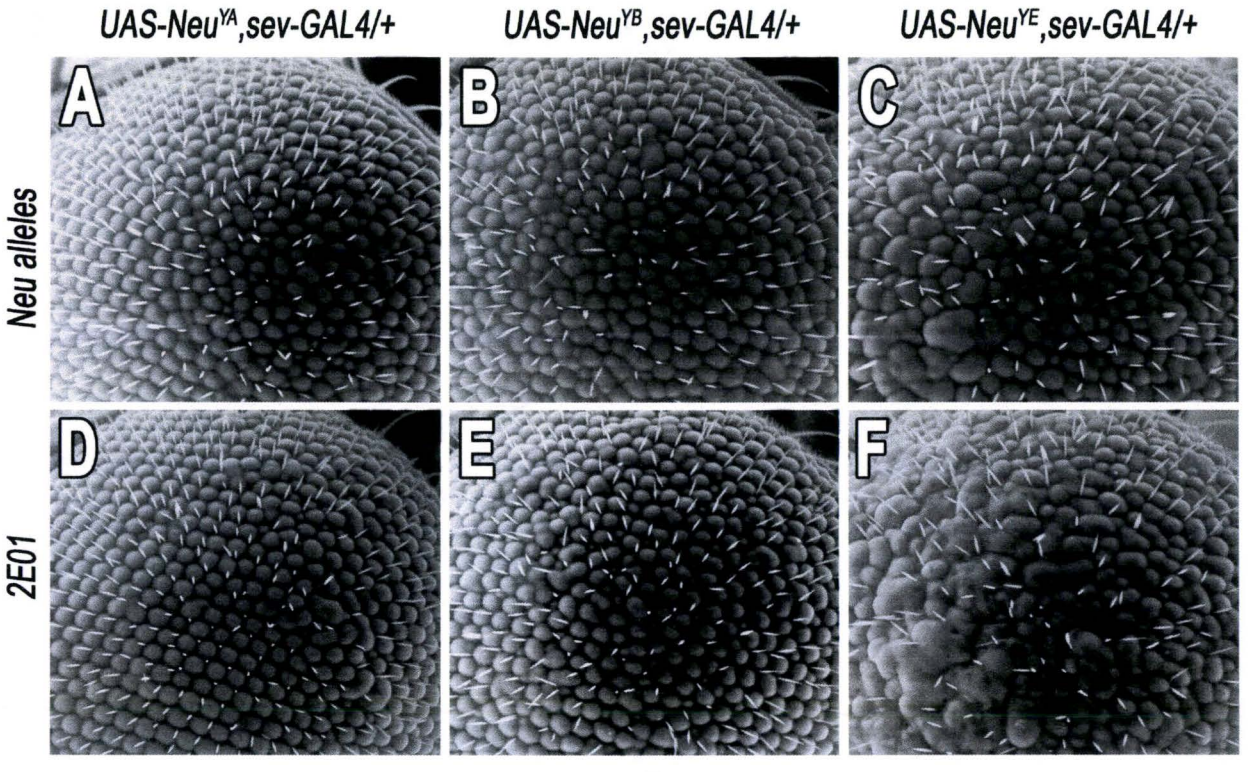
UAS-Neu^YA,sev-GAL4/+
UAS-Neu^YB,sev-GAL4/+
UAS-Neu^YE,sev-GAL4/+
Neu alleles
2E01
A
B
C
D
E
F

Figure 3.8: *CG7777*^{KG08662} mutant shows strong enhancement of the *Drosophila*-EGFR (*Elp*^{B1}) eye phenotype. The novel enhancer, CG7777 strongly enhanced the *Neu*^{YA} rough eye phenotypes (compare A and B). This dual specific (YA and YE) novel gene also showed strong genetic interaction with the *Neu*^{YAE} and the gain-of function DER Ellipse mutant, *Elp*^{B1}, while enhancing the eye phenotypes significantly (compare C and D; E and F). However, a non- genetic interaction was observed with the Sev-Torso chimera (G and H). Images were taken at X150 magnification on an ESEM (also see supplement 3.9 for other magnifications). Transgenes are indicated on the top right of each panel. Bar indicated 300 μm.

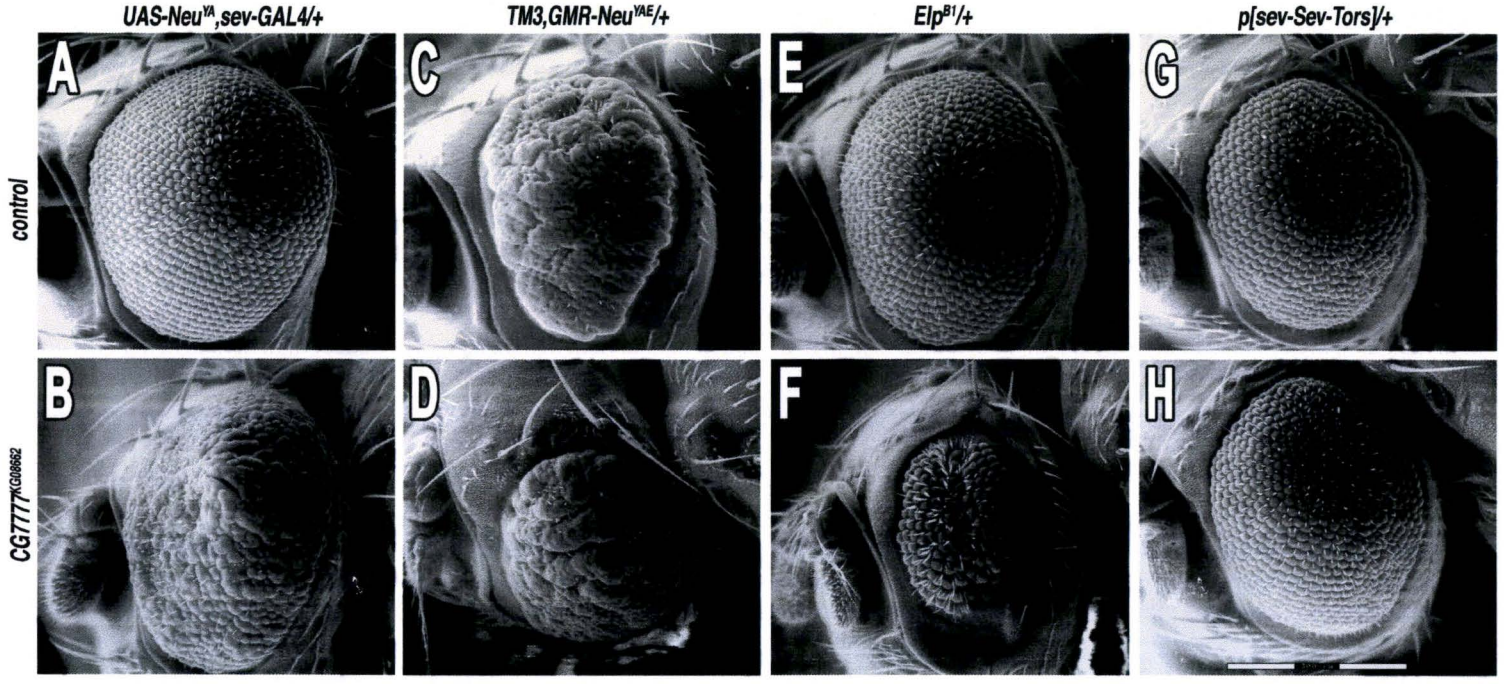
UAS-Neu^YA,sev-GAL4/+
TM3,GMR-Neu^YAE/+
Elp^B1/+
p[sev-Sev-Tors]/+
control
CG7777^KG08662
A
B
C
D
E
F
G
H

defined precise excision or the undefined imprecise excision by the *P*-element can be used to generate expected mutation to map the novel loci.

We have previously postulated that Neu^{YA} may reduce the RTK signaling possibly by recycling the receptors back to the plasma membrane or by facilitating trafficking of the signaling molecules for the lysosomal degradation (Chapter 2). If our hypothesis is true, one, from such a Neu^{YA} screening, would expect to isolate modifier genes that either contributes to the receptor recycling or to receptor degradation. The Blast search results indicate that the CG7777 is the sole *Drosophila* homolog of human Aquaporin 4 (AQP 4). The aquaporins (AQPs) are integral membrane proteins whose main function is to transport water across cell membranes in response to osmotic gradients. If final mapping identifies the candidate to be CG7777 or AQP 4, it is possible that this protein signals through EGFR mediated pathway. We would also expect to see phenotypic enhancement of Neu^{YA} as seen in $Neu^{YA}/p[CG7777]$ heterozygote (Fig. 3.8). This enhanced eye phenotypes is possibly due to increased or a longer duration of EGFR signaling resulting from the modulation of two above-mentioned signal attenuation steps.

3.4 Discussion:

The short generation time and large number of progeny have made *Drosophila melanogaster* one of the best model systems for performing large-scale genetic screening for mutations that affect a given process. The *GMR* enhancer/promoter initiates expression in the eye disc, in rows 4–6, posterior to the Morphogenetic Furrow (MF), when the photoreceptors R2, R3, R4, R5, and R8 are already present and photoreceptors R1 and R6 are joining the ommatidial precluster (Wolff and Ready 1993). Here, we show that *GMR*-induced expression of the Neu^{YAE} allele results in rough-eye phenotypes suitable for the identification of both suppressor and enhancer mutations specific to particular *Neu* pTyr. For large-scale genetic screening, a dominant modifier screen is the most efficient; as it allows identifying the effectors based on the phenotypic enhancement or suppression in the F1 (First generation) progeny. However, many redundant genes with no apparent phenotypes (or lethality), when mutated to a loss of function, are very difficult to identify in such screens (Adams et al., 2000; Miklos and Rubin, 1996). In this regard, cell culture-based RNAi quantitative screenings have been more efficient (Friedman and Perrimon, 2007).

In this study we screened a total of 61,241 F1 progeny and isolated 856 (1.3%) modifiers. Out of 856 modifiers, 195 (0.3%) bred to the F2 generation (Table 3.1). The low percentage of isolation of F1 modifiers was likely due to the selection of only strong modifiers. In order to map the modifiers in an efficient manner, we chose to study the modifiers, which were homozygous lethal and specific to either the Neu^{YA} or Neu^{YE} (Table 3.2, 3.3, 3.4; Supplement 3.5 and Supplement 3.6).

During meiotic recombination mapping at least 1500 progeny from each modifier was screened to determine the rate of recombination. However, more often this number showed to be insufficient, as a significant recombination chromosomal distance was calculated between two alleles of the same complementation group. The relative wide spread distribution on both the 2nd and 3rd chromosome arms and a significant number of hits at the same loci (allelic) signify the saturation of our mutagenesis (Fig. 3.3). However, we expected that no modifier could be isolated either in the X or in the 4th chromosome. *Drosophila* male carries a single copy of X-chromosome and be hemizygous lethal for any lethal mutation on this chromosome. On the other hand, a shorter 4th chromosomal arm is quite unlikely to have a hit with our administered EMS concentration.

In this report we chose to map one suppressor and most of the enhancer groups, having at least two members in them, to be most efficient with available time, manpower and genetic tools. Further mapping of the rest of the modifiers is likely to identify more novel genes those attenuate RTK signaling, at least in *Drosophila.*

3.4.1 Identification of the 2nd chromosome 2S02 suppressor group as *lilliputian*

The identification of *lilli* in our screen validates our screening. *Lilli* has been identified as a dominant suppressor of ectopic phenotypes in at least 10 screens (Anderson et al. 2005; Luschnig et al. 2004; Li and Li 2003; Su et al. 2001; Li et al. 2000; Rebay et al. 2000; Greaves et al. 1999; Neufeld et al. 1998; Dickson et al. 1996;

Perrimon et al. 1996). Our deficiency mapping identified the same non-complementing deletions as with all the groups, which also identified *lilli* (Su et al., 2001; Rebay et al., 2000; Newfeld et al., 1998). The transcription factor, *lilli* is known to have interactions with various pathways, such as the Ras, Dpp/TGF-β and ecdysteroid pathways, that are known to influence Notch signaling (Hasson and Paroush, 2006; Sundaram, 2005; Su et al., 2001). Ecdysteroids are insect molting hormones in arthropods that induce signals required for postembryonic development (Kozlova and Thummel, 2000).

lilli was earlier described as a member of the FMR2/LAF4 multigene family (Gecz et al., 1997; Nilson et al., 1997). FMR2 was identified as a mutation that causes Fragile-X mental retardation syndrome, the most common form in inherited mental retardation in humans. On the other hand, LAF4 was identified as a chromosomal translocation that result in Burkitt's lymphoma, associated with highly malignant tumors in the most common childhood cancer (reviewed in Su et al., 2000). FMR2 is highly expressed in the fetal brain, while LAF4 is highly expressed in fetal lymphoid tissue, particularly in pre-B cells (Jin and Warren, 2000; Ma and Sta DT, 1996). The other members of FMR2/LAF4 family includes, AF5 and AF4. These human proteins are nuclear proteins capable of DNA binding and transcriptional activation (Li et al., 1998). The *Drosophila-lilliputian* has >51% amino acid similarity with these human proteins (Su et al., 2001).

lilli suppressed the rough-eye phenotypes induced by both Neu^{YA} and Neu^{NYPD}. Here, we reason that *lilli* is specific to the phosphorylation deficient, Neu^{NYPD} not to Neu^{YA} signaling in *Drosophila*. As YA has inhibitory role upon NYPD, it is easily

understandable that a suppressed NYPD signaling pathway is omnipresent in the Neu^{YA} genetic background. Therefore, the phenotypic suppression of Neu^{YA} by *lilli* is due to the suppressed level of Neu^{NYPD}. We firmly suggest that *lilli* is a positive regulator of NYPD signaling in *Drosophila.*

For the Neu^{NYPD} verification, we used the *GMR-GAL4* driven misexpression, as this system is more sensitive than that of *sev-GAL4* (Chapter 2). The suppression of Neu^{NYPD} eye phenotypes by *lilli* is likely due to the signaling potentials of Neu^{NYPD} through the binding of c-Src kinase at the catalytic/kinase domain of this oncogene. It has been shown that while all the phosphotyrosines are mutated or absent, the phosphorylation deficient *Neu* allele, Neu^{NYPD} is efficiently tyrosine phosphorylated (Kim et al., 2005). In particular, Neu^{NYPD} signals through the association with c-Src in rat1 fibroblast *in vivo* (Kim et al., 2005). Another study showed that c-Src weakly phosphorylated with tyrosine residues in the catalytic domain of the PDGF-β receptor (Hansen et al., 1996; Kypta et al., 1990). Therefore, the suppression of Neu^{NYPD} phenotypes may be due to a positive role of c-Src with *lilli*. Collectively, the identification of *lilli* and its specificity to NYPD not only validates our genetic screening but also the suggested inhibitory role of YA over NYPD.

3.4.2 *Lilliputian* modifies the phenotype induced by the sevenless receptor tyrosine kinase

The *lilli* gene is required for normal cytoskeleton organization, proper cell size determination, and embryo segmentation. *lilli* interacts genetically with each of the Wnt,

AKT, and EGFR pathways (Gu and Nelson 2003; Su et al., 2001; Tang et al., 2001; Wittwer et al., 2001). In order to verify the *lilli* with the YA-interacting receptor tyrosine kinases, such as *Drosophila*-DER and Sevenless receptor tyrosine kinase, we made heterozygotes of *lilli* mutations with various ectopically expressed alleles (Fig 3.5). The Neu^{YA} specific suppressor, *lilli* showed no genetic interaction with Neu^{YB}, Neu^{YE} and the gain-of-function DER mutant, Elp^{B1}. However, *lilli* mutant completely suppressed the rough eye phenotypes of Sev-Torso chimera (also see S5). This suppression suggests a complete disruption of the 4 cone cells in the cluster to R7-cell fates, which are characteristic to the ectopic expression of the *sev* enhancer/promoter. It has been reported that in *lilli* mutant clones, although the photoreceptor rhabdomeres were smaller but cell-fate specification was not disrupted (Tang et al. 2001; Wittwer et al. 2001). Therefore, we suggest that the transcription factor, *lilli* may (1) directly repress the expression of R7-cell fate determinant, such as the transcription factor *prospero,* resulting in supernumerary R7 cells in the Sev-Torso chimeric flies, or may (2) increase the expression of the cone cell specific transcription factor *dPax2* in the heterozygote reverting the extra R7 cells to cone cell-fate, resulting in smoother eye surface.

On the other hand, *lilli* didn't result in significant level of suppression of the eye phenotypes induced by the gain-of-function DER allele, Elp^{B1}. The lack of interaction may be due to the involvement of a parallel signaling pathway to EGFR during the *Drosophila* eye development. In fact, *lilli* was shown to function in the Dpp/TGF-β signaling pathway in parallel to the Ras-MAPK signaling during the dorsal ventral boundary formation in the developing *Drosophila* wing (Bejarano et al., 2008). It has also

been shown that gain-of-function Torso RTK signaling triggered ectopic Dpp and STAT signaling resulting in the patterning defects during the embryogenesis (Li and Li, 2003).

3.4.3 Identification of the 2nd chromosome 2E01 group near *CG7777*

We have previously shown that Neu^{YA} attenuates RTK signaling, at least in EGFR and Sevenless receptor tyrosine kinase, possibly by recycling the signal competent receptors to the plasma membrane or by facilitating lysosome-mediated receptor degradation (chapter 2). We thought that the identification of genes that negatively regulate the Neu^{YA} signaling would reveal the candidates attenuating RTK signaling in *Drosophila*. Therefore, we put much of our effort in mapping the enhancers isolated from this genetic screen. On the 2nd chromosome, 2E01 complementation group comprises 3 members, including 2E01, 2E11 and 2E12. These enhancers failed to complement with the smallest available deficiency, Df(2R)BSC160, uncovering 8 genes, including *CG30026, CG34054, CG7763, CG7777, CG33472, E(Pc), inv* and *CG30034*. Due to the unavailability of the mutant alleles for each of these loci, we failed to verify all the candidates in this region.

However, we ruled out *E(Pc)* and *inv* as the potential candidates (data not shown). Interestingly, 2E01 enhancers were lethal over the *P*-element insert at the locus CG7777, (P{SUPor-P}CG7777KG08662). The *P*-element insert in CG7777 selectively enhanced the rough eye phenotypes of Neu^{YA} (Fig. 3.6). Originally identified as an enhancer, the dual specific (YA and YE) modifier showed no genetic interactions with other Neu alleles, including Neu^{YB} (Fig. 3.7). However, a strong phenotypic enhancement was

shown in the $Elp^{B1}/CG7777^{KG08662}$ heterozygote. At this point we cannot conclude that the candidate gene is to be the *CG7777*, as there is no available *CG7777* deficiency or mutant line in the public stock centres. Further screen with the RNAi lines of *CG7777* and other members of that Deficiency is worth doing to identify the bonafide candidate.

The blast search results indicate that the CG7777 is the sole *Drosophila* homolog of human Aquaporin 4 (AQP 4). The aquaporins (AQPs) are integral membrane proteins whose main function is to transport water across cell membranes in response to osmotic gradients. Out of 13 human AQPs, more than 10 are expressed in the eye. In human eye tissue, AQP4 is the predominant and is expressed in the Muller glial cells. It has been shown that the level of AQP4 expression is associated with environmentally driven manipulations of light activity on the retina and the development of myopia (Goodyear et al., 2009). Moreover, a recent study with the Alveolar Type II (ATII) cell of rats shows that the Oleic acid-induced acute lung injury results in the activation of MAPK signaling pathway and up-regulation of AQP-4 mRNA expression (Fang et al., 2009).

However, the specificity of CG7777 with Neu^{NYPD} is yet to be verified. A strong phenotypic enhancement both in the $Elp^{B1}/CG7777^{KG08662}$ and $Neu^{YA}/CG7777^{KG08662}$ heterozygote is possibly due to an increased signaling resulting from reduced receptor recycling back to the plasma membrane or a slower trafficking to the endosome for lysosomal degradation. Recently, AQP4 has been reviewed as an important player regulating multiple steps in adult neurogenesis, including cell proliferation, specification, differentiation and cell migration (Zheng et al., 2010). However, the role AQP4 in endocytosis as a means of RTK signal attenuation is yet to be explored.

If final mapping identifies the candidate to be CG7777 or AQP 4, it is possible that this gene signals through EGFR-mediated pathway. We would also expect to see phenotypic enhancement of Neu^{YA}, as seen in Neu^{YA}/*p[CG7777]* heterozygote (Fig. 3.6). This enhanced eye phenotype will possibly be due to increased or a longer duration of EGFR signaling resulting from the modulation of two above-mentioned signal attenuation steps. The involvement of CG7777 in the Neu^{YA}-mediated RTK signal attenuation is worth verifying with the various components of receptor recycling and lysosomal degradation pathways. The genetic interaction of amorphous alleles, such as Rab 5, Rab 11, Hrs (for recycling) and Vps, and Ept (for lysosomal degradation) would verify this hypothesis.

In summary, our screen has identified numerous known components or mediators of the oncogenic rat-Neu/ErbB2 and (possibly) the novel gene CG7777. We anticipate that the unmapped suppressors and enhancers will identify many of the known genes linked to various processes like, the Ras-Raf-MAPK signaling pathway, receptor intracellular trafficking, receptor recycling or lysosomal degradation. We anticipate that this modifier collection will provide a rich resource for further investigations of the molecular mechanisms of RTK signaling attenuation.

CHAPTER 4: CONCLUSIONS AND PROSPECTS

4.0 Conclusions and Prospects

The structure and function of many SH2/PTB proteins in signaling is conserved in model organisms like *Caenorhabditis elegans* and *Drosophila* and a number of studies have taken the advantage of the well-characterized signal transduction pathways in *Drosophila* to screen for proteins that interact with vertebrate transgenes (Moghal and Sternberg, 2003; Jackson et al., 2002; Kazantsev et al., 2002; Rubinsztein, 2002; Bhandari and Shashindra, 2001; Worby and Margolis, 2000;). *Drosophila* has extensively been used to study human diseases, such as Alzheimer's, Parkinson's and Huntington, and to discover drugs targeting human heart diseases (Doumnis et al., 2009; Botella et al., 2009; Iijima and Iijima, 2009; Moloney et al., 2009; Akasaka and Ocorr, 2009; Ocorr et al., 2007). However, this is the first detailed study of the pTyr 1028 of rat-Neu/ErbB2 revealing its negative signaling capability *in vivo*.

Our genetic data, obtained from both eye and wing tissue experiments, suggests that Neu^{YA} inhibits signaling from other 'add-back' *Neu* alleles, perhaps by forming a heterodimer. The reduction of phenotypic expression of these 'add-back' alleles may be due to the reduction of Tyrosine phosphorylation levels that correspond to intracellular signal activation. Neu^{YA} may also prevent other RTKs, such as DER, at least DER^{DN} from forming dimers with the endogenous DER, or Neu^{YA} may remove wildtype DER from the cell surface. Other signal attenuating steps, such as receptor-mediated endocytosis, receptor recycling and lysosomal degradation is required for *Neu*-mediated signal attenuation. However, this attenuating process works in a YA-independent manner. Furthermore, genetics data also suggests that during impaired endocytosis, receptor

recycling and lysosomal degradation, cells may up-regulate a novel pathway in attenuating YA-mediated signaling that involves the RTK-negative regulator, *Sprouty*, and the hepatocyte growth factor regulated tyrosine kinase substrate, *Hrs*. Therefore, a genome wide YA-modifier screen is not only important for revealing the components of this pTyr specific signaling pathway in *Drosophila* but also for better understanding of RTKs attenuation.

In order to identify the signaling components of rat-Neu^{YA} in *Drosophila*, I screened a total of 61,241 F1 progeny and isolated 856 F1 dominant modifiers (enhancers/suppressors) of the YA rough eye phenotype, out of which 195 bred to the F2 generation (Table 3.1). In order to map these modifiers in an efficient manner, I chose to study the modifiers, which were homozygous lethal, had at least 2 members in the same complementation group, and were specific either to Neu^{YA}, Neu^{NYPD} or Neu^{YE} (Table 3.2; Fig. 3.3). Finally, I identified the known gene, *Lilliputian*, the potential novel gene, CG7777 and many other unmapped enhancers and suppressors.

The screen designed with the *GMR*-enhancer/promoter fused to the Neu^{YAE}, *GMR::*Neu^{YAE} is the best-sensitized and available tool for identifying the dominant modifiers using the *Drosophila* indispensable adult tissue, such as eye tissue. Promoters are not affected by the dosage compensation and a similar sevenless-enhancer/promoter (*sev::*ras^{V12}) fusion construct was successfully used to identify the downstream components of the Ras signaling pathway (Karim et al., 1996). *GMR-GAL4* drivers showed more sensitivity than that of Sevenless (*sev*) in the *Drosophila* eye tissue (Chapter 2). Hence the more sensitized *GMR::*Neu^{YAE} screen is expected to identify more

modifiers at ease than that of *sev::Neu*^{YAE} or a dosage dependent *GMR-GAL4* driven misexpression of *Neu*^{YAE}.

The mutagenesis rate depends on the EMS concentration, the fly strain, administration methods and Lab surroundings (Bokel, 2008). In consistent with other experiments, the standard 25 mM EMS concentration (Grigliatti, 1998), treated on the isogenized OregonR starter strain, generated 34.9% single X-linked lethal mutation, corresponding to approximately one mutation per chromosome (Data shown in Hossain, 2005; M.Sc. thesis). The identification of low percentage of F2 modifiers (0.3%) may be due to the selection of modifiers with strong phenotypes in both eyes. Moreover, the modifiers having no apparent phenotype while haplosufficient cannot be identified in such a screen. However, the saturation of this sensitized screening is expected, as many of the complementation groups have multiple members or allelic to each other.

In this study, the major difficulties arose during the mapping of the modifiers using meiotic recombinant techniques and during validating the identified candidates with the known mutants. During meiotic recombination mapping, the rate of recombination, calculated from a progeny size of 1500, was not precise enough to locate a calculated rough molecular position that can be identified within a range of few hundred-kilo base pairs deletion in both upstream and downstream of the mutations. The rough mapping could be refined with the two molecularly mapped p-elements (Mullins et al., 1989; O'Hare and Rubin, 1983). The pairs of *P*-elements are selected so that a particular mutation can be flanked by both of them (*P*-elements). The recombination rate of any of these *P*-elements and the mutation is calculated in percentage. This percentile

value roughly corresponds to the centi Morgan (cM) value between the particular *P*-element and the mutation.

On the other hand, the SNP mapping procedure could have been employed to refine our rough mapping position. Even though SNP mapping is well established in other model organism, such as *C. elegans*, the SNP library for *Drosophila* is available for a limited number of strains (Chen et al., 2008). Therefore, in order to consider the SNP mapping for a particular *Drosophila* strain, one should characterize and isogenize all the SNPs before starting the mutagen administration.

Finally, the fine mapping and validation of the several novel modifiers was impossible as there were neither mutation of interested genes or single gene disruption stocks publicly available at the time of mapping. Even though the RNAi stocks, available in Vienna, don't cover the entire *Drosophila* genome, it remains to be explored to map our several potential modifiers. Moreover, the molecularly defined precise excision or the undefined imprecise excision by the *P*-element can be used to generate expected mutation that may circumvent the mapping scheme in future.

In conclusion, our screen efficiently identified and validated the known gene Lilliputian, a member of the FMR2/LAF4 multigene family that is responsible for Fragile-X mental retardation syndrome and Burkitt's lymphoma in human (Su et al., 2002). The identification of *lilli* also validates our mutagenesis screen and supports the authenticity of other modifiers, such as CG7777 and many unmapped candidates. Further study with the unmapped modifiers and available genetic tools may identify and validate many of the known and novel genes linked to various processes, including the Ras-Raf-

MAPK signaling, receptor intracellular trafficking, receptor recycling, lysosomal degradation or even RTK regulation pathways. The sequence verification and molecular characterization of the identified *lilli* alleles is worth doing in better understanding the genetic interaction of this molecule with the rat-Neu^{YA}.

The future study remains to verify the novel gene, CG7777 and other modifiers to be mapped, with the available RNAi transgenes. Sequence analysis and molecular characterization of these novel modifiers and other novel modifiers may shed light on better understanding of the Neu^{YA}-mediated RTK regulation and may open the avenue of designing better drugs targeting ErbB2 or other RTK signal attenuation pathway components.

REFERENCES:

Akasaka, T., Ocorr, K. (2009) Drug discovery through functional screening in the *Drosophila* heart. *Methods Mol Biol.* **577:** 235-49.

Alvarado, D., Klein, DE., Lemmon, MA. (2009) ErbB2 resembles an autoinhibited invertebrate epidermal growth factor receptor. *Nature.* **461(7261):** 287-91.

Ande, S.R., Chen, J., Maddika, S. (2009) The ubiquitin pathway: an emerging drug target in cancer therapy. *Eur J Pharmacol.* **625(1-3):** 199-205.

Anderson, D., Koch, C.A., Grey, L., Ellis, C., Moran, M.F., Pawson, T. (1990). Binding of SH2 domains of phospholipase C gamma 1, GAP, and Src to activated growth factor receptors. *Science.* **250:** 979–982.

Bach, E.A., Vincent, S., Zeidler, M.P., Perrimon, N. (2003) A sensitized genetic screen to identify novel regulators and components of the Drosophila janus kinase/signal transducer and activator of transcription pathway. *Genetics.* **165(3):** 1149-66.

Bache, KG., Brech, A., Mehlum, A., Stenmark, H. (2003) Hrs regulates multivesicular body formation via ESCRT recruitment to endosomes. *J Cell Biol.* 162(3): 435-42.

Bacus, S.S., Chin, D., Yarden, Y., Zelnick, C.R., Stern, D.F. (1996) Type 1 receptor tyrosine kinases are differentially phosphorylated in mammary carcinoma and differentially associated with steroid receptors. *Am J Pathol.* 148: 549–558.

Baker, N and Rubin, G.M. (1989) Effect on eye development of dominant mutations in Drosophila homologue of the EGF receptor. *Nature.* **340(6229):** 150-3.

Baker, NE., Yu, S., Han, D. (1996) Evolution of proneural atonal expression during distinct regulatory phases in the developing *Drosophila* eye. *Curr Biol.* **6(10):** 1290-301.

Baker, NE. and Zitron, AE. (1995) Drosophila eye development: Notch and Delta amplify a neurogenic pattern conferred on the morphogenetic furrow by scabrous. *Mech Dev.* **49(3):** 173-89.

Baker, N.E., Yu, S., and Han, D. (1996). Evolution of proneural atonal expression during distinct regulatory phases in the developing Drosophila eye. *Curr Biol* **6:**1290–1301.

Baker, N.E. and Yu, S.Y. (2001). The EGF receptor defines domains of cell cycle progression and survival to regulate cell number in the developing Drosophila eye. *Cell* **104:** 699–708.

Bakrim, A., Maria, A., Sayah, F., Lafont, R., Takvorian, N. (2008) Ecdysteroids in spinach (Spinacia oleracea L.): biosynthesis, transport and regulation of levels. *Plant Physiol Biochem.* **46(10):** 844-54.
Baonza, A., Casci, T., Freeman, M. (2001) A primary role for the epidermal growth factor receptor in ommatidial spacing in the *Drosophila* eye. *Curr Biol.* **11(6):** 396-404.

Barbacci, EG., Guarino, BC., Stroh, JG., Singleton, DH., Rosnack, KJ., Moyer, JD., Andrews, GC. (1995) The structural basis for the specificity of epidermal growth factor and heregulin binding. *J Biol Chem.* **270(16):** 9585-9.

Bargmann, C.I., Hung, M.C., and Weinberg, R.A. (1986). Multiple Independent Activations of the Neu Oncogene by A Point Mutation Altering the Transmembrane Domain of P185, *Cell.* **45:** 649-657.

Bargmann, C.I., and Weinberg, R.A. (1988). Oncogenic Activation of the Neu-Encoded Receptor Protein by Point Mutation and Deletion, *EMBO J. 7:* 2043-2052.

Bargmann, C.I. and Weinberg, R.A. (1988) Oncogenic activation of the neu-encoded receptor protein by point mutation and deletion. *EMBO J.* **7(7):** 2043-52.

Baselga, J. and Swain, S.M. (2009). Novel anticancer targets: revisiting ERBB2 and discovering ERBB3. *Nat Rev Cancer.* **9(7):** 463-75.

Baselga, J. and Norton, L. (2002). Focus on breast cancer. *Cancer Cell.* **1:** 319-322.

Beerli, R.R., Grausporta, D., Woodscook, K., Chen, X.M., Yarden, Y., and Hynes, N.E. (1995) Neu Differentiation Factor Activation of Erbb-3 and Erbb-4 Is Cell-Specific and Displays A Differential Requirement for Erbb-2, *Mol. Cell. Biol. 15:* 6496-6505.

Bell, C.A., Tynan, J.A., Hart, K.C., Meyer, A.N., Robertson, S.C., and Donoghue, D.J. (2000) Rotational coupling of the transmembrane and kinase domains of the Neu receptor tyrosine kinase, *Mol. Biol. Cell. 11:* 3589-3599.

Bhandari, P., Shashidhara, LS. (2001) Studies on human colon cancer gene APC by targeted expression in *Drosophila. Oncogene.* **20(47):** 6871-80.

Bier, E. and Bodmer, R. (2004) *Drosophila,* an emerging model for cardiac disease. *Gene.* **342(1):** 1-11.

Bokel, C. (2008) EMS screen: From Mutagenesis to Screening and Mapping. *Methods Mol. Biol.* **420:** 119-138.

Bourguignon, L., Lan, K-H., Singleton, P., Lin, S-Y., Yu, D., Hung, M.C. (2002) Localizing the EGF receptor – Reply. *Nat Cell Biol* **4:** E22–E23, 2002

Bradshaw, J.M., Waksman, G. (2002) Molecular recognition by SH2 domains. *Adv Protein Chem.* 61: 161-210.

Braid, L.R. and Verheyen, E.M. (2008) Drosophila nemo promotes eye specification directed by the retinal determination gene network. *Genetics.* **180(1):** 283-99.

Brand, A.H. and Perrimon, N. (1993) Targeted gene expression as a means of altering cell fates and generating dominant phenotypes. *Development.* **118(2):**401-15.

Brett, T.J. & Traub, L.M. (2006) Molecular structures of coat and coat-associated proteins: function follows form. *Curr. Opin. Cell Biol.* **18:** 395–406.

Bright, N.A., Gratian, M.J., Luzio, J.P. (2005) Endocytic delivery to lysosomes mediated by concurrent fusion and kissing events in living cells. *Curr Biol.* **15(4):** 360-5.

Bromberg, J.F., Wrzeszczynska, M.H., Devgan, G., Zhao, Y., Pestell, R.G., Albanese, C., Darnell, J.E. Jr. (1999) Stat3 as an oncogene. *Cell.* **98:** 295–303.

Burke, C.L., Lemmon, M.A., Coren, B.A., Engelman, D.M. and Stern, D.F. (1997) Dimerization of the p185neu transmembrane domain is necessary but not sufficient for transformation. *Oncogene.* **14(6):** 687-96.

Ceresa, B.P. (2006). Regulation of EGFR endocytic trafficking by rab proteins. *Histol Histopathol.* **21(9):** 987-93.

Chan, R., Hardy, W., Laing, M., Hardy, S. and Muller, W.J. (2002) The catalytic activity of the ErbB2 receptor tyrosine kinase is essential for embryonic development. *Mol and Cell Biol.* **22**: 1073-1078.

Chan, R., Hardy, W.R., Dankort, D., Laing, M.A. and Muller, W.J. (2004) Modulation of ErbB2 signaling during development: a threshold level of ErbB2 signaling is required for development. *Development.* **131**: 5551-5560.

Chen, M.L., Green, D., Liu, L., Lam, Y.C., Mukai, L., Rao, S., Ramagiri, S., Krishnan, K.S., Engel, J.E., Lin, J.J., Wu, C.F. (2002) Unique biochemical and behavioral alterations in Drosophila shibire(ts1) mutants imply a conformational state affecting dynamin subcellular distribution and synaptic vesicle cycling. *J Neurobiol.* **53(3):** 319-29.

Chen, P., Rodriguez, A., Erskine, R., Thach, T., Abrams, J.M. (1998). Dredd, a novel effector of the apoptosis activators reaper, grim, and hid in Drosophila. *Dev. Biol.* **201(2):** 202-216.

Cho, HS., Mason, K., Ramyar, KX., Stanley, AM., Gabelli, SB., Denney, DW. Jr, Leahy, DJ. (2003) Structure of the extracellular region of HER2 alone and in complex with the Herceptin Fab. *Nature.* **421:** 756–760.

Citri, A., Skaria, KB., Yarden, Y. (2003) The deaf and the dumb: the biology of ErbB-2 and ErbB-3. *Exp Cell Res.* **284(1):** 54-65.

Citri, A., Alroy, I., Lavi, S., Rubin, C., Xu, W., Grammatikakis, N., Patterson, C., Neckers, L., Fry, DW., Yarden, Y. (2002) Drug-induced ubiquitylation and degradation of ErbB receptor tyrosine kinases: implications for cancer therapy. *EMBO J.* **21:** 2407–2417.

Clarke, R.B. (2003) p27KIP1 phosphorylation by PKB/Akt leads to poor breast cancer prognosis. *Breast Cancer Res.* **5:** 162–163.

Cohen, SY., Quentel, G., Guiberteau, B., Coscas, GJ. (1993) Retinal vascular changes in congenital hypertrophy of the retinal pigment epithelium. *Ophthalmology.* 100(4): 471-4.

Cotton, L.M., O'Bryan, M.K., Hinton, B.T. (2008) Cellular signaling by fibroblast growth factors (FGFs) and their receptors (FGFRs) in male reproduction. *Endocr Rev.* **29(2):** 193-216.

Craven, R.J., Lightfoot, H, Cance, W.G. (2003) A decade of tyrosine kinases: from gene discovery to therapeutics. *Surg Oncol.* **12:** 39–49.

Dankort, D.L., Wang, Z., Blackmore, V., Moran, M.F. and Muller, W.J. (1997) Distinct tyrosine autophosphorylation sites negatively and positively modulate neu-mediated transformation. *Mol Cell Biol.***17(9):** 5410-25.

Dankort, D., Jeyabalan, N., Dumont, D.J. and Muller, W.J. (2001) Multiple ErbB-2/Neu Phosphorylation Sites Mediate Transformation through Distinct Effector Proteins. *J Biol Chem.* **276(42):** 38921-8.

Deng, WP., Nickoloff, JA. (1992) Site-directed mutagenesis of virtually any plasmid by eliminating a unique site. *Anal Biochem.* **200(1):** 81-8.

De Camilli, P., Takei, K., McPherson, P.S. (1995) The function of dynamin in endocytosis. *Curr Opin Neurobiol.* **5(5):** 559-65.

Dickson, BJ., Van Der Straten, A., Dominguez, M., Hafen, E. (1996) Mutations modulating Raf signaling in Drosophila eye development. *Genetics.* 142: 163–171.

Di Fiore, PP., Pierce, JH., Kraus, MH., Segatto, O., King, CF., and Aaronson, SA. (1967). ErbB-2 is a potent oncogene when over- expressed in NIH 3T3 cells. *Science.* **237:** 178-182.

Dikic, I. and Giordano, S. (2003) Negative receptor signalling. *Curr Opin Cell Biol.* **15(2):** 128-35.

Dikic, I. (2003) Mechanisms controlling EGF receptor endocytosis and degradation. *Biochem Soc Trans.* **31(Pt 6):** 1178-81.

Dokucu, ME., Zipursky, SL., Cagan, RL. (1996) Atonal, rough and the resolution of proneural clusters in the developing *Drosophila* retina. *Development.* **122(12):** 4139-47.

Dominguez, M. and Casares, F. (2005) Organ specification-growth control connection: new in-sights from the Drosophila eye-antennal disc. *Dev Dyn.* **232:** 673–684.

Dinan, L., Lafont, R. (2006) Effects and applications of arthropod steroid hormones (ecdysteroids) in mammals. *J Endocrinol.* **191(1):** 1-8.

Doroquez, D.B. and Rebay, I. (2006) Signal integration during development: mechanisms of EGFR and Notch pathway function and crosstalk. *Crit Rev Biochem Mol Biol.* **41:** 339-85.

Ellis, MC., O'Neill, EM., Rubin, GM. (1993) Expression of *Drosophila* glass protein and evidence for negative regulation of its activity in non-neuronal cells by another DNA-binding protein. *Development.* **119(3):** 855-65.

Fantl, W.J., Johnson, D.E., and Williams, L.T. (1993) Signaling by Receptor Tyrosine Kinases, *Annu. ReV. Biochem.* ***62:*** 453-481.

Feng, SM., Sartor, CI., Hunter, D., Zhou, H., Yang, X., Caskey, LS., Dy, R., Muraoka-Cook, RS., Earp, HS. 3rd. The HER4 cytoplasmic domain, but not its C-terminus, inhibits mammary cell proliferation. *Mol. Endocrinol.* **21:** 1861–1876.

Floyd, S. and De Camilli, P. (1998) Endocytosis proteins and cancer: a potential link? *Trends Cell Biol.* **8(8):** 299-301.

Frank, B., Hemminki, K., Wirtenberger, M., Bermejo, J.L., Bugert, P., Klaes, R., Schmutzler, R.K., Wappenschmidt, B., Bartram, C.R., and Burwinkel, B. (2005) The rare ERBB2 variant Ile654Val is associated with an increased familial breast cancer risk, *Carcinogenesis.* **26:** 643-647.

Franklin, MC., Carey, KD., Vajdos, FF., Leahy, DJ., de Vos, AM., Sliwkowski, MX. (2004) Insights into ErbB signaling from the structure of the ErbB2–pertuzumab complex. *Cancer Cell.* **5:** 317–328.

Freeman, M. (1996). Reiterative use of the EGF receptor triggers differentiation of all cell types in the Drosophila eye. *Cell.* **87:** 651-660.

Freeman, M. (1997). Cell determination strategies in the Drosophila eye. *Development.* **124:** 261-270.

Freeman, M. (2002). A fly's eye view of EGF receptor signalling. *EMBO J.* **21:** 6635-6642.

Friedman, A., Perrimon, N. (2006) A functional RNAi screen for regulators of receptor tyrosine kinase and ERK signalling. *Nature.* **444(7116):** 230-4.

Fleishman, SJ., Schlessinger, J., Ben-Tal, N. (2002) A putative molecular-activation switch in the transmembrane domain of erbB2. *Proc Natl Acad Sci USA.* **99(25):** 15937-40.

Ganguly, A., Jiang, J., Y.T. (2005) *Drosophila* WntD is a target and an inhibitor of the Dorsal/Twist/Snail network in the gastrulating embryo. *Development.* **132(15):** 3419-29.

Gecz, J., S. Bielby, G. Sutherland and J. Mulley. (1997) Gene structure and subcellular localization of FMR2, a member of a new family of putative transcription activators. *Genomics.* **44:** 190.

Greenwood, S. and Struhl, G. (1999) Progression of the morphogenetic furrow in the Drosophila eye: the roles of Hedgehog, Decapentaplegic and the Raf pathway. *Development.* **126:** 5795–5808.

Gruenberg, J. and Stenmark, H. (2004). The biogenesis of multivesicular endosomes. *Nat. Rev. Mol. Cell. Biol.* **5:** 317-323.

Gu, Y. and Nelson, DL. (2003) FMR2 function: insight from a mouse knockout model. *Cytogenet Genome Res.* **100(1-4):** 129-39.

Hansen, K., Johnell, M., Siegbahn, A., Rorsman, C., Engström, U., Wernstedt, C., Heldin, CH., Rönnstrand, L. (1996) Mutation of a Src phosphorylation site in the PDGF beta-receptor leads to increased PDGF-stimulated chemotaxis but decreased mitogenesis. *EMBO J.* **15(19):** 5299-313.

Hanson PI, Shim S, Merrill SA. (2009) Cell biology of the ESCRT machinery. *Curr Opin Cell Biol.* **21(4):** 568-74.

Hasson, P. and Paroush, Z. (2006) Crosstalk between the EGFR and other signalling pathways at the level of the global transcriptional corepressor Groucho/TLE. *Br J Cancer.* **94(6):** 771-5.

Hay, B.A., Maile, R. and Rubin GM. (1997) P element insertion-dependent gene activation in the Drosophila eye. *Proc Natl Acad Sci U S A.* **94(10):** 5195-200.

Herbst JJ, Opresko LK, Walsh BJ, Lauffenburger DA, Wiley HS. (1994) Regulation of postendocytic trafficking of the epidermal growth factor receptor through endosomal retention. *J Biol Chem.* **269(17):** 12865-73.

Higashijima, S., Kojima, T., Michiue, T., Ishimaru, S., Emori, Y., and Saigo, K. (1992) Dual Bar homeo box genes of Drosophila required in two photoreceptor cells, R1 and R6, and primary pigment cells for normal eye development. *Genes Dev.* **6:** 50–60.

Huang, S., Shu, L., Dilling, M.B., Easton, J., Harwood, F.C., Ichijo, H., Houghton, P.J. (2003) Sustained activation of the JNK cascade and rapamycin- induced apoptosis are suppressed by p53/p21(Cip1). *Mol Cell.* **11:** 1491–1501.

Huang, A. and Rubin, G. (2000) A misexpression screen identifies genes that can modulate RAS1 pathway signaling in *Drosophila melanogaster*. *Genetics* **156**: 1219-1230.

Hunter, T. (2000) Signaling-2000 and beyond. *Cell.* **100**: 113-127.

Hynes, N.E. and stern, D.F. (1994) The biology of ErbB-2/Neu/HER-2 and its role in cancer. *Biochim.Biophys Acta.* **1198**: 165-184.

Hyun, TS., and Ross, TS. (2004) HIP1: trafficking roles and regulation of tumorigenesis. *Trends Mol Med.* **10(4):** 194-9.

Iijima-Ando, K. and Iijima, K. (2004) Transgenic Drosophila models of Alzheimer's disease and tauopathies. *Brain Struct Funct.* **214(2-3):** 245-62.

Izumi, Y., Xu, L., di Tomaso, E., Fukumura, D. & Jain, R. K. (2002) Tumor biology: Herceptin acts as an anti-angiogenic cocktail. *Nature.* **416:** 279–280.

Jackson, R.G., Wiedau-Pazos M, Sang T.K., Wagle, N., Brown, C.A., Massachi, S. and Geschwind, D.H. (2002) Human wild-type tau interacts with wingless pathway components and produces neurofibrillary pathology in *Drosophila*. *Neuron.* **34(4):** 509-19.

Jaehne, J., Urmacher, C., Thaler, HT., Friedlander-Klar, H., Cordon-Cardo, C., Meyer, HJ. (1992). Expression of Her2/neu oncogene product p185 in correlation to

clinicopathological and prognostic factors of gastric carcinoma. *J. Cancer Res. Clin. Oncol.* **118:** 474–479

Jin, P., and S. Warren. (2000) Understanding the molecular basis of Fragile X syndrome. Hum. Mol. Genet. **9:** 901–908.

Jakubowski, J., Kornfeld, K. (1999) A local, high-density, single-nucleotide polymorphism map used to clone Caenorhabditis elegans cdf-1. *Genetics.* **153(2):** 743-52.

Jarman, A.P., Grell, E.H., Ackerman, L., Jan, L.Y., and Jan, Y.N. (1994) Atonal is the proneural gene for Drosophila photoreceptors. *Nature.* **369:** 398–400.

Jarman, A.P., Sun, Y., Jan, L.Y., and Jan, Y.N. (1995) Role of the proneural gene, atonal, in formation of Drosophila chordotonal organs and photoreceptors. *Development.* **121:** 2019–2030.

Kamio T, Shigematsu K, Sou H, Kawai K, Tsuchiyama H. (1990) Immunohistochemical expression of epidermal growth factor receptors in human adrenocortical carcinoma. *Hum Pathol.* **21:** 277–282.

Karim, FD., Chang, HC., Therrien, M., Wassarman, DA., Laverty, T., Rubin, GM. (1996) A screen for genes that function downstream of Ras1 during *Drosophila* eye development. *Genetics.* **143(1):** 315-29.

Katzmann, DJ., Odorizzi, G. and Emr, SD. (2002) Receptor downregulation and multivesicular-body sorting. *Nat. Rev. Mol. Cell Biol.* **3:** 893–905.

Kazantsev, A., Walker, H.A., Slepko, N., Bear, J.E., Preisinger, E., Steffan, J.S., Zhu, Y.Z., Gertler, F.B., Housman, D.E., Marsh, J.L., and Thompson, L.M. (2002) A bivalent Huntingtin binding peptide suppresses polyglutamine aggregation and pathogenesis in *Drosophila. Nat Genet.* **30(4):** 367-76.

Kenyon, K.L., Ranade, S.S., Curtiss, J., Mlodzik, M., and Pignoni, F. (2003) Coordinating proliferation and tissue specification to promote regional identity in the Drosophila head. *Dev Cell.* **5:** 403–414.

Kim, A., Liu, B., Ordonez-Ercan, D., Alvarez, KM., Jones, LD., McKimmey, C., Edgerton, SM., Yang, X., Thor, AD. (2005) Functional interaction between mouse erbB3 and wild-type rat c-neu in transgenic mouse mammary tumor cells. *Breast Cancer Res.* **7(5):** R708-18.

Kim, HJ., Taylor, LJ., Bar-Sagi, D. (2007) Spatial regulation of EGFR signaling by Sprouty2. *Curr Biol.* **17(5):** 455-61.

Kumar, J.P. and Moses, K. (2001) The EGF receptor and notch signaling pathways control the initiation of the morphogenetic furrow during Drosophila eye development. *Development.* **128:** 2689–2697.

Kumar, R. and Hung, M.C. (2005) Signaling intricacies take center stage in cancer cells. *Cancer Res.* **65:** 2511–2515.

Kumar, J. P., Hsiung, F., Powers, M. and Moses, K. (2003). Nuclear translocation of activated MAP kinase is developmentally regulated in the developing Drosophila eye. *Development.* **130:** 3703-3714.

Kumar, J. P., Tio, M., Hsiung, F., Akopyan, S., Gabay, L., Seger, R., Shilo, B.-Z. and Moses, K. (1998). Dissecting the roles of the Drosophila EGF receptor in eye development and MAP kinase activation. *Development.* **125:** 3875-3885.

Kundra, V., Escobedo, J.A., Kazlauskas, A., Kim, H.K., Rhee, S.G., Williams, L.T. and Zetter, B.R. (1994) Regulation of chemotaxis by the platelet-derived growth factor receptor-beta. *Nature.* **367(6462):** 474-6.

Kurada, P and White, K. (1998) Ras promotes cell survival in *Drosophila* by downregulating hid expression. *Cell.* **95**: 191-196.

Kypta, R.M., Goldberg, Y., Courtneidge, S.A. (1990) Association between the PDGF receptor and members of the Src family of tyrosine kinases. *Cell.* 62(3): 481-92.

Lane, HA., Beuvink, I., Motoyama, AB., Daly, JM., Neve, RM., Hynes, NE. (2000) ErbB2 potentiates breast tumor proliferation through modulation of p27Kip1–Cdk2 complex formation: receptor overexpression does not determine growth dependency. *Mol. Cell. Biol.* **20:** 3210–3223.

Lanoue, BR. and Jacobs, JR. (1999) Rhomboid function in the midline of the Drosophila CNS. *Dev Genet.* **25(4):** 321-30.

Lai, K.M., Olivier, J.P., Gish, G.D., Henkemeyer, M., McGlade, J., Pawson, T. (1995) A Drosophila shc gene product is implicated in signaling by the DER receptor tyrosine kinase. *Mol Cell Biol.* **15(9):** 4810-8.

Le Borgne, R., Bardin, A., Schweisguth, F. (2005) The roles of receptor and ligand endocytosis in regulating Notch signaling. *Development.* **132(8):** 1751-62.

Le, XF., Claret, FX., Lammayot, A., Tian, L., Deshpande, D., LaPushin, R., Tari, AM., Bast, RC. Jr. (2003) The role of cyclin-dependent kinase inhibitor p27Kip1 in anti-HER2 antibody-induced G1 cell cycle arrest and tumor growth inhibition. *J. Biol. Chem.* **278:** 23441–23450.

Lee, K.F., Simon, H., Chen, H., Bates, B., Hung, M.C., and Hauser, C. (1995) Requirement for neuregulin receptor erbB2 in neural and cardiac development. *Nature.* **378**: 394-398.

Lee, KF., Simon, H., Chen, H., Bates, B., Hung, MC., Hauser, C. (1995) Requirement for neuregulin receptor erbB2 in neural and cardiac development. *Nature.* **378(6555):** 394-8.

Lesa, G.M. and Sternberg, P.W. (1997) Positive and negative tissue-specific signaling by a nematode epidermal growth factor receptor. *Mol Biol Cell.* **8(5):** 779-93.

Lesokhin AM, Yu SY, Katz J, Baker NE. (1999) Several levels of EGF receptor signaling during photoreceptor specification in wild-type, Ellipse, and null mutant Drosophila. *Dev Biol.* **205(1):** 129-44.

Liang J, Zubovitz J, Petrocelli T, Kotchetkov R, Connor MK, Han K, Lee JH, Ciarallo S, Catzavelos C, Beniston R, Franssen E, Slingerland JM (2002) PKB/Akt phosphorylates p27, impairs nuclear import of p27 and opposes p27-mediated G1 arrest. *Nat Med.* **8:** 1153–1160.

Li, L., and Cohen, SN. (1996) Tsg101: a novel tumor susceptibility gene isolated by controlled homozygous functional knockout of allelic loci in mammalian cells. *Cell.* **85:** 319–329.

Li Y, Dowbenko D, Lasky LA (2002) AKT/PKB phosphorylation of p21Cip/WAF1 enhances protein stability of p21Cip/WAF1 and promotes cell survival. J Biol Chem. **277:** 11352–11361.

Li, E., You, M., and Hristova, K. (2006) FGFR3 dimer stabilization due to a single amino acid pathogenic mutation, *J. Mol. Biol.* ***356*:** 600-612.

Li E. and Hristova K. (2006) Role of receptor tyrosine kinase transmembrane domains in cell signaling and human pathologies. *Biochemistry.* **45:** 6241–6251.

Lin, S.Y., Makino, K., Xia, W., Matin, A., Wen, Y., Kwong, K.Y., Bourguignon, L., Hung, M.C. (2001) Nuclear localization of EGF receptor and its potential new role as a transcription factor. *Nat Cell Biol.* **3:** 802–808.

Lipponen, P., Eskelinen, M. (1994) Expression of epidermal growth factor receptor in bladder cancer as related to established prognostic factors, oncoprotein (c-erbB-2, p53) expression and long-term prognosis. *Br J Cancer.* **69:** 1120–1125, 1994

Liu, E., Thor, A., He, M., Barcos, M., Ljung, BM., Benz, C. (1992). The HER2 (c-erbB-2) oncogene is frequently amplified in *in situ* carcinomas of the breast. *Oncogene.* **7:** 1027–1032.

Liu, B.A., Jablonowski, K., Raina, M., Arcé, M., Pawson, T., Nash, P.D. (2006) The human and mouse complement of SH2 domain proteins-establishing the boundaries of phosphotyrosine signaling. *Mol Cell.* **22(6):** 851-68.

Livneh, E., Glazer, L., Segal, D., Schlessinger, J., and Shilo, B.Z. (1985) The Drosophila EGF receptor gene homolog: conservation of both hormone binding and kinase domains. *Cell.* **40:** 599–607.

Lo, H-W., Xia, W., Wei, Y., Ali-Seyed, M., Huang, S.F., Hung, M-C. (2005) Novel prognostic value of nuclear EGF receptor in breast cancer. *Cancer Res.* 65: 338–348.

Luschnig, S., Moussian, B., Krauss, J., Desjeux, I., Perkovic, J., Nüsslein-Volhard, C. (2004) An F1 genetic screen for maternal-effect mutations affecting embryonic pattern formation in *Drosophila melanogaster. Genetics.* **167(1):** 325-42.

Ma, C., and Staudt, L. (1996) LAF4 encodes a lymphoid nuclear protein with transactivation potential that is homologous to AF4, the gene fused to MLL in t(4;11) leukemias. *Blood.* **87:** 743–745.

Marmor, M.D., Yarden, Y. (2004) Role of protein ubiquitylation in regulating endocytosis of receptor tyrosine kinases. *Oncogene.* **23(11):** 2057-70.

Marone, R., Hess, D., Dankort, D., Muller, W.J., Hynes, N.E., Badache, A. (2004) Memo mediates ErbB2-driven cell motility. *Nat Cell Biol.* **6(6):** 515-22.

Marti, U., Ruchti, C., Kampf, J., Thomas, G.A., Williams, E.D., Peter, H.J., Gerber, H., Burgi, U. (2001) Nuclear localization of epidermal growth factor and epidermal growth factor receptors in human thyroid tissues. *Thyroid.* **11:** 137–145.

Martin, L., Blanpain, C., Garnier, P., Wittamer, V., Parmentier, M., Vita, C. (2001) Structural and functional analysis of the RANTES-glycosaminoglycans interactions. *Biochemistry.* **40(21):** 6303-18.

Melicharek, D., Shah, A., DiStefano, G., Gangemi, A.J., Orapallo, A., Vrailas-Mortimer, A.D., Marenda, D.R. (2008). Identification of novel regulators of atonal expression in the developing Drosophila retina. *Genetics.* **180(4):** 2095-110.

Miklos, GL., Rubin, GM. (1996) The role of the genome project in determining gene function: insights from model organisms. *Cell.* **86(4):** 521-9.

Moghal, N., Sternberg, P.W. (2003) The epidermal growth factor system in Caenorhabditis elegans. *Exp Cell Res.* 284(1): 150-9.

Mukherjee, S., Tessema, M., Wandinger-Ness, A. (2006) Vesicular trafficking of tyrosine kinase receptors and associated proteins in the regulation of signaling and vascular function. *Circ Res.* **98(6):** 743-56.

Mullins, MC., Rio, DC., Rubin, GM. (1989) cis-acting DNA sequence requirements for P-element transposition. **Genes Dev.** 3(5): 729-38.

Münster, P.N., Marchion, D.C., Basso, A.D. & Rosen, N. (2002) Degradation of HER2 by ansamycins induces growth arrest and apoptosis in cells with HER2 overexpression via a HER3, phosphatidylinositol 3-kinase–AKT-dependent pathway. *Cancer Res.* **62:** 3132–3137.

Negro, A., Brar, BK., Gu, Y., Peterson, KL., Vale W., Lee, KF. (2006) ErbB2 is required for G proteincoupled receptor signaling in the heart. *Proc. Natl Acad. Sci. USA.* **103:** 15889–15893.

Neufeld, TP., Tang, AH., Rubin, GM. (1998) A genetic screen to identify components of the sina signaling pathway in Drosophila eye development. *Genetics.* **148(1):** 277-86.

Nickerson, D. P., Russell, M. R. & Odorizzi, G. (2007) A concentric circle model of multivesicular body cargo sorting. *EMBO Rep.* **8:** 644–650.

Nilson, I., Reichel, M., Ennas, M., R. Greim, R., Knorr, C. (2001) Exon/intron structure of the human AF4 gene, amember of the AF4/LAF4/FMR2 gene family coding for a nuclear protein with structural alterations in acute leukaemia. *Br. J. Haematol.* **98:** 157–169.

Ocorr, K., Akasaka, T., Bodmer, R. (2007) Age-related cardiac disease model of Drosophila. *Mech Ageing Dev.* **128(1):** 112-6.

O'Hare, K. and Rubin, GM. (1983) Structures of P transposable elements and their sites of insertion and excision in the Drosophila melanogaster genome. *Cell.* **34(1):** 25-35.

Owens, MA., Horten, BC., Da Silva, MM. (2004). HER2 amplification ratios by fluorescence *in situ* hybridization and correlation with immunohistochemistry in a cohort of 6556 breast cancer tissues. *Clin. Breast Cancer.* **5:** 63–69.

Oved, S., Mosesson, Y., Zwang, Y., Santonico, E., Shtiegman, K., Marmor, MD., Kochupurakkal, BS., Katz, M., Lavi, S., Cesareni, G., Yarden, Y. (2006) Conjugation to Nedd8 instigates ubiquitylation and down-regulation of activated receptor tyrosine kinases. *J Biol Chem.* **281(31):** 21640-51.

Pappu, K.S. and Mardon, G. (2004). Genetic control of retinal specification and determination in Drosophila. *Int J Dev Biol.* **48:** 913–924.

Park, K., Han, S., Kim, H. J., Kim, J. & Shin, E. (2006). HER2 status in pure ductal carcinoma *in situ* and in the intraductal and invasive components of invasive ductal carcinoma determined by fluorescence *in situ* hybridization and immunohistochemistry. *Histopathology.* **8:** 702–707.

Park, O.K., Schaefer, T.S., Nathans, D. (1996) In vitro activation of Stat3 by epidermal growth factor receptor kinase. *Proc Natl Acad Sci U SA.* **93:** 13704–13708.

Patel, N.H. (1994). Imaging neuronal subsets and other cell types in whole-mount Drosophila embryos and larvae using antibody probes. *Methods Cell Biol.* **44: 445–487.**

Pawson, T. and Nash, P. (2000) Protein-protein interactions define specificity in signal transduction. *Genes Dev.* **14**: 1027-1047.

Pinkas-Kramarski, R., Soussan, L., Waterman, H., Levkowitz, G., Alroy, I., Klapper, L., Lavi, S., Seger, R., Ratzkin, BJ., Sela, M., Yarden, Y. (1996). Diversification of Neu differentiation factor and epidermal growth factor signaling by combinatorial receptor interactions. *EMBO J.* **15:** 2452–2467

Perez, EA. and Baweja, M. (2008) HER2-positive breast cancer: current treatment strategies. *Cancer Invest.* **26(6):** 545-52.

Perrimon, N., Lanjuin, A., Arnold, C., Noll, E. (1996) Zygotic lethal mutations with maternal effect phenotypes in Drosophila melanogaster. II. Loci on the second and third chromosomes identified by P-element-induced mutations. *Genetics.* **144(4):** 1681-92.

Peschard, P. and Park M. (2003) Escape from Cbl-mediated downregulation: a recurrent theme for oncogenic deregulation of receptor tyrosine kinases. *Cancer Cell.* **(6):** 519-23.

Peters, KG., Marie, J., Wilson, E., Ives, HE., Escobedo, J., Del Rosario, M., Mirda, D., Williams, LT. (1992) Point mutation of an FGF receptor abolishes phosphatidylinositol turnover and Ca2+ flux but not mitogenesis. *Nature.* **358(6388):** 678-81.

Petti, L.M., Irusta, P.M., and DiMaio, D. (1998) Oncogenic activation of the PDGF *â* receptor by the transmembrane domain of p185(neu). *Oncogene. **16:*** 843-851.

Perrimon, N., Engstrom, L.and Mahowald, A.P. (1985) A pupal lethal mutation with a paternally influenced maternal effect on embryonic development in *Drosophila melanogaster. Dev Biol.* **110(2):** 480-91.

Portera, CC., Walshe, JM., Rosing, DR., Denduluri, N., Berman, AW., Vatas, U., Velarde, M., Chow, CK., Steinberg, SM., Nguyen, D., Yang, SX., Swain, SM. (2008)

Cardiac toxicity and efficacy of trastuzumab combined with pertuzumab in patients with human epidermal growth factor receptor 2-positive metastatic breast cancer. *Clin. Cancer Res.* **14:** 2710–2716 (2008).

Raiborg, C. & stenmark, H. (2009) The EsCRT machinery in endosomal sorting of ubiquitylated membrane proteins. *Nature.* **458:** 445–452.

Ramjaun, AR., Downward, J. (2007). Ras and phosphoinositide 3-kinase: partners in development and tumorigenesis. *Cell Cycle.* **6(23):** 2902-5.

Ranson, M. (2004) Epidermal growth factor receptor tyrosine kinase inhibitors. *British J. Cancer.* **90**: 2250-2255.

Raz, E., Schejter, E.D., Shilo, B.Z. (1991) Interallelic complementation among DER/flb alleles: implications for the mechanism of signal transduction by receptor-tyrosine kinases. *Genetics.* **129(1)**: 191-201.

Rebay, I. and Rubin, GM. (1995) Yan functions as a general inhibitor of differentiation and is negatively regulated by activation of the Ras1/MAPK pathway. *Cell.* **81(6):** 857-66.

Rebay, I., Chen, F., Hsiao, F., Kolodziej, PA., Kuang, BH., Laverty, T., Suh, C., Voas, M., Williams, A., Rubin, GM. (2000) A genetic screen for novel components of the Ras/Mitogen-activated protein kinase signaling pathway that interact with the yan gene of Drosophila identifies split ends, a new RNA recognition motif-containing protein. *Genetics.* **154(2):** 695-712.

Ready, D.F., Hanson, T.E., and Benzer, S. (1976). Development of the Drosophila retina, a neurocrystalline lattice. *Dev Biol.* **53:** 217–240.

Reich, A. and Shilo, BZ. (2002) Keren, a new ligand of the Drosophila epidermal growth factor receptor, undergoes two modes of cleavage. *EMBO J.* **21(16):** 4287-96.

Riese, DJ. and Stern, DF. (1998) Specificity within the EGF family/ErbB receptor family signaling network. *Bioessays.* **20(1):** 41-8.

Reithmacher, D., Sonnennberg-Riethmacher, E., Brinkmann, V., Yamaai, T., Lewin, G.R. and Birchmeier, C. (1997) Severe neuropathies in mice with targeted mutations in the ErbB3 receptor. *Nature*. **389**: 725-730.

Roch, F., Jimenez, G. and Casanova, J. (2002) EGFR signalling inhibits Capicua-dependent repression during specification of Drosophila wing veins. *Development.* **129(4):** 993-1002.

Rodrigues, A.B., Werner, E., Moses, K. (2005) Genetic and biochemical analysis of the role of Egfr in the morphogenetic furrow of the developing Drosophila eye. *Development.* **132(21):** 4697-707.

Roignant, J.Y., Treisman, J.E. (2009). Pattern formation in the Drosophila eye disc. *Int J Dev Biol.* **53(5-6):** 795-804.

Rørth, P., Szabo, K., Bailey, A., Laverty, T., Rehm, J., Rubin, GM., Weigmann, K., Milán, M., Benes, V., Ansorge, W., Cohen, SM. (1998) Systematic gain-of-function genetics in Drosophila. *Development.* **125(6):** 1049-57.

Rorth, P. (1996) A modular misexpression screen in Drosophila detecting tissue-specific phenotypes. *Proc Natl Acad Sci U S A.* **93(22):** 12418-22.

Rubinsztein, D.C. (2002) Lessons from animal models of Huntington's disease. *Trends Genet.* **18(4):** 202-9. Review.

Sadowski, L., Pilecka, I., Miaczynska, M. (2008) Signaling from endosomes: location makes a difference. *Exp Cell Res.* **315(9):** 1601-9.

Schechter, A.L., Stern, D.F., Vaidyanathan, L., Decker, S.J., Drebin, J.A., Greene, M.I., and Weinberg, R.A. (1984) The Neu Oncogene: An Erb-B-Related Gene Encoding A 185,000-Mr Tumor-Antigen, *Nature.* ***312*:** 513-516.

Schlessinger, J. (2003) Autoinhibition control. *Science.* ***300*:** 750-752.

Schlessinger, J. (2000) Cell signaling by receptor tyrosine kinases, *Cell.* ***103*:** 211-225.

Schlessinger, J. (2000) Cell signaling by receptor tyrosine kinases. *Cell.* **103**: 211-225.

Schlessinger, J. and Ullrich, A. (1992) Growth factor signaling by receptor tyrosine kinases. *Neuron.* **9(3):** 383-91. Review.

Schlessinger, J., Lemmon, MA. (2006) Nuclear signaling by receptor tyrosine kinases: the first robin of spring. *Cell.* **127(1):** 45-8.

Schnepp, B., Grumbling, G., Donaldson, T., Simcox, A. (1996) Vein is a novel component in the Drosophila epidermal growth factor receptor pathway with similarity to the neuregulins. *Genes Dev.* **10(18):** 2302-13.

Settle, M., Gordon, M.D., Nadella, M., Dankort, D., Muller, W. and Jacobs, J.R. (2003) Genetic identification of effectors downstream of Neu (ErbB-2) autophosphorylation sites in a Drosophila Model. *Oncogene.* **22:** 1916-1926.

Shilo, B.Z. (2003). Signaling by the Drosophila epidermal growth factor receptor pathway during development. *Exp Cell Res.* **284:** 140–149.

Shilo, B.Z., and Raz, E. (1991) Developmental control by the Drosophila EGF receptor homolog DER. *Trends Genet.* 7**(11-12):** 388-92. Review.

Shilo, B.Z. (2005) Regulating the dynamics of EGF receptor signaling in space and time. *Development.* **132:** 4017–4027.

Shin, I., Yakes, FM., Rojo, F., Shin, NY., Bakin, AV., Baselga, J., Arteaga, CL. (2002) PKB/Akt mediates cell-cycle progression by phosphorylation of p27(Kip1) at threonine 157 and modulation of its cellular localization. *Nat Med.* **8:** 1145–1152.

Shtiegman K, Yarden Y. (2003) The role of ubiquitylation in signaling by growth factors: implications to cancer. *Semin Cancer Biol.* **13(1):** 29-40.

Silver, S.J. and Rebay, I. (2005) Signaling circuitries in development: insights from the retinal determination gene network. *Development.* **132:** 3–13.

Simon, MA., Bowtell, DD., Dodson, GS., Laverty, TR., and Rubin, GM. (1991) Ras1 and a putative guanine nucleotideexchange factor perform crucial steps in signaling by the sevenless- protein tyrosine kinase. *Cell.* **67:** 701–716.

Slamon, D.J. *et al.* (1987) Human breast cancer: correlation of relapse and survival with amplification of the HER-2/*neu* oncogene. *Science.* **235:** 177–182.

Sonnenfeld, M.J., Jacobs, J.R. (1994). Mesectodermal cell fate analysis in Drosophila midline mutants. *Mech Dev.* **46(1):** 3-13.

Spector, NL., Xia, W., Burris, H., Hurwitz, H., Dees, EC., Dowlati, A., O'Neil, B., Overmoyer, B., Marcom, PK., Blackwell, KL., Smith, DA., Koch, KM., Stead, A., Mangum, S., Ellis, MJ., Liu, L., Man, AK., Bremer, TM., Harris, J., Bacus, S. (2005) A study of the biological effects of lapatinib (GW572016), a reversible inhibitor of ErbB1 and ErbB2 tyrosine kinases, on tumor growth and survival pathways in patients with advanced malignancies. *J. Clin. Oncol.* **23:** 2502–2512.

Sporn, M.B., Todaro, G.J. (1980) Autocrine secretion and malignant transformation of cells. *N Engl J Med.* **303:** 878–880.

Sorkin, A. and von Zastrow, M. (2009) Endocytosis and signalling: intertwining molecular networks. *Nat Rev Mol Cell Biol.* **10(9):** 609-22.

Sorkin, A. (2004) Cargo recognition during clathrin-mediated endocytosis: a team effort. *Curr. Opin. Cell Biol.* **16:** 392–399.

Sorkin, A., Goh, L.K. (2008) Endocytosis and intracellular trafficking of ErbBs. *Exp Cell Res.* **314(17):** 3093-106.

Simon, M.A. (2000) Receptor tyrosine kinases: Specific outcomes from general signals. *Cell.* **103**: 13-15.

Spradling, A.C., Stern, D., Beaton, A., Rhem, E.J., Laverty, T., Mozden, N., Misra, S. and Rubin, G.M. (1999) The Berkeley *Drosophila* Genome Project gene disruption project: Single P-element insertions mutating 25% of vital *Drosophila* genes. *Genetics.* **153(1):** 135-77.

Stove, C. and Bracke, M. (2004) Roles for neuregulins in human cancer. *Clin Exp Metastasis.* **21(8):** 665-84.

Stern, D. and Kamps, M.P. (1988) EGF-stimulated tyrosine phosphorylation of p185neu: a potential model for receptor interactions. *EMBO J.* **7:** 995-1001.

Stern, M.J., Marengere, L.E., Daly, R.J., Lowenstein, E.J., Kokel, M., Batzer, A., Olivier, P., Pawson, T. and Schlessinger, J. (1993) The human GRB2 and Drosophila Drk genes can functionally replace the Caenorhabditis elegans cell signaling gene sem-5. *Mol Biol Cell.* **4(11):** 1175-88.

Sturtevant, M.A. and Bier, E. (1995) Analysis of the genetic hierarchy guiding wing vein development in *Drosophila. Development.* **121(3):** 785-801.

Stuttfeld, E. and Ballmer-Hofer, K. (2009) Structure and function of VEGF receptors. *IUBMB Life.* **61(9):** 915-22.

Sundaram, MV. (2005) The love-hate relationship between Ras and Notch. *Genes Dev.* **19:** 1825–1839.

Su, M.A., Wisotzkey, R.G. and Newfeld, S.J. (2001) A screen for modifiers of decapentaplegic mutant phenotypes identifies lilliputian, the only member of the Fragile-X/Burkitt's lymphoma family of transcription factors in Drosophila melanogaster. *Genetics.* **157:** 717–725.

Takeuchi, K., Ito, F. (2010) EGF receptor in relation to tumor development: molecular basis of responsiveness of cancer cells to EGFR-targeting tyrosine kinase inhibitors. *FEBS J.* **277(2):** 316-26.

Therrien, M., Morrison, DK., Wong, AM., Rubin, GM. (2000) A genetic screen for modifiers of a kinase suppressor of Ras-dependent rough eye phenotype in Drosophila. *Genetics.* **156(3):** 1231-42.

Therrien, M., Chang, H.C., Solomon, N.M., Karim, F.D., Wassarman, D.A. and Rubin, G.M. (1995) KSR, a novel protein kinase required for RAS signal transduction. *Cell.* **83(6):** 879-88.

Tzahar, E., Waterman, H., Chen, X., Levkowitz, G., Karunagaran, D., Lavi, S., Ratzkin, BJ., Yarden, Y. (1996) A hierarchical network of interreceptor interactions determines signal transduction by Neu differentiation factor/neuregulin and epidermal growth factor. *Mol. Cell. Biol.* **16:** 5276–5287.

Valius, M. and Kazlauskas, A. (1993) Phospholipase C-gamma 1 and phosphatidylinositol 3 kinase are the downstream mediators of the PDGF receptor's mitogenic signal. *Cell.* **73(2):** 321-34.

Venter, J.C., Smith, H.O., Hood, L. (1996). A new strategy for genome sequencing. **Nature. 381(6581):** 364-6.

Vermeij, J., Teugels, E., Bourgain, C., Xiangming, J., Veld, P., Ghislain, V., Neyns, B., De Grève, J. (2008) Genomic activation of the EGFR and HER2-neu genes in a significant proportion of invasive epithelial ovarian cancers. *BMC Cancer.* **8:** 3.

Viglietto, G., Motti, M.L., Bruni, P., Melillo, R.M., D'Alessio, A., Califano, D., Vinci, F., Chiappetta, G., Tsichlis, P., Bellacosa, A., Fusco, A., Santoro, M. (2002) Cytoplasmic relocalization and inhibition of the cyclindependent kinase inhibitor p27(Kip1) by PKB/Akt-mediated phosphorylation in breast cancer. *Nat Med.* **8 :** 1136–1144.

von Zastrow, M., Sorkin, A. (2007) Signaling on the endocytic pathway. *Curr Opin Cell Biol.* 19(4): 436-45.

Webster, M.K., and Donoghue, D.J. (1996) Constitutive activation of fibroblast growth factor receptor 3 by the transmembrane domain point mutation found in achondroplasia, *EMBO J.* **15:** 520-527.

Wiley, HS. (2003) Trafficking of the ErbB receptors and its influence on signaling. *Exp Cell Res.* **284(1):** 78-88.

Winters, Z.E., Hunt, N.C., Bradburn, M,J,, Royds, J.A., Turley, H., Harris, A.L., Norbury, C.J. (2002) Subcellular localisation of cyclin B, Cdc2 and p21(WAF1/CIP1) in breast cancer. association with prognosis. *Eur J Cancer.* **37:** 2405–2412.

Wittwer, F., van der Straten, A., Keleman, K., Dickson, BJ., Hafen, E. (2001) Lilliputian: an AF4/FMR2-related protein that controls cell identity and cell growth. *Development.* **128(5):** 791-800.

Wolff, T. and Ready, D.F. (1991). The beginning of pattern formation in the Drosophila compound eye: the morphogenetic furrow and the second mitotic wave. *Development.* **113:** 841–850.

Xia, W., Chen, J.S., Zhou, X., Sun, P.R., Lee, D.F., Liao, Y., Zhou, B.P., Hung, M.C. (2004) Phosphorylation/cytoplasmic localization of p21Cip1/ WAF1 is associated with HER2/neu overexpression and provides a novel combination predictor for poor prognosis in breast cancer patients. *Clin Cancer Res.* **10:** 3815–3824, 2004

Xu, T. and Rubin, GM. (1993) Analysis of genetic mosaics in developing and adult Drosophila tissues. *Development.* **117(4):** 1223-37.

Yang, L. and Baker, N.E. (2003). Cell cycle withdrawal, progression, and cell survival regulation by Egfr and its effectors in the differentiating Drosophila eye. *Dev. Cell.* **4:** 359-369.

Yarden, Y. & Sliwkowski, M.X. (2001) Untangling the ErbB signalling network. *Nature Rev. Mol. Cell Biol.* **2:** 127–137.

Yarden, Y and Sliwkowski, M.X. (2000) untangling the ErbB signaling network. *Mol. Cell Biol.* **2:** 127-137.

Yaziji, H., Goldstein, LC., Barry, TS., Werling, R., Hwang, H., Ellis, GK., Gralow, JR., Livingston, RB., Gown, AM. (2004) HER-2 testing in breast cancer using parallel tissue-based methods. *J. Am. Med. Assoc.* **291:** 1972–1977.

Yu, A., Rual, JF., Tamai, K., Harada, Y., Vidal, M., He, X., Kirchhausen, T. (2007) Association of dishevelled with the clathrin ap-2 adaptor is required for frizzled endocytosis and planar cell polarity signaling. *Dev. Cell.* **12:** 129–141.

Zerial, M. and McBride, H. (2001) Rab proteins as membrane organizers. *Nat Rev Mol Cell Biol.* **2(2):** 107-17.

Zhou, B.P., Liao, Y., Xia, W., Spohn, B., Lee, M.H., Hung, M.C. (2001) Cytoplasmic localization of p21Cip1/WAF1 by Akt-induced phosphorylation in HER-2/neu-overexpressing cells. *Nat Cell Biol.* **3:** 245–252.

Zhou, B.P., Liao, Y., Xia, W., Zou, Y., Spohn, B., Hung, M.C. (2001) HER-2/ neu induces p53 ubiquitination via Akt-mediated MDM2 phosphorylation. *Nat Cell Biol.* **3:** 973–982.

APPENDIX

Supplement 2.1: Mis-expression of *Neu* alleles produces distinct wing phenotypes. *Neu* alleles were mis-expressed at the wing margin with p[C96] GAL4 driver. The activated Neu^{NT} showed the most severe wing phenotype that includes vein branching (asterisks), vein deltas (arrowheads) and wing notches (arrows) (H). Neu^{NYPD} showed a nearly wild type wing margin along with a very small vein delta (B). Neu^{YA} showed ectopic vein formation in the anterior half of the wing blade (C). A gradual increasing severity of wing notches phenotypes were observed in Neu^{YC} (E), Neu^{YD} (F), and Neu^{YE} (G) respectively. The transgenes are indicated at the bottom left of each panel. (Hossain, 2005; M.Sc. thesis).

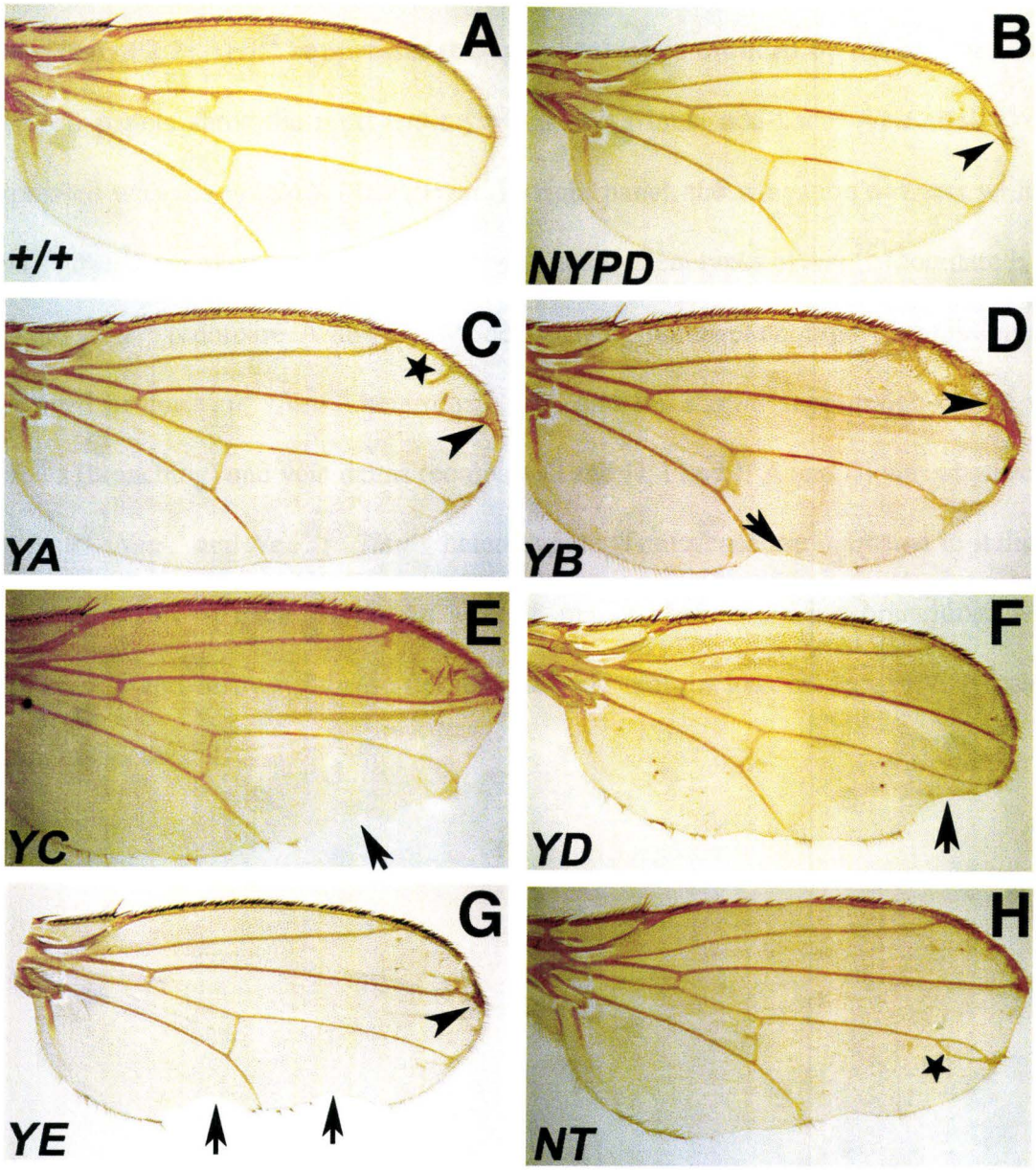
A
+/+
B
NYPD
C
YA
D
YB
E
YC
F
YD
G
YE
H
NT

Supplement 2.2: Neu^{YA} suppresses the eye phenotypes induced by other *Neu* alleles. The left panels show the representing wings of various 'add-back' *Neu* alleles, mis-expressed with the *p[C96]-GAL4* driver. In right panel, the wings are *in trans* with the Neu^{YA}. Neu^{YA} completely suppressed the wing notch phenotypes of Neu^{YE} (compare E and F) and Neu^{YB} (compare A and B). Moderate wing notch phenotype suppression was observed in the Neu^{YD}/Neu^{YA} heterozygote (C and D). Partial suppression of the vein defects (branching) and vein deltas (compare G and H; I and J; A and B) was observed in the Neu^{NT}/Neu^{YA} and Neu^{NYPD}/Neu^{YA} heterozygote. Transgenes are indicated in italics at the bottom left of each panel. An asterisk marks show the wing branching, while arrowheads and arrows indicate deltas and wing margin loss respectively. (Hossain, 2005; M.Sc. thesis).

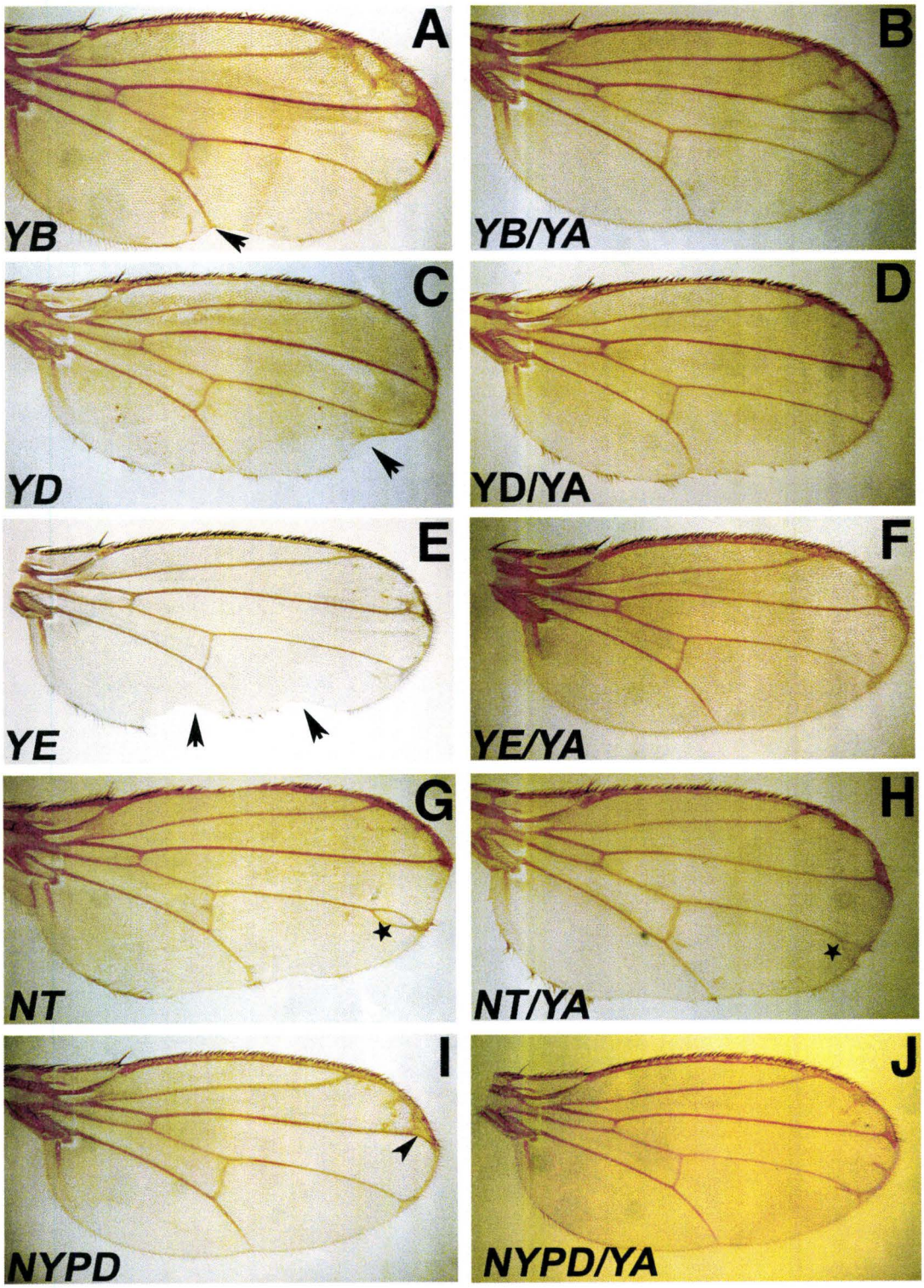
A
YB
B
YB/YA
C
YD
D
YD/YA
E
YE
F
YE/YA
G
NT
H
NT/YA
I
NYPD
J
NYPD/YA

Supplement 2.3: Mis-expression of *Neu* 'add-back' alleles produces distinct eye phenotype. The mis-expression of eye phenotype was induced with the *GMR-GAL4* driver. The ommatidial and the adjacent bristles are regularly spaced in the adult eye of *p[GMR-GAL4]* flies raised at 18°C (A). Activated Neu^{NT} produces the severe phenotypes that include greatly reduced eye size and complete loss of ommatidial shape and eye bristles (H). An irregular bristle arrangement along with noticeably flattened ommatidial discs were found in the *Neu* flies (D). A near wild type ommatidial shape and arrangement were observed in both Neu^{YA} (C) and Neu^{NYPD} (B) flies. However, in Neu^{NYPD}, paired bristles were distributed throughout the whole eye surface (see also Fig.3). On the other hand, several groups of three bristles at a time was observed in the case of Neu^{YA}. The eye phenotype of Neu^{YC} (E) and Neu^{YA} (F) and Neu^{YE} (G) were also graded severe. Transgenes are indicated at the bottom left of each panel. (Hossain, 2005; M.Sc. thesis).

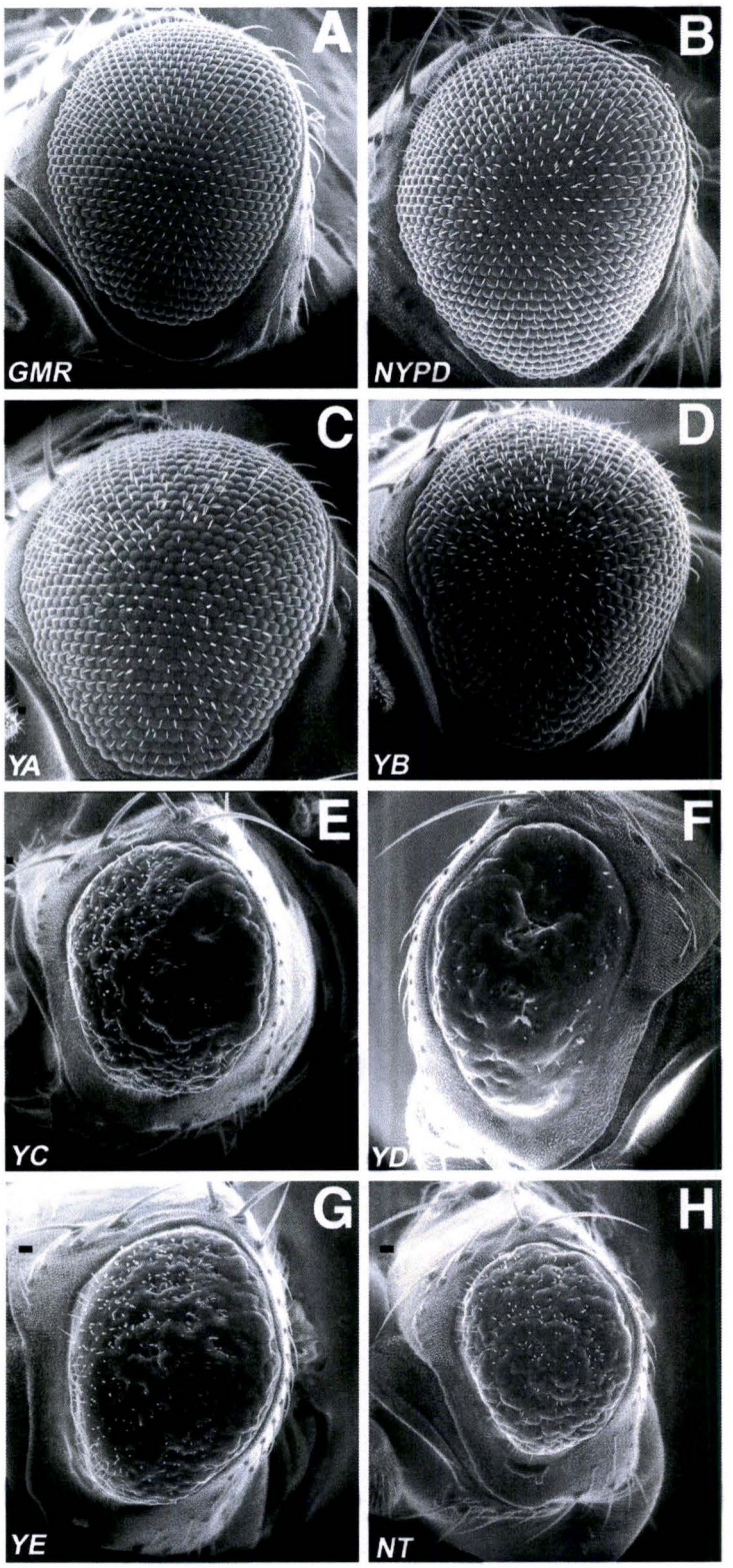
A
GMR
B
NYPD
C
YA
D
YB
E
YC
F
YD
G
YE
H
NT

Supplement 2.4: *Neu^{YA}* suppresses the DER (DEgfr)- induced eye phenotypes. Expression of wild type *Drosophila* EGF receptor (*DER^{WT}*) in the eye with *GMR-GAL4* driver resulted in a rough eye (A) with severely reduced ommatidial facets and bristles in the colourless area (I, upper part of the eye)) and irregularly fused facets in the rest of the eye (II). The rough eye phenotypes were greatly reduced in *p[UAS-DER^{WT}]/p[GMR-GAL4]; p[UAS-Neu^{YA}]/+* adults (B). A comparatively reduced colourless region of the eye was also observed with increased numbers of bristles and ommatidial facets (III) and the rest of the eye surface had almost regularly shaped facets (IV). The complete disruption of ommatidial facet structures with irregularly spaced bristles (C) was seen in the gain of function allele (*DER^{A877T}*) (Genotype: *p[UAS-DER^{WT}]/p[GMR-GAL4]*). A similar phenotype, with even more reduced bristle numbers, was seen in the *p[UAS-DER^{A877T}]/p[GMR-GAL4]; p[UAS-Neu^{YA}]/+* adults (D). However, the phenotype (E), due to a dominant negative allele of *DER (DER^{DN}),* was noticeably suppressed in the *p[UAS-DER^{DN}]/p[GMR-GAL4]; p[UAS-Neu^{YA}]/+* adults (F). The top left caption indicates the heterozygote of *GMR-GAL4* and the particular allele, while top left caption indicates the heterozygote of *Neu^{YA}* and the particular *DER* allele while expressed with *GMR-GAL4.* (Hossain, 2005; M.Sc. thesis).

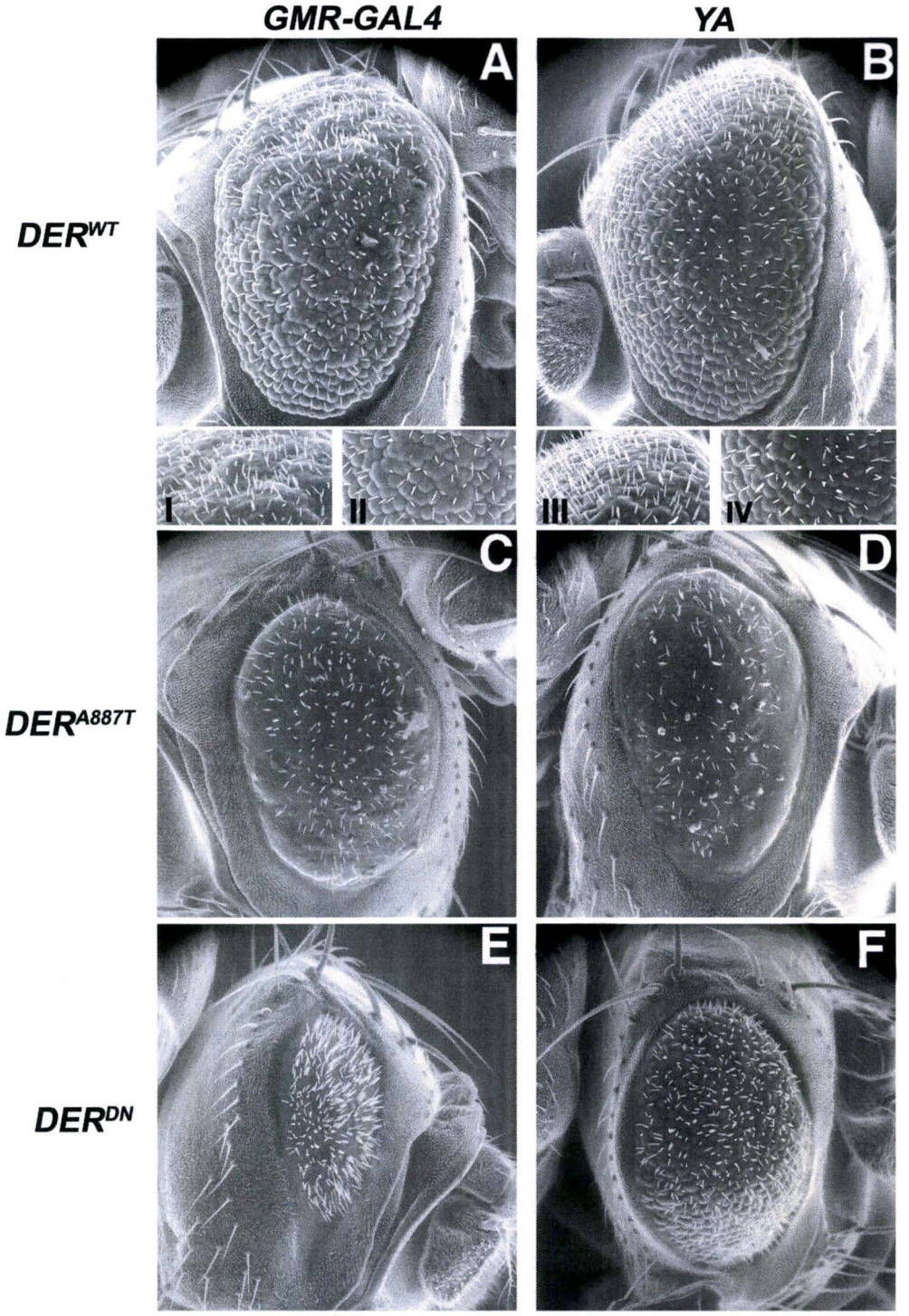
GMR-GAL4
YA
DER^WT
DER^A887T
DER^DN
A
B
C
D
E
F
I
II
III
IV

Supplement 2.5: The Paired t-test results for $DER^{ACT}/+$ and DER^{ACT}/Neu^{YA}

Paired *t* test results

P value and statistical significance:
The two-tailed P value equals 0.0245
By conventional criteria, this difference is considered to be statistically significant.

Confidence interval:
The mean of Group One minus Group Two equals -67.33
95% confidence interval of this difference: From -113.56 to -21.10

Intermediate values used in calculations:
t = 6.2668
df = 2
standard error of difference = 10.745

Learn more:

GraphPad's web site includes portions of the manual for GraphPad Prism that can help you learn statistics. First, review the meaning of P values and confidence intervals. Next check whether you chose an appropriate test. Then learn how to interpret results from an unpaired or paired *t* test. These links include GraphPad's popular *analysis checklists*.

Review your data:

Group	Group One	Group Two
Mean	832.33	899.67
SD	13.01	27.02
SEM	7.51	15.60
N	3	3

Supplement 2.6: The Paired t-test results for $DER^{WT}/+$ and DER^{WT}/Neu^{YA}

Paired *t* test results

P value and statistical significance:
The two-tailed P value equals 0.2830
By conventional criteria, this difference is considered to be not statistically significant.

Confidence interval:
The mean of Group One minus Group Two equals 21.33
95% confidence interval of this difference: From -41.77 to 84.44

Intermediate values used in calculations:
t = 1.4545
df = 2
standard error of difference = 14.667

Learn more:

GraphPad's web site includes portions of the manual for GraphPad Prism that can help you learn statistics. First, review the meaning of P values and confidence intervals. Next check whether you chose an appropriate test. Then learn how to interpret results from an unpaired or paired *t* test. These links include GraphPad's popular *analysis checklists*.

Review your data:

Group	Group One	Group Two
Mean	792.67	771.33
SD	16.56	15.18
SEM	9.56	8.76
N	3	3

Supplement 2.7: The Paired t-test results for $Elp^{B1}/+$ and Elp^{B1}/Neu^{YA}

Paired *t* test results

P value and statistical significance:

The two-tailed P value equals 0.0082

By conventional criteria, this difference is considered to be very statistically significant.

Confidence interval:

The mean of Group One minus Group Two equals -130.00

95% confidence interval of this difference: From -180.97 to -79.03

Intermediate values used in calculations:

t = 10.9739

df = 2

standard error of difference = 11.846

Learn more:

GraphPad's web site includes portions of the manual for GraphPad Prism that can help you learn statistics. First, review the meaning of P values and confidence intervals. Next check whether you chose an appropriate test. Then learn how to interpret results from an unpaired or paired *t* test. These links include GraphPad's popular *analysis checklists*.

Review your data:

Group	Group One	Group Two
Mean	534.33	664.33
SD	15.04	20.11
SEM	8.69	11.61
N	3	3

Supplement 2.8: The Paired t-test results for *sev-Torso/+* and *sev-Torso /Neu*^{YA}

Paired *t* test results

P value and statistical significance:

The two-tailed P value equals 0.0062

By conventional criteria, this difference is considered to be very statistically significant.

Confidence interval:

The mean of Group One minus Group Two equals -244.33

95% confidence interval of this difference: From -327.63 to -161.04

Intermediate values used in calculations:

t = 12.6211

df = 2

standard error of difference = 19.359

Learn more:

GraphPad's web site includes portions of the manual for GraphPad Prism that can help you learn statistics. First, review the meaning of P values and confidence intervals. Next check whether you chose an appropriate test. Then learn how to interpret results from an unpaired or paired *t* test. These links include GraphPad's popular *analysis checklists*.

Review your data:

Group	Group One	Group Two
Mean	574.67	819.00
SD	16.56	17.00
SEM	9.56	9.81
N	3	3

Supplement 2.9: The intensity of Anti-pTyr Antibody Fluorescence in cells expressed under the control of I-76-D GAL4 driver.

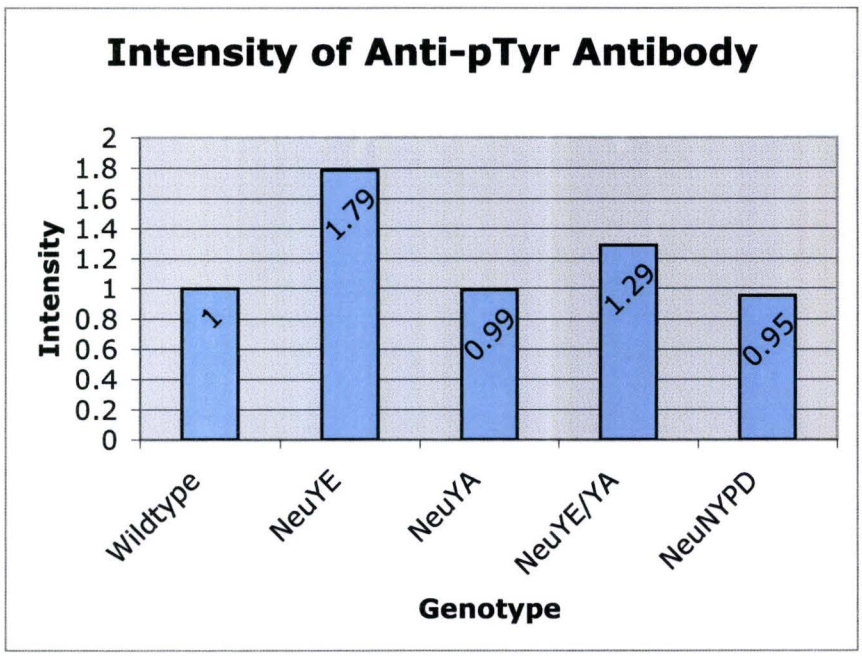

Supplement 2.10: *Neu*^{YA} downregulates the phosphorylation level of the other 'add-back' *Neu* alleles. The *Twist-GAL4* driver expresses the gene of interest (*UAS-GFP*) at the ventral ectoderm during the stage 6-12 of developing embryos. A number of cells of the epidermis show higher, while the others (surrounding cells) show minimal level of GFP expression (A). The phosphorylation level in control (wild type) embryo is at a minimal level (B). The mis-expressed *Neu*^{YE} embryos show higher levels of phosphorylation in many of the epidermal cells at the ventral region (C), while only a few cells show similar level of phosphorylation in *Neu*^{YA} (D). However, a reduced level of phosphorylation is evident in *Neu*^{YE}/*Neu*^{YA} heterozygote (E). Finally, a higher phosphorylation level than that of *Neu*^{YA} is seen in *Neu*^{NYPD} (F).

All Images were taken at 63X lens and 5.62X magnification on a Leica confocal microscope. Scale bar indicates 5 μm.

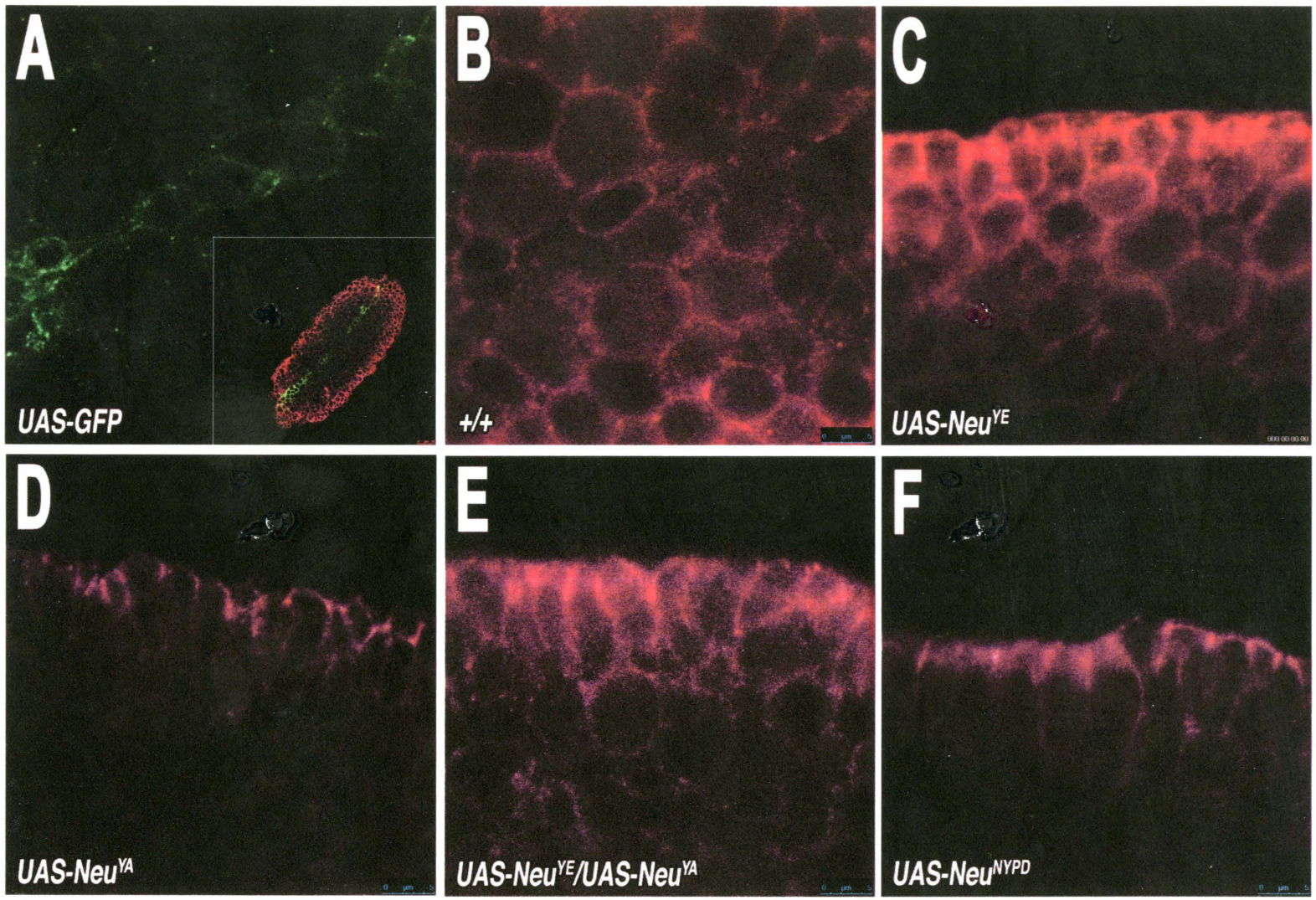
A
UAS-GFP
B
+/+
C
UAS-Neu^YE
D
UAS-Neu^YA
E
UAS-Neu^YE/UAS-Neu^YA
F
UAS-Neu^NYPD

Supplement 2.11: Dosage sensitive modifier screen of RTK regulators. The haplosuficient of the negative regulator of RTK, *Sprouty* suppressed the Neu^{YA} eye phenotype, while enhanced the phenotypes of Neu^{YE} and Neu^{YAE}. However, most of the other tested regulators were insensitive to various *Neu* alleles.

Supplement 2.11: Summary data of *Neu*^{YA} interactions with various regulators of RTK and receptor mediated endocytotic pathway.

Alleles		*Neu* Modification			Roles in RTKs Regulation	Mammalian relatives	References
		YA	*YE*	*YAE*			
Regulators:							
drk^{10626}	Downstream of receptor kinase	N	N	N	Acts as an adaptor protein and plays important role in Signaling of Receptor Tyrosine Kinase.	Grb2	Feller SM et al., 2002.
Kek1	Kekkon1	N	E	E	EGFR inhibitor protein. Acts in a negative feedback loop to modulate the activity of the EGFR tyrosine kinase	---	Ghiglione C et al., 1999.
Px	Plexin	N	N	N	A functional semaphoring receptor signaling in axon guidance.	----	Vikis et al., 2000.
Spry5	Sprouty	S	E	E	Membrane-anchored Phosphoprotein Inhibitors of Growth Factor Signaling	Sprouty	Impagnatiello et al., 2001.
Ebi^{CSS-6}	Ebi	N	S	S	ebi regulates epidermal growth factor receptor signaling pathways in *Drosophila*.	---	Dong et al., 1999
Src^{42A}	Src Oncogene at 42A	N	N	N	An Oncogene with Tyrosine Kinase activity.	FRK (Fyn-related Kinase)	Zhang et al., 1999.
Src^{64B}	Src Oncogene at 64B	N	N	N	An Oncogene with Tyrosine Kinase activity.	FRK (Fyn-related Kinase)	Li et al., 1999.

S: Suppression, E: Enhancement, N: No-interaction

Supplement 3.1: Mutants and pUAST lines used in this study.

All mutants and pUAST lines used are reported in the following table.

pUAST lines	Genetics	Reference
GMRGAL4 Source: Rubin's Lab Freeman's Lab.	Driver line containing yeast transcription factor, GAL4, under the control of glass multimer reporter (GMR).	Hay et al., 1997.
C96 Source: Boulianne	Enhancer trap P-insert line containing yeast transcription factor, GAL4. C96 expression has been observed in imaginal discs and adult wing margins (Settle et al., 2003)	Kim et al., 1998; Gustafson and Boulianne, 1996; Stewart et al., 2001.
UAS-DER^{wildtype} (11-9) Source: N. Baker	*Drosophila* epidermal growth factor receptor	Baker and Rubin, 1989.
DER-Ellipse (DER^{ElpB1}) Source: N. Baker	Gain of function mutant of DEgfr	Baker and Rubin, 1989.
UAS-DER^{A887T} (12-4) Source: N. Baker	Constitutively active DEgfr that contains an alanine to threonine mutation at residue number 887.	Lesokhin et al., 1999.
UAS-DER^{DN} Source: M. Freeman	Dominant negative *Drosophila* Egfr receptor	Freeman, 1996.
Downstream of Receptor kinase (drk^{10626}) Source: S. Simon	SH3/SH2 adaptor protein involved in Ras protein signal transduction.	Simon et. al., 1993; Spradling et al., 1999.
Kekkon1 (Kek1) Source: Ghiglione	EGFR inhibitor protein. Acts in a negative feedback loop to modulate the activity of the EGFR tyrosine kinase.	Ghiglione C et al., 1999.
Sprouty (Spry^{05}) Source: Bloomington	Membrane-anchored Phosphoprotein Inhibitors of Growth Factor Signaling	Impagnatiello et al., 2001.
Plexin (Px)		
Ebi (Ebi^{CSS-6}) Source: Bloomington	ebi regulates epidermal growth factor receptor signaling pathways in *Drosophila.*	Dong et al., 1999

Src Oncogene at 42A (Src^{42A}) Source: Bloomington	An Oncogene with Tyrosine Kinase activity.	Zhang et al., 1999.
Src Oncogene at 64B (Src^{64B}) Source: Bloomington	An Oncogene with Tyrosine Kinase activity.	Li et al., 1999.
Alpha-adaptin Source: Spradling	Formation of intracellular transport vesicle and/or Selection of cargo for entry into vesicle	Boehm and Bonificiano, 2001.
Epidermal Growth Factor Receptor Substrate Clone 15 ($Eps\text{-}15^{EP2513}$) Source: Bloomington	Link signaling receptors to a clathrin coat. Plays role in the assembly of clathrin-coated pits.	Brett and Traub, 2006.
Expanded (Ex^{K12913}) Source: Caltech	Functions cooperatively with Merlin to modulate receptor Endocytosis.	Boedigheimer et al.,1997.
Clathrin Heavy chain (Chc^{1}) Source: Bazinet	Formation of invaginated pits on the plasma membrane and subsequent budding of vesicles.	Bazinet et al., 1993.
Merlin (Mer^{4}) Source: Fehon	Merlin and Expanded function cooperatively to modulate receptor endocytosis and signaling.	Maitra S et al., 2006.
Rab5 ($Rab5^{K08232}$) Source: Kiss	Small GTPase that plays a key role in the early endocytotic pathway.	Zerial and McBride, 2001.
Hepatocyte Growth Factor regulated tyrosine kinase substrate (Hrs^{D28}) Source: Bellen	Hrs regulates endosome membrane invagination. Plays role in receptors sorting in intraluminal vescicles.	Lloyd et al., 2002.
Rab11 ($Rab11^{2JD1}$) Source: Rawls	Small GTPase that plays a key role in the early endocytotic pathway regulation. Rab11 regulates recycling through the pericentriolar recycling endosome.	Sonnichsen, 2000.
Effet (Eff^{8}) Source: Dura	Functions as E1 Ubiquitin protein	Flauvarque et al., 2001.
Ubiquitin Activating	Ubiquitin Activating	Lee, 2008.

Enzyme ($Uba1^{05642}$) Source: Spradling	Enzyme, E1. Controls apoptosis autonomously and Tissue growth non-autonomously.	
Ubiquitin Activating Enzyme ($Uba1^{s3484}$) Source: Spradling	Ubiquitin Activating Enzyme, E1. Controls apoptosis autonomously and Tissue growth non-autonomously.	Lee, 2008.
Casitas B-Lineage ($Cbl^{KG03080}$) Source: Schupbach	Functions as an E3 ligase, and Lymphoma catalyse the formation of a covalent bond between ubiquitin and Cbl's protein substrates-typically a receptor tyrosine kinase.	Traub, 2006.
Scribble ($Scrib^{KG04161}$) Source: Bender	Functions in Ubiquitin-mediated degradation.	Takizawa S et al., 2006.
Vacuolar Protein Sorting (Vps^{25}) Source: Jongens	Involved in Golgi to Lysosome trafficking.	Pevsner J et al., 1999.
Erupted (Ept^{2}) Source: Moberg	Encodes components of Endosomal sorting complex required for transport (ESCRT).	Giebel and Wodarz, 2006.

Supplement 3.2: Bloomington Deficiency Stocks used in this study

Stock	Deficiency strain	Break pint	Description
6608	Df(2L)BSC16	21C3-4;21C6-8	Df(2L)BSC16, net[1] cn[1]/SM6a
8673	Df(2L)BSC107	21C5-D1	w[1118];Df(2L)BSC107, P+PBac{XP5.WH5} BSC107/CyO
3084	Df(2L)ast2	21D1-2;22B2-3	Df(2L)ast2/SM1
3133	Df(2L)dp-79b	22A2-3;22D5-E1	Df(2L)dp-79b, dp[DA]cn[1]/ In(2LR)bw[V1], b[1] bw[V1]
7144	Df(2L)BSC37	22D2-3;22F1-2	Df(2L)BSC37/CyO
6648	Df(2L)dpp[d14]	22E4-F2;22F3-23A1	Df(2L)dpp[d14]/In(2LR)Gla, wg[Gla-1]
90	Df(2L)C144	22F4-23A1;23C2-4	Df(2L)C144, $dpp^{d\text{-}ho}$ ed^{1}/In(2LR)Gla, $wg^{Gla\text{-}1}$ Bc^{1} $Egfr^{E1}$
1567	Df(2L)JS17	23C1-2;23E1-2	Df(2L)JS17, dpp[d-ho]/CyO, P{ry[+t7.2]=en1}wg[en11]
490	Df(2L)E110	25F3-26A1;26D3-11	In(1)w[m4]; Df(2L)E110/CyO
6299	Df(2L)BSC5	26B1-2;26D1-2	Df(2L)BSC5, w[+mC]/SM6a
6338	Df(2L)BSC6	26D3-E1;26F4-7	Df(2L)BSC6, dp[ov1] cn[1]/SM6a
6374	Df(2L)BSC7	26D10-E1;27C1	w[1118]; Df(2L)BSC7/CyO
2414	Df(2L)spd[j2]	27C1-2;28A	w[*]; Df(2L)spd[j2], wg[spd j2]/CyO,P{ry[+t7.2]=ftz/ lacB}E3
5420	Df(2L)Dwee1-W05	27C2-3;27C4-5	w[*]; Df(2L)Dwee1 W05/CyO; P{ry[+t7.2] =ftz/lacC}1
4956	Df(2L)XE-3801	27E2;28D1	Df(2L)XE-3801/CyO, P{ry[+t7.2]=sevRas1. V12}FK1
7147	Df(2L)BSC41	28A4-B1;28D3-9	Df(2L)BSC41, dp[ov1] cn[1]/CyO
9502	Df(2L)BSC142	28C3;28D3	w[1118]; Df(2L)BSC142, P+PBac{XP5.WH5} BSC142/CyO
140	Df(2L)Trf-C6R31	28DE;28DE	y[1] w[67c23]; Df(2L)Trf-C6R31/CyO
7807	Df(2L)Exel7034	Df(2L)Exel7034	P+PBac{XP5.RB3} Exel7034/CyO

Stock	Deficiency strain	Break pint	Description
179	Df(2L)TE29Aa-11	28E4-7;29B2-C1	ln(1)w[m4h], y[1]; Df(2L)TE29Aa-11, dp[*]/CyO
8836	Df(2L)BSC111	28F5;29B1	w[1118]; Df(2L)BSC111, P+PBac{XP5.WH5} BSC111/CyO
9298	Df(2L)ED611	29B4;29C3	w[1118]; Df(2L)ED611, P{w[+mW.Scer\ FRT.hs3]=3'.RS5+3.3'} ED611/SM6a254
2892	Df(2L)N22-14	29C1-2;30C8-9	Df(2L)N22-14/CyO
6478	Df(2L)BSC17	30C3-5;30F1	Df(2L)BSC17/SM6a
1045	Df(2L)Mdh	30D-30F;31F	Df(2L)Mdh, cn[1]/Dp(2;2)Mdh3, cn[1]
8469	Df(2L)BSC50	30F4-5;31B1-4	Df(2L)BSC50/SM6a
3366	Df(2L)J2	31B;32A	y[*]; Df(2L)J2/SM1
9503	Df(2L)BSC143	31B1;31D9	w[1118]; Df(2L)BSC143, P+PBac{XP5.WH5} BSC143/CyO
7142	Df(2L)BSC32	32A1-2;32C5-D1	Df(2L)BSC32/SM6a, bw[k1]
9505	Df(2L)BSC145	32C1;32C5	w[1118]; Df(2L)BSC145, P+PBac{XP5.WH5} BSC145/CyO
7143	Df(2L)BSC36	32D1;32D4-E1	Df(2L)BSC36/SM6a, bw[k1]
5869	Df(2L)FCK-20	32D1;32F1-3	Df(2L)FCK-20, dp[ov1] bw[1]/CyO, P{ry[+t7.2] =sevRas1.V12}FK1
3079	Df(2L)Prl	32F1-3;33F1-2	Df(2L)Prl, Prl[1] nub[Prl]/CyO
6999	Df(2L)BSC30	34A3;34B7-9	Df(2L)BSC30/SM6a, bw[k1]
9594	Df(2L)BSC159	34B4;34C4	w[1118]; Df(2L)BSC163, P+PBac{XP5.WH5} BSC163/CyO
3138	Df(2L)b87e25	34B12-C1;35B10-C1	Df(2L)b87e25/CyO
9506	Df(2L)BSC147	34C1;34C6	w[1118]; Df(2L)BSC147, P+PBac{XP5.RB3} BSC147/CyO
6092	Df(2L)b80e3, Dp(2;2)GYS, pr[1] bw[1]/CyO		
6056	Df(2L)64j, L[2]/CyO, Adh[nB]		
3588	Df(2L)TE35BC-24	35B4-6;35F1-7	Df(2L)TE35BC-24, b[1] pr[1] pk[1] cn[1] sp[1]/CyO
1491	Df(2L)r10	35D1;36A6-7	Df(2L)r10, cn[1]/CyO

Stock	Deficiency strain	Break pint	Description
2583	Df(2L)cact-255rv64	35F-36A;36D	Df(2L)cact-255rv64, cact[chif64]/CyO; ry[506]
420	Df(2L)TW137	36C2-4;37B9-C1	Df(2L)TW137, cn[1] bw[1]/CyO, Dp(2;2)M(2)m[+]
567	Df(2L)pr-A16	37B2-12;38D2-5	Df(2L)pr-A16, cn[1] bw[1]/CyO
167	Df(2L)TW161	38A6-B1;40A4-B1	Df(2L)TW161, cn[1] bw[1]/CyO
7531	Df(2L)Exel6049	39E7;40D3	w[1118]; Df(2L)Exel6049, P{w[+mC]=XP-U} Exel6049/CyO
9510	Df(2L)BSC151	40A5;40E5	w[1118]; Df(2L)BSC151, P+PBac{XP5.WH5} BSC151/CyO
4308	Df(2R)nap14/CyO	41B-42B1	
1007	Df(2R)nap9	42A1-2;42E6-F1	Df(2R)nap9/Dp(2;2)BG, In(2LR)Gla, wg[Gla-1]
1888	Df(2R)ST1	42B3-5;43E15-18	Df(2R)ST1, Adh[n5] pr[1] cn[*]/CyO
3368	Df(2R)cn9	42E;44C	Df(2R)cn9/CyO, amos[Roi1] sp[*]
198	Df(2R)H3C1	43F;44D3-8	w[118]; Df(2R)H3C1/CyO
201	Df(2R)H3E1	44D1-4;44F12	w[118]; Df(2R)H3E1/CyO
3591	Df(2R)Np5	44F10;45D9-E1	w[1]; Df(2R)Np5, In(2LR)w45-32n, cn[1]/CyO
4966	Df(2R)w45-30n	45A6-7;45E2-3	w[1]; Df(2R)w45-30n, cn[1]/CyO
6917	Df(2R)BSC29	45D3-4;45F2-6	Df(2R)BSC29, cn[1] bw[1] sp[1]/CyO
9410	Df(2R)BSC132	45F6;46B12	w[1118]; Df(2R)BSC132, P+PBac{XP5.WH5} BSC132/SM6a
1743	Df(2R)B5	46A;46C	w[1118]; Df(2R)B5, px[1] sp[1]/CyO, Adh[nB]
1702	Df(2R)X1	46C;47A1	Df(2R)X1, Mef2[X1]/CyO, Adh[nB]
596	Df(2R)stan2, b[1] pr[1] P{ry[+t7.2]=neoFRT}42D/CyO	46F1-47B	
520	Df(2R)E3363/CyO	47A3-47E	
190	Df(2R)en-A	47D3;48B2	Df(2R)en-A/CyO

Stock	Deficiency strain	Break pint	Description
3518	Df(2R)Jp1	51D3-8;52F5-9	w[a] N[fa-g];Df(2R)Jp1/CyO
3520	Df(2R)Jp8	52F5-9;52F10-53A1	w[a] N[fa-g]; Df(2R)Jp8, w[+]/CyO
7886	w[1118]; Df(2R)Exel7142,P+PBac{XP5.WH5}Exel7142/CyO		
7888	w[1118]; Df(2R)Exel7144, P+PBac{XP5.RB3}Exel7144/CyO		
7445	Df(2R)BSC49	53D9-E1;54B5-10	Df(2R)BSC49/SM6a
7414	Df(2R)BSC44	54B1-2;54B7-10	Df(2R)BSC44/SM6a
9596	Df(2R)BSC161	54B2;54B17	w[1118]; Df(2R)BSC161, P+PBac{XP5.WH5} BSC161/CyO
5680	Df(2R)robl-c	54B17-C4;54C1-4	Df(2R)robl-c/CyO, y[+]
5574	Df(2R)k10408	54C1-4;54C1-4	y[1] w[67c23]; Df(2R)k10408,P{w[+mC] =lacW}mthl3[k10408] CG4827[k10408] /CyO
7441	Df(2R)BSC45	54C8-D1;54E2-7	Df(2R)BSC45, w[+mC]/SM6a
6779	Df(2R)14H10Y-53	54D1-2;54E5-7	y[1] w[67c23] Df(2R)14H10Y-53/SM6a
6780	Df(2R)14H10W-35	54E5-7;55B5-7	y[1] w[67c23]; Df(2R)14H10W-35/SM6a
1547	Df(2R)PC4	55A;55F	Df(2R)PC4/CyO
757	Df(2R)P34	55E2-4;56C1-11	y[1] w[*]/Dp(1;Y)y[+]; Df(2R)P34/CyO
6866	Df(2R)BSC26	56C4;56D6-10	Df(2R)BSC26/CyO
6647	Df(2R)BSC22	56D7-E3;56F9-12	Df(2R)BSC22/SM6a
3467	Df(2R)AA21	56F9-17;57D11-12	Df(2R)AA21, c[1] px[1] sp[1]/SM1
7896	Df(2R)Exel7162	56F11;56F16	w[1118]; Df(2R)Exel7162, P+PBac{XP5.WH5} Exel7162/CyO
6609	Df(2R)BSC19 5	6F12-14;57A4	Df(2R)BSC19, cn[1] bw[1]/SM6a
5246	Df(2R)Egfr5	57D2-8;58D1	Df(2R)Egfr5, b[1] pr[1] cn[1] sca[1]/CyO, P{ry[+t7.2] =sevRas1.V12}FK1
3124	Df(3L)fz-GF3b	70C1-2;70D4-5	Df(3L)fz-GF3b, P{w[+tAR] ry[+t7.2AR]=wA[R]} 66E/TM6B, Tb[+]
3126	Df(3L)fz-M21	70D2-3;71E4-5	Df(3L)fz-M21, st[1]/TM6
6551	Df(3L)XG5	71C2-3;72B1-C1	Df(3L)XG5/TM3, Sb[1] Ser[1]

Stock	Deficiency strain	Break pint	Description
3640	Df(3L)brm11	71F1-4;72D1-10	Df(3L)brm11/TM6C, cu[1] Sb[1] ca[1]
2993	Df(3L)st-f13	72C1-D1;73A3-4	Df(3L)st-f13, Ki[1] rn[roe-1] p[p]/TM6B, Tb[1]
2998	Df(3L)81k19	73A3;74F	Df(3L)81k19/TM6B, Tb[1]
6411	Df(3L)BSC8	74D3-75A1;75B2-5	Df(3L)BSC8/TM3, Ser[1]
2608	Df(3L)W10	75A6-7;75C1-2	Df(3L)W10, ru[1] h[1] Sb[sbd-2]/TM6B, Tb[1]
2990	Df(3L)Cat	75B8;75F1	Df(3L)Cat, kni[ri-1] Sb[sbd1] e[*]/TM3, Ser[1]
2990	Df(3L)Cat, kni[ri-1] Sb[sbd-1] e[*]/TM3, Ser[1]		
8082	Df(3L)ED4782	75F2;76A1	w[1118]; Df(3L)ED4782, P{w[+mW.Scer\FRT. hs3]=3'.RS5+3.3'} ED4782/TM6C, cu[1] Sb[1]
6754	Df(3L)fz2	75F10-11;76A1-5	w[*]; Df(3L)fz2/TM6B, Tb[1]
8085	w[1118];Df(3L)ED4799,P{w[+mW.Scer\FRT.hs3]=3'.RS5+3.3'}ED4799/TM6C, cu[1] Sb[1]		
6646	Df(3L)BSC20	76A7-B1;76B4-5	Df(3L)BSC20, st[1] ca[1]/TM6B, Tb[1]
3617	Df(3L)kto2	76B1-2;76D5	Df(3L)kto2/TM6B, Tb[1]
5126	Df(3L)XS533	76B4;77B	Df(3L)XS533/TM6B, Sb[1] Tb[1] ca[1]
2052	Df(3L)rdgC-co2	77A1;77D1	Df(3L)rdgC-co2, th[1] st[1] in[1] kni[ri-1] p[p]/ TM6C, cu[1] Sb[1] Tb[1] ca[1]
3127	Df(3L)ri-79c	77B-C;77F-78A	Df(3L)ri-79c/TM3, Sb[1]
5878	Df(3L)ri-XT1	77E2-4;78A2-4	Df(3L)ri-XT1, ru[1] st[1] e[1] ca[1]/TM3, P{w[+ m*]=Ubx-lacZ.w[+]} TM3, Sb[1]
4429	Df(3L)ME107	77F3;78C8-9	Df(3L)ME107, mwh[1] red[1] e[1]/TM1, red[*]
4430	Df(3L)Pc-2q	78C5-6;78E3-79A1	Df(3L)Pc-2q, ry[506]/TM2
3007	Df(3R)ry615	87B11-13;87E8-11	Df(3R)ry615/TM3, Sb[1] Ser[1]
1534	Tp(3;Y)ry506-85C	87D1-2;88E5-6	Tp(3;Y)ry506-85C/MKRS
383	Df(3R)ea	88E7-13;89A1	Df(3R)ea, kni[ri-1] p[p]/TM3, Ser[1]
3468	Df(3R)slo8	96A2-7;96D2-4	Df(3R)slo8/Dp(3;3)Su[8]

Stock	Deficiency strain	Break pint	Description
7681	Df(3R)Exel6202	96C9;96E2	w[1118]; Df(3R)Exel6202, P{w[+mC]=XP-U}Exel6202 /TM6B, Tb[1]
7682	Df(3R)Exel6203	96E2;96E6	w[1118]; Df(3R)Exel6203, P{w[+mC]=XP-U}Exel6203 /TM6B, Tb[1]
2447	e[4] E(spl)[1]		
9500	Df(3R)BSC140	96F1;96F10	w[1118]; Df(3R)BSC140, P+PBac{XP5.WH5} BSC140/TM6B, Tb[+]
5601	Df(3R)Espl3	96F1;97B1	Df(3R)Espl3/TM6C, cu[1] Sb[1] Tb[1] ca[1]
1910	Df(3R)Tl-P	97A;98A1-2	Df(3R)Tl-P, e[1] ca[1]/TM3, Ser[1]
823	Df(3R)D605	97E3;98A5	Df(3R)D605/TM3, Sb[1] Ser[1]
9529	Df(3R)IR16	97F1-2;98A	w[*]; Df(3R)IR16/TM3, Sb[1]
7412	Df(3R)BSC42	98B1-2;98B3-5	Df(3R)BSC42, st[1] ca[1]/TM3, Sb[1]
1425	y[1] w[1]; Df(3R)M37, kni[ri-1]/TM3, Sb[1]		
430	Df(3R)3450	98E3;99A6-8	w[1118]; Df(3R)3450/TM6B, Tb[1]

Supplement 3.3: Enhancers showed a wide range of rough-eye phenotype. The enhancers to be mapped in this study were selected only if they showed a very strong eye phenotype compared to the control *GMR-Neu*^{YAE} flies (A and B). Some of these enhancers that fit our criteria were given names based on their linkage to the particular chromosome and initial 'E' followed by the specific numeric number (See C-J). Enhancers showed smaller eyes with fewer bristles and rougher eye surface (C-L). However, the enhancers, such as E218, that did not comprise the fit list were not named or studied further (K and L). Images were taken at X150 and X300 magnifications on an ESEM. Bar indicates 150 μm for B, D, F, H, J and L.

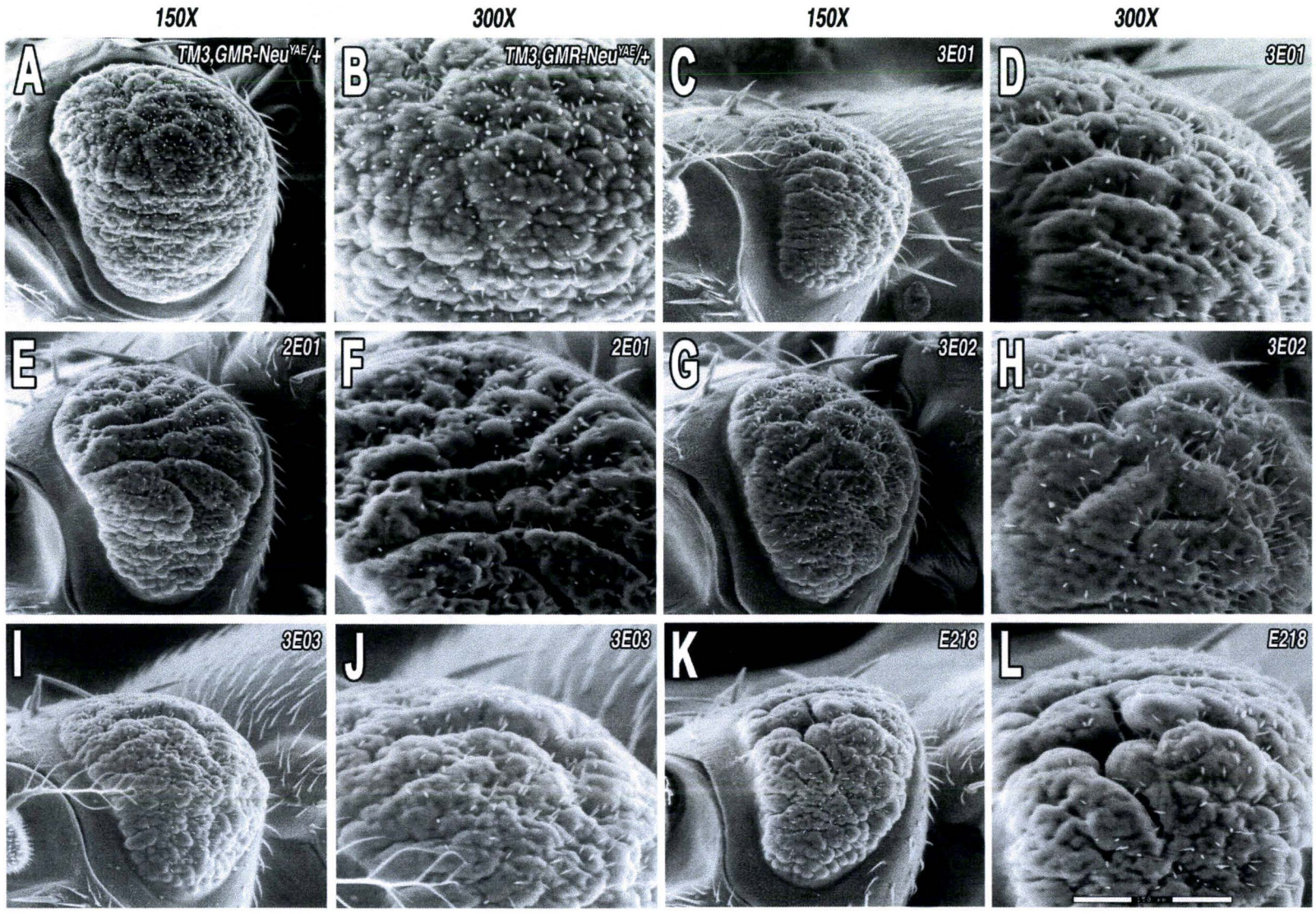
150X
300X
150X
300X
A
TM3,GMR-Neu^YAE/+
B
TM3,GMR-Neu^YAE/+
C
3E01
D
3E01
E
2E01
F
2E01
G
3E02
H
3E02
I
3E03
J
3E03
K
E218
L
E218

Supplement 3.4: Suppressors showed a wide range of eye phenotype. The suppressors to be mapped in this study were selected only if they showed a very strong eye phenotype compared to the control *GMR-Neu*^{YAE} flies (A and B). The suppressors that fit our criteria were named according to their linkage to the particular chromosome and initial 'E' followed by a numeric identifier (See C-J). Suppressors were identified for larger eyes with more regular bristles and ommatidial facets (C-L). However, the suppressors, such as S011, failed to our fit list and were not named or studied further (C and D). Images were taken at X150 and X300 magnifications on an ESEM. Bar indicates 150 μm for B, D, F, H, J and L.

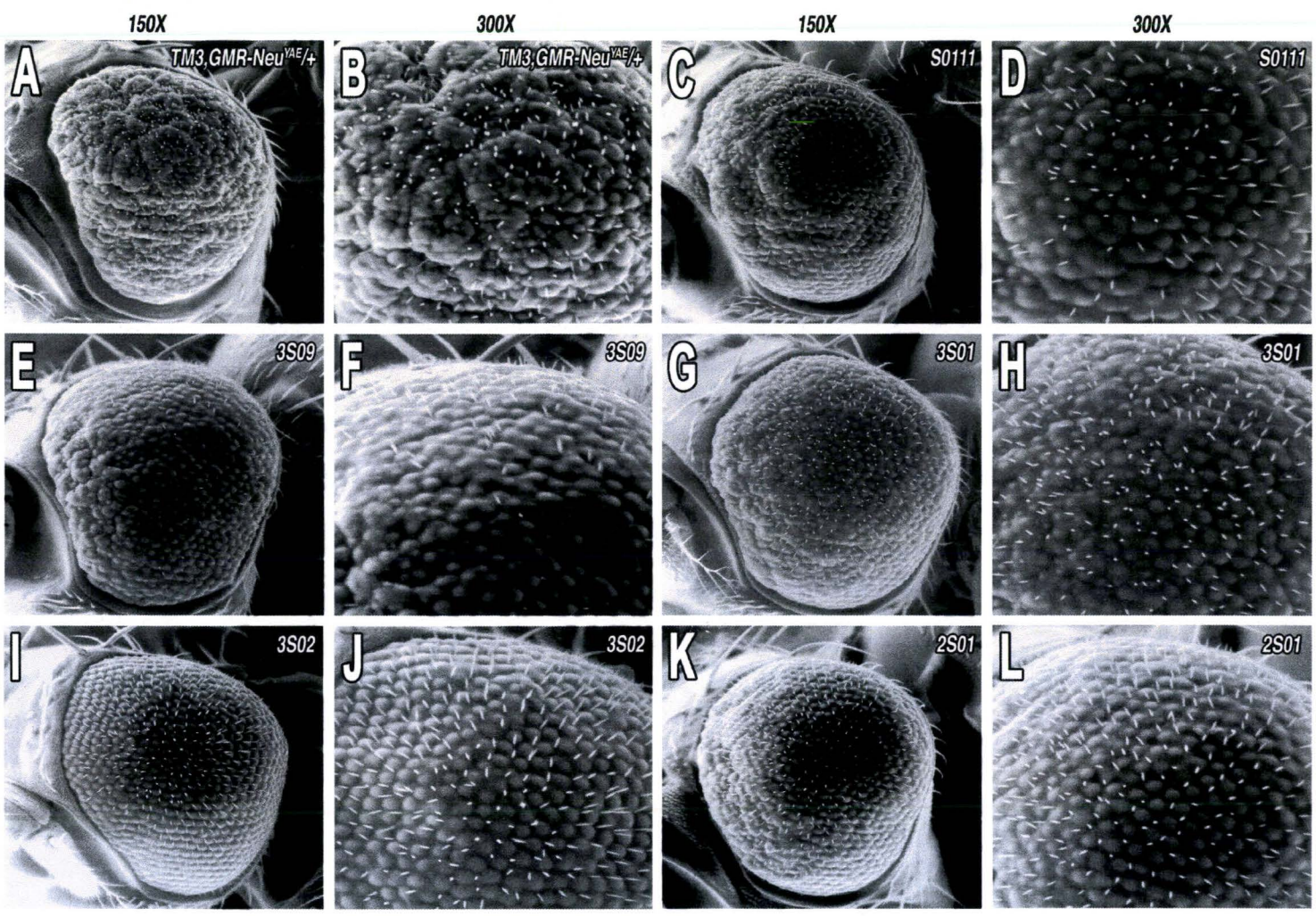
150X
300X
150X
300X
A
TM3,GMR-Neu^{YAE}/+
B
TM3,GMR-Neu^{YAE}/+
C
S0111
D
S0111
E
3S09
F
3S09
G
3S01
H
3S01
I
3S02
J
3S02
K
2S01
L
2S01

Supplement 3.5: Neu allele specificity of the 2nd-chromosome enhancers. (Panel A, B and C) Second chromosomal enhancers were verified for their genetic interactions with the *Neu*^{YA}, *Neu*^{YB}, and *Neu*^{YE}. A genetic interaction was assigned only when the modifier showed either suppression of enhancement of specific Neu allele *in trans*. Photographs from each genotype were taken at least at X150 and X300 magnification. The top panels are the misexpression of various Neu alleles and the particular modifier *in trans,* is indicated at the left of each row. Bar indicates 150 μm for the X300 magnifications.

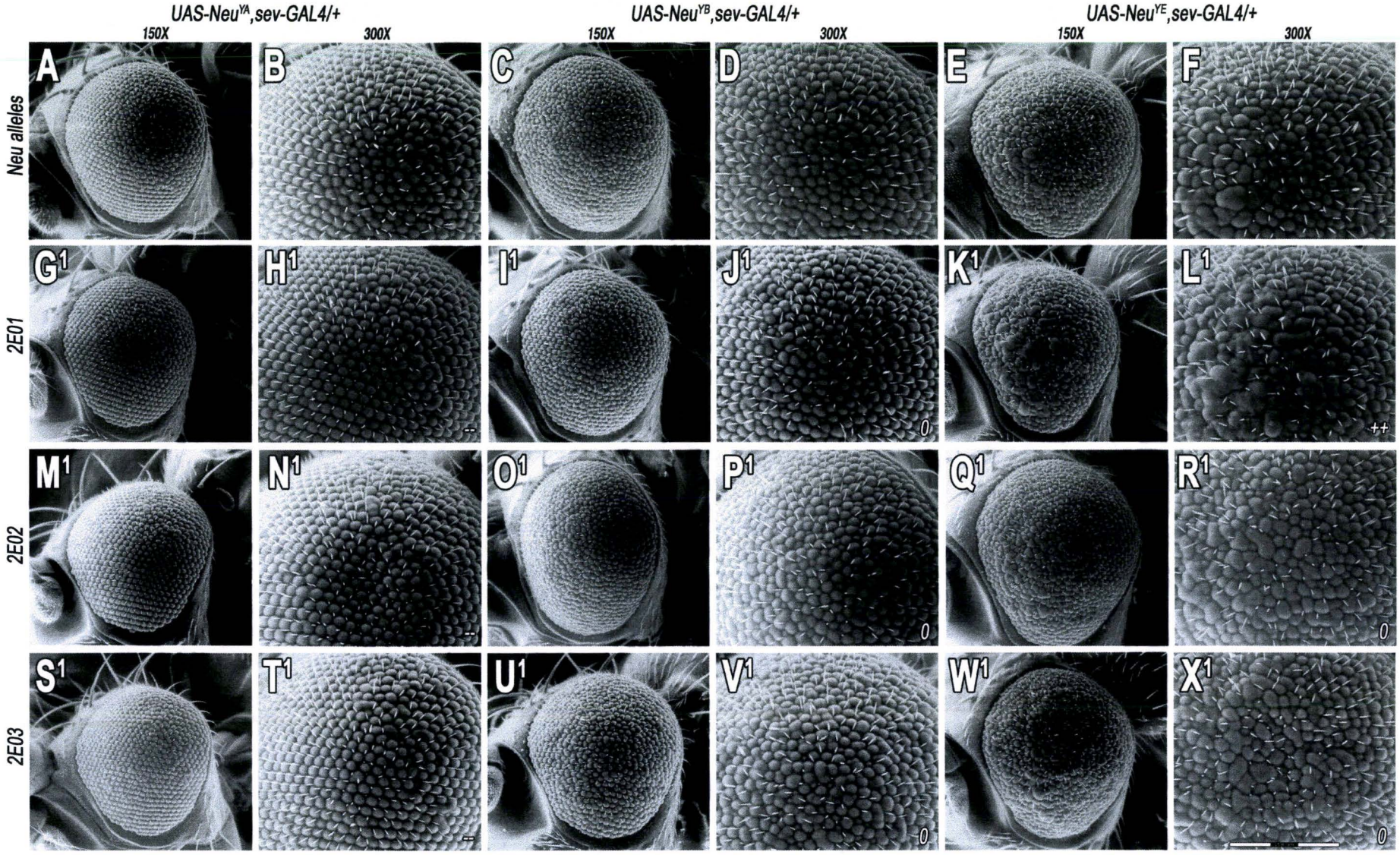
UAS-Neu^YA,sev-GAL4/+
UAS-Neu^YB,sev-GAL4/+
UAS-Neu^YE,sev-GAL4/+
150X
300X
150X
300X
150X
300X
Neu alleles
2E01
2E02
2E03
A
B
C
D
E
F
G1
H1
I1
J1
K1
L1
M1
N1
O1
P1
Q1
R1
S1
T1
U1
V1
W1
X1
--
0
++

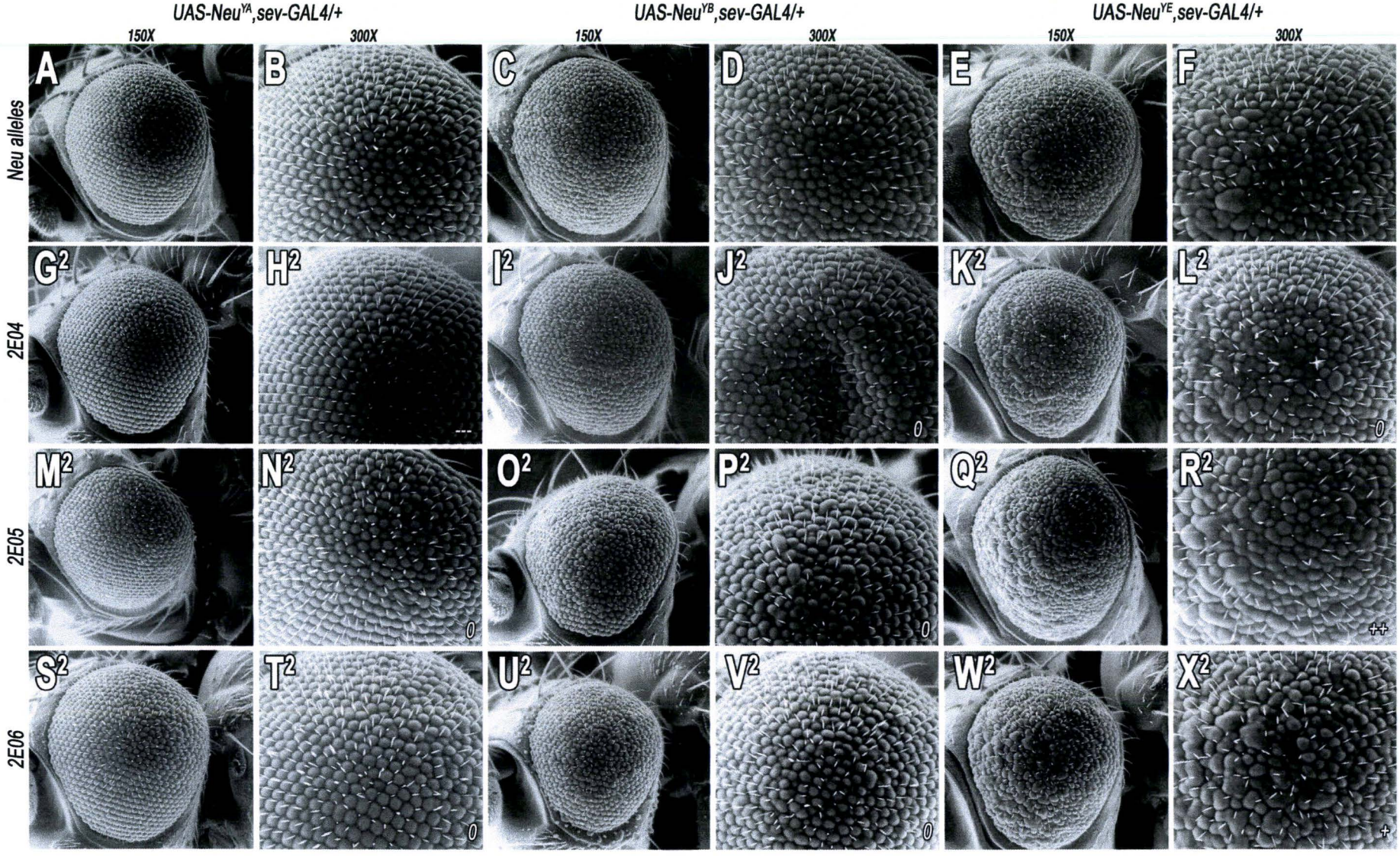
UAS-Neu^YA,sev-GAL4/+
UAS-Neu^YB,sev-GAL4/+
UAS-Neu^YE,sev-GAL4/+
150X
300X
150X
300X
150X
300X
Neu alleles
2E04
2E05
2E06
A
B
C
D
E
F
G2
H2
I2
J2
K2
L2
M2
N2
O2
P2
Q2
R2
S2
T2
U2
V2
W2
X2

0
0
0
0
0
++
+

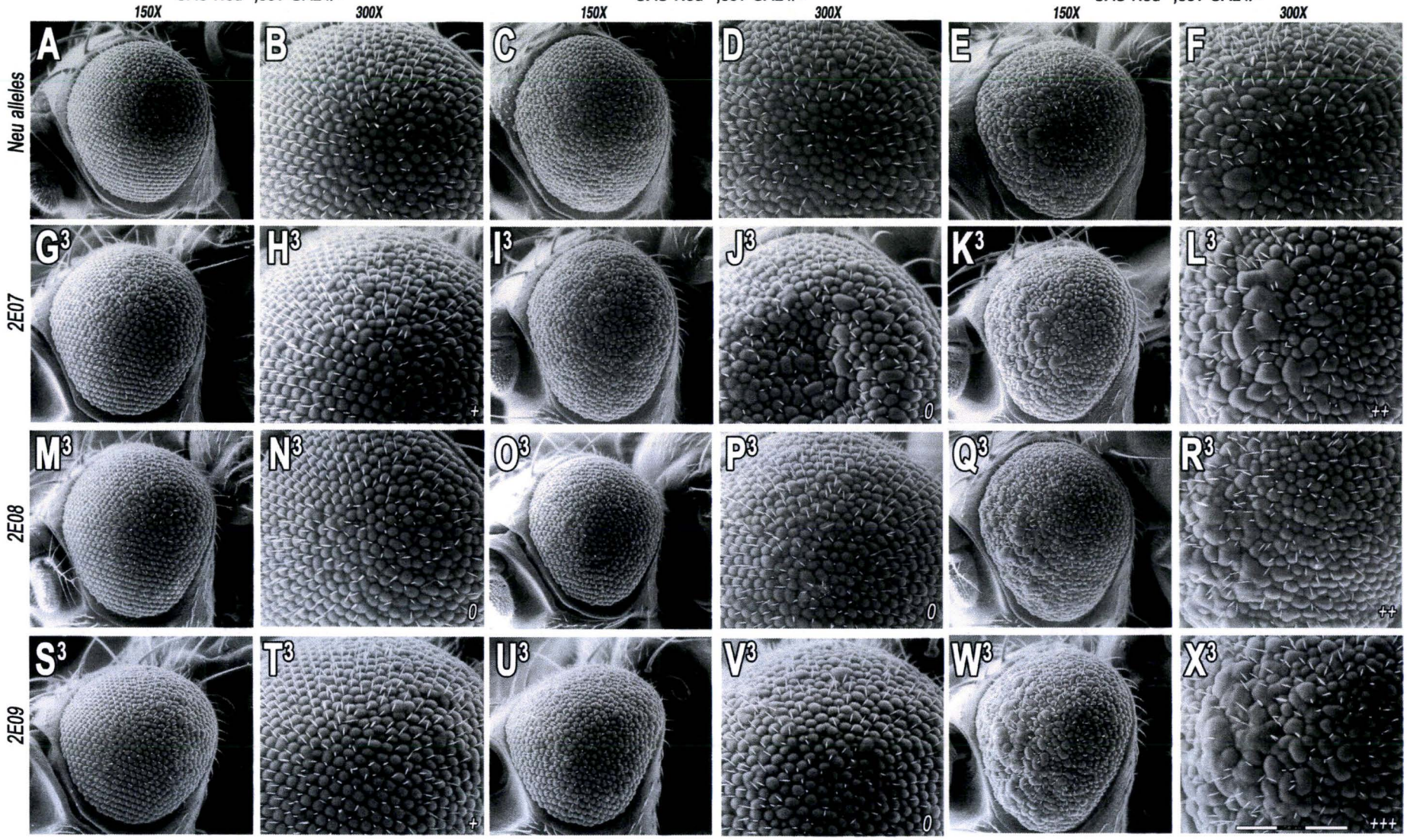
UAS-Neu^YA,sev-GAL4/+
UAS-Neu^YB,sev-GAL4/+
UAS-Neu^YE,sev-GAL4/+
150X
300X
150X
300X
150X
300X
Neu alleles
2E07
2E08
2E09
A
B
C
D
E
F
G3
H3
I3
J3
K3
L3
M3
N3
O3
P3
Q3
R3
S3
T3
U3
V3
W3
X3
+
0
0
++
0
++
+
0
+++

Supplement 3.6: Neu allele specificity of the 3rd-chromosome enhancers. (Panel A, B and C) Third chromosomal enhancers were verified for their genetic interactions with the Neu^{YA}, Neu^{YB}, and Neu^{YE}. A genetic interaction was assigned only when the modifier showed either suppression of enhancement of specific Neu allele *in trans*. Photographs from each genotype were taken at least at X150 and X300 magnification. The top panels are the misexpression of various Neu alleles and the particular modifier *in trans* is indicated at the left of each row. Bar indicates 150 μm for the X300 magnifications.

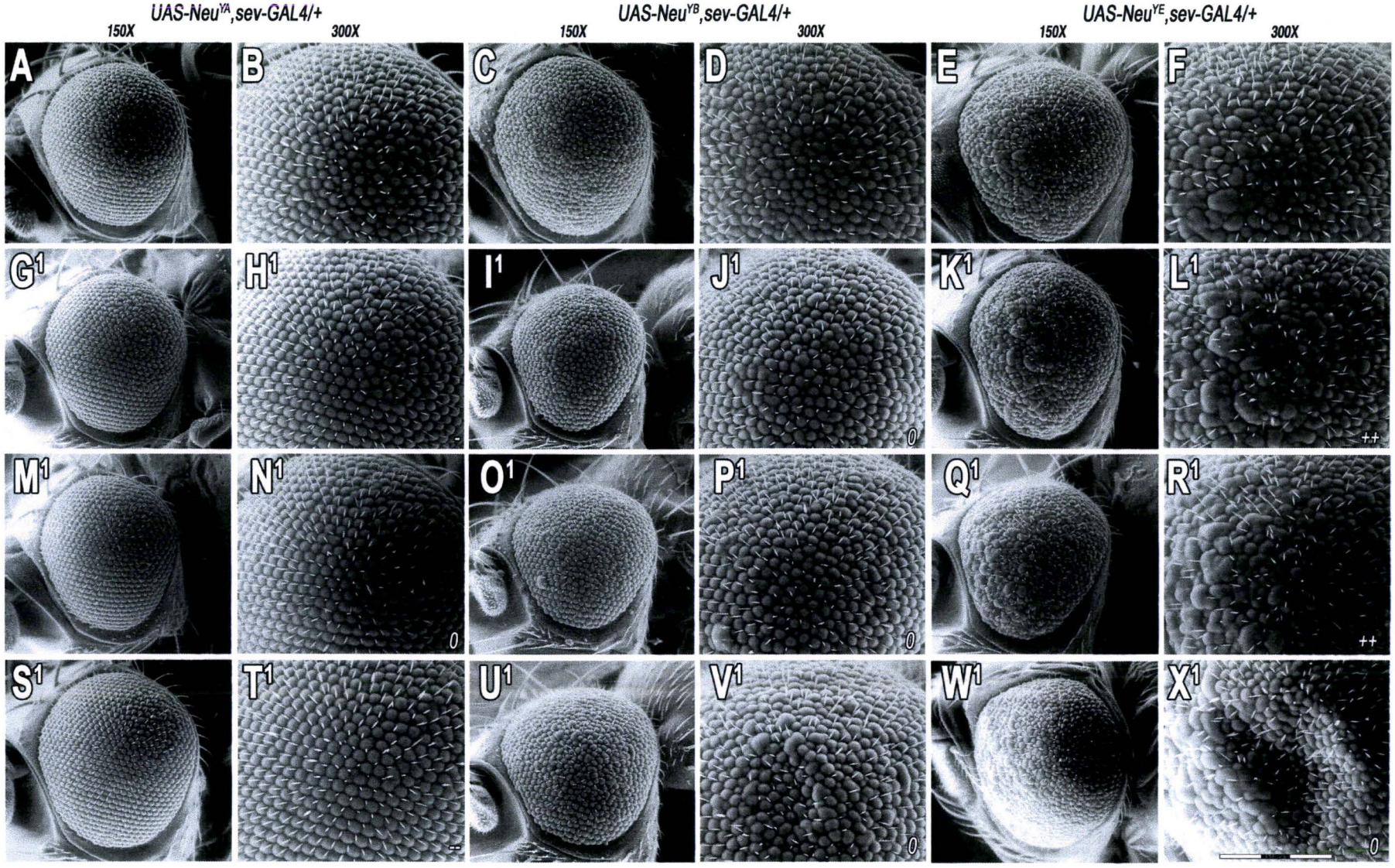
UAS-Neu^YA,sev-GAL4/+
UAS-Neu^YB,sev-GAL4/+
UAS-Neu^YE,sev-GAL4/+
150X
300X
150X
300X
150X
300X
Neu alleles
3E01
3E02
3E03
A
B
C
D
E
F
G1
H1
I1
J1
K1
L1
M1
N1
O1
P1
Q1
R1
S1
T1
U1
V1
W1
X1
0
++
0
++
0
0
0
--
0

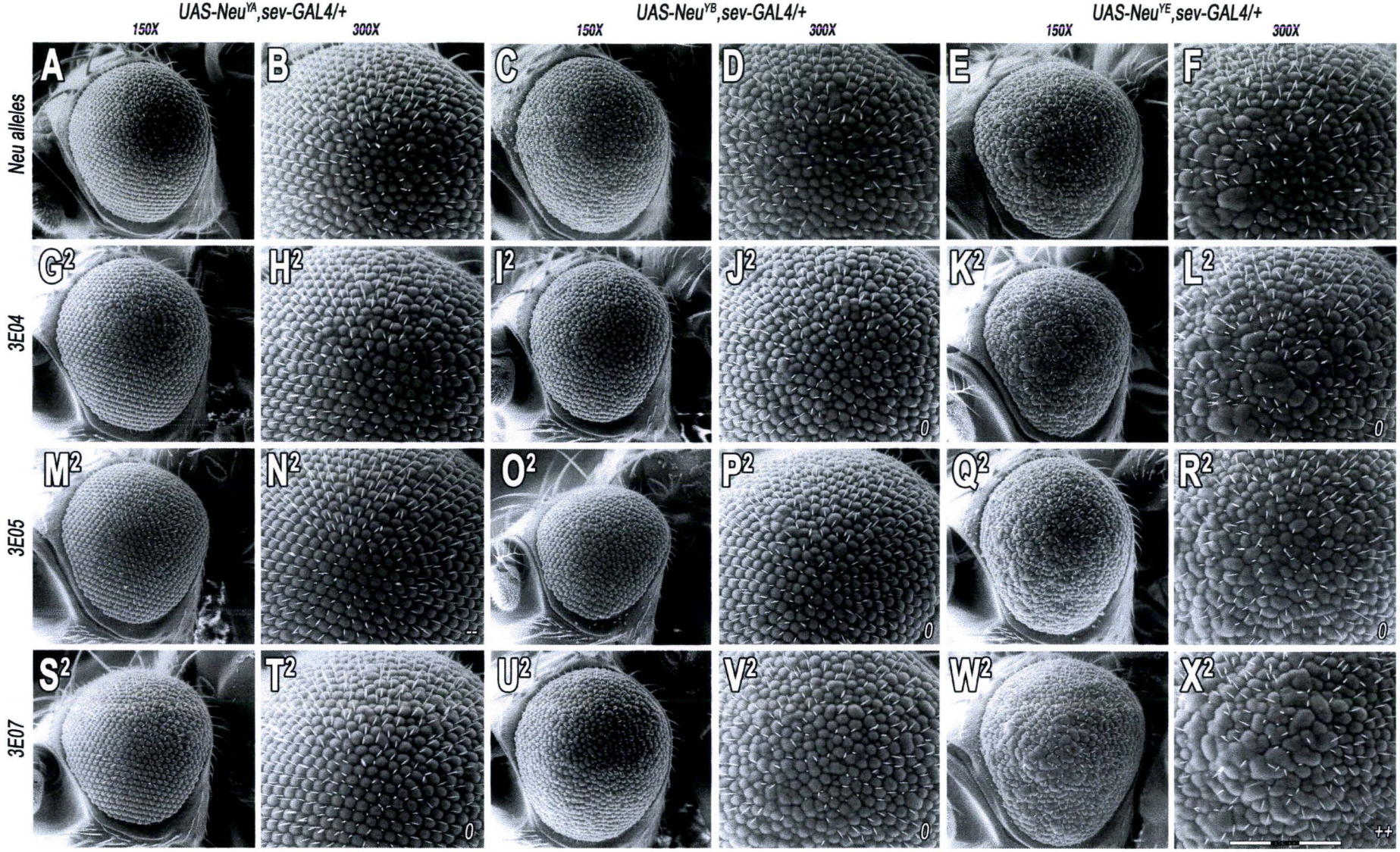
UAS-Neu^YA,sev-GAL4/+
UAS-Neu^YB,sev-GAL4/+
UAS-Neu^YE,sev-GAL4/+
150X
300X
Neu alleles
3E04
3E05
3E07
A
B
C
D
E
F
G2
H2
I2
J2
K2
L2
M2
N2
O2
P2
Q2
R2
S2
T2
U2
V2
W2
X2
0
++

Supplement 3.7: Determination of the rough map position using meiotic recombination. (A) Shows the summary data obtained from the meiotic recombination experiments with the 2nd chromosome modifier, 2S02. (B) Shows the calculation for the rough map position determination for the 2S02. (C) Approximate map position of the 2nd chromosome modifiers (Suppressors/Enhancers). (D) Approximate map position of the 3rd chromosome modifiers (Suppressors/Enhancers).

(A)

Table: Summary data of the recombination of the 2nd chromosome modifier, 2S02 (data obtained from 1463 F1 progeny).

Number of recombinant lines	*al*[1] 21C1-C1	*dp*[1] 24F4-25A1	*b*[1] 34D1-D1	*pr*[1] 38B5-B9	*c*[1] 52D3-D7	*px*[1] 58E4-E8	*sp*[1] 60C1-C2	Modifier Present
6	**+**	**+**	**-**	**-**	**-**	**-**	**-**	**Y**
3	**+**	**+**	**+**	**-**	**-**	**-**	**-**	**Y**
1	**+**	**+**	**+**	**+**	**-**	**-**	**-**	**Y**
3	**+**	**+**	**+**	**+**	**+**	**-**	**-**	**Y**
1	**-**	**+**	**+**	**+**	**+**	**+**	**+**	**Y**
1	-	+	-	-	-	+	+	Y
1	-	+	-	-	+	-	-	Y
6	-	-	+	+	+	+	+	N
2	-	-	-	+	-	-	-	N
1	-	-	-	-	+	-	-	N
1	-	-	-	-	+	+	+	N
4	+	-	-	-	-	-	-	N
1	+	-	+	-	-	-	-	N
1	-	-	+	+	+	+	+	N

+: Wildtype gene, **-:** Marker chromosome, **Y:** Modifier Present, **N:** Modifier Absent, **Shaded box:** Single recombinants and Modifiers present, **White box:** Either double recombinants or modifiers absent.

(B)

Relative distance of the modifier from al^1 to b^1 = No. of recombinants with al^1 present (1) : No. of recombinants with b^1 present (6)

Molecular distance from al^1 to b^1 = (21C1-21C1) ≈ (34D1-34D1)
= 382,778 bp ≈ 13,822,549 bp
= 13,439,771 bp

Rough distance from al^1 to the 2S02 =13,439,771/(sum of ratio)
= 13,439,771/7
= 1,919,967 bp (roughly)

Rough distance from 2S02 to b^1 = 13,439,771- 1,919,967
= 11,519,804 bp (roughly)

* The rough distance was calculated using at least 2 pair of markers.

(C)

Approximate map location of the 2nd Chromosome modifiers (determined from the meiotic recombination experiments)

Modifiers	Approximate calculated rough position (in bp)	Approximate calculated rough map location (in cytological division)
2S02	2L: 2,298,083	22D1
2S04	2L: 2,686,536	23A2
2S05	2L: 3,838,415	24C8
2S06	2L: 2,298,083	22D1
2S07	2L: 7,102,663	27E2
2S03	2R: 9,981,494	50E4
2S08	2R: 9,115,800	49F2
2S10	2R: 2,190,243	39A2
2E07	2L: 6,329,443	26C3
2E04	2L: 11,584,484	32F5
2E13	2R: 1,594,184	35D6
2E14	2R: 1,900,645	37B11
2E02	2R: 2,765,404	42D6
2E04	2R: 2,765,404	42D6
2E01	2R: 5,036,553	45A1
2E11	2R: 5,450,757	45D2
2E12	2R: 5,551,221	45E
2E03	2R: 11,857,365	53D1
2E09	2R: 12,792,795	53D
2E10	2R: 13,449,892	54C

Modifiers in the same shaded box are allelic or in the same complementation group. Even though their map position varies based on the recombination data, they fail to complement the same deleted region during Df mapping (complete Df mapping results in Chapter 3).

(D)

Approximate map location of the 3rd Chromosome modifiers (determined from the meiotic recombination experiments)

Modifiers	Approximate calculated rough position (in bp)	Approximate calculated rough map location (in cytological division)
3S03	3L: 15,224,708	71C1
3S05	3L: 13,586,616	70A
3S11	3L: 15,376,248	72A1
3S12	3L: 15,564,886	72D1
3S10	3L: 15,190,029	71B1
3S13	3L: 16,229,086	72D10
3S04	3L: 20,793,567	77B
3S06	3L: 20,887,667	77B
3S02	3R: 9,253,157	87E2
3S09	3R: 9,335,224	87E2
3E01	3L: 15,376,248	72A1
3E03	3L: 14,990,695	71B1
3E10	3L: 15,190,029	71A2
3E06	3L: 13,586,616	70B2
3E04	3L: 15,306,613	71C1
3E05	3L: 14,569,471	70B3
3E08	3R: 21,747,011	95D2

Modifiers in the same shaded box are allelic or in the same complementation group. Even though their map position varies based on the recombination data, they fail to complement the same deleted region during Df mapping (complete Df mapping results in Chapter 3).

Supplement 3.8: *lilli* mutant shows suppression of the Sev-Torso chimeric eye phenotype. In heterozygote with the control flies, $lilli^{A17\text{-}2}$ mutant shows eye phenotype suppression with the Neu^{YA} (compare A and B), while no phenotypic interaction with the Neu^{YB} (compare C and D) and Neu^{YE} (compare E and F). This YA specific modifier suppressed the rough-eye phenotype of Sev-Torso chimeric adults, suggesting a genetic interaction of these two alleles (compare K and L). However, $lilli^{A17\text{-}2}$ mutant had no effect on the *Drosophila*-EGFR Ellipse-mutant, Elp^{B1}, suggesting no genetic interaction between these two RTK alleles (compare I and J). Images were taken at X150, X300 and X800 magnifications on an ESEM. Transgenes are indicated on the left of row. Bar indicates 50 μm.

Panel-A
UAS-Neu^YA,sev-GAL4/+
UAS-Neu^YA,sev-GAL4/lilliA17-2
UAS-Neu^YB,sev-GAL4/+
UAS-Neu^YB,sev-GAL4/lilliA17-2
UAS-Neu^YE,sev-GAL4/+
UAS-Neu^YE,sev-GAL4/lilliA17-2
150X
300X
800X
A
B
C
D
E
F
G
H
I
J
K
L
M
N
O
P
Q
R

Panel-B
UAS-Neu^YNPD/+; GMR-GAL4/+
UAS-Neu^NYPD/+; GMR-GAL4/lilli^A17-2
TM3,GMR-Neu^YAE/+
TM3,GMR-Neu^YAE/lilli^A17-2
Elp^B1/+
Elp^B1/lilli^A17-2
150X
300X
800X
A
B
C
D
E
F
G
H
I
J
K
L
M
N
O
P
Q
R

Supplement 3.9: CG7777 mutant shows strong enhancement of the *Drosophila*-EGFR (Elp^{B1}) eye phenotypes. The novel enhancer, CG7777 strongly enhanced the Neu^{YA} rough eye phenotype (compare A and B). This dual (YA and YE) specific novel gene also showed a strong genetic interaction with the Neu^{YAE} and the gain-of-function DER Ellipse-mutant, Elp^{B1}, while enhancing the eye phenotypes significantly (compare C and D; E and F). However, a non-genetic interaction was observed with the Sev-Torso chimera (G and H). Images were taken at X150 magnifications on an ESEM (also see the supplement for other magnifications). Transgenes are indicated on the top centre of each panel. Bar indicates 300 μm.

Panel-A

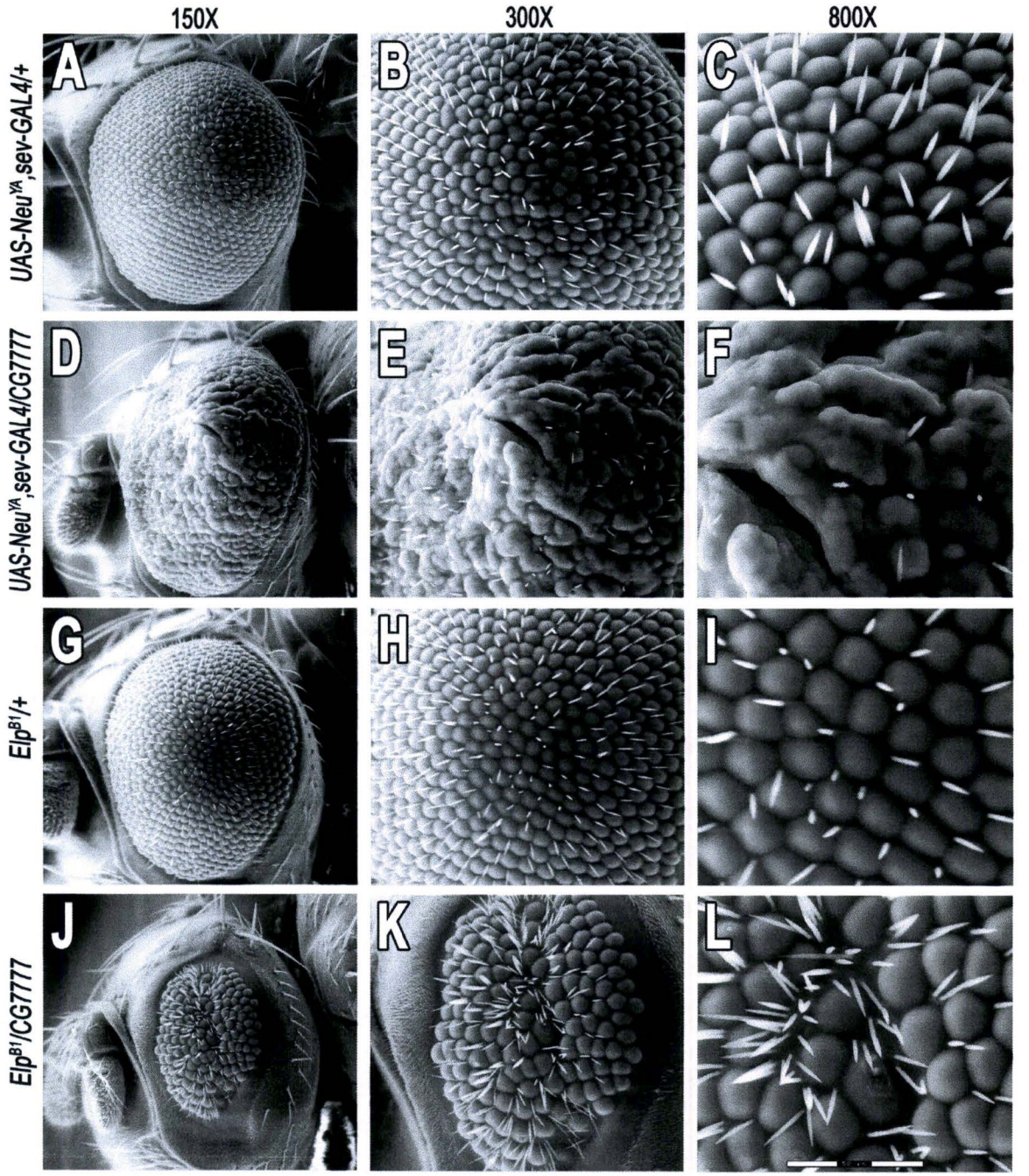
150X
300X
800X
UAS-Neu^YA,sev-GAL4/+
UAS-Neu^YA,sev-GAL4/CG7777
Elp^B1/+
Elp^B1/CG7777
A
B
C
D
E
F
G
H
I
J
K
L

Panel-B

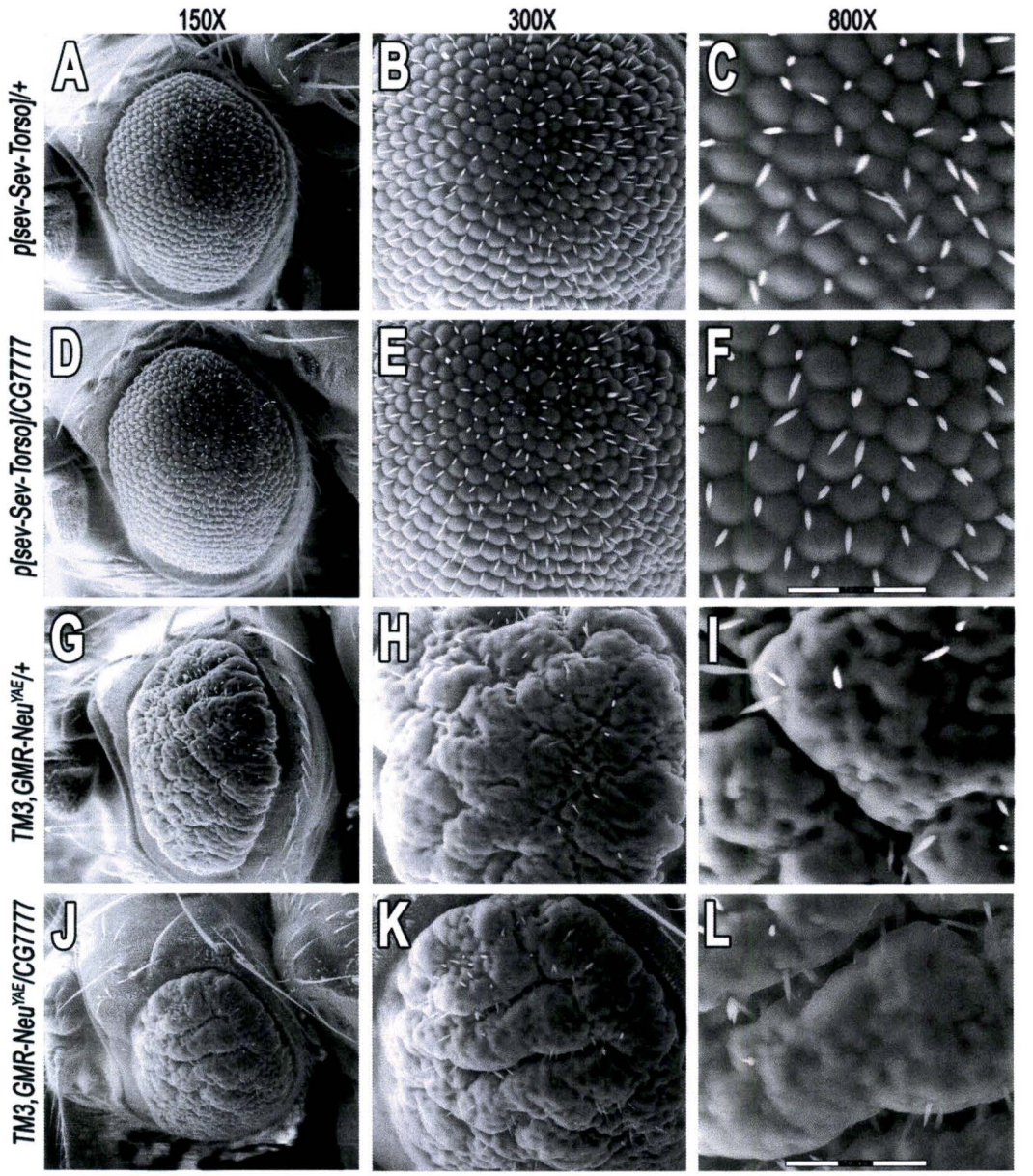
150X
300X
800X
p[sev-Sev-Torso]/+
p[sev-Sev-Torso]/CG7777
TM3,GMR-Neu^YAE/+
TM3,GMR-Neu^YAE/CG7777
A
B
C
D
E
F
G
H
I
J
K
L